MES BULLETIN OF

APPLIED SCIENCES

NAAC Accredited with 'A' Grade

EXECUTIVE EDITORS

Prof. ACHALA L. NARGUND & Prof. N. M. BUJURKE

Post Graduate Department of Mathematics and

Research Centre in Applied Mathematics

M E S College of Arts, Commerce and Science

15th cross, Malleswaram, Bengaluru - 560003.

MES BULLETIN OF APPLIED SCIENCES

MES BULLETIN OF APPLIED SCIENCES

(Working Papers)

EXECUTIVE EDITORS

Prof. ACHALA L. NARGUND   &   Prof. N. M. BUJURKE

Dedicated to

Pʀᴏꜰ. H. S. SHARADAMMA

POST GRADUATE STUDENTS EDITION

TABLE OF CONTENTS

Study of Sine-Gordon equation

C.V. Anitha[1], C.S. Asha[2] and L.N. Achala[3]

[1,2,3]P. G. Department of Mathematics and Research Centre in Applied Mathematics

M. E. S. College of Arts, Commerce and Science

15th cross, Malleswaram, Bangalore - 560003.

Email ID: [1]anithavenkatareddy28@gmail.com, [2]ashacs1980@gmail.com, [2]anargund1960@gmail.com

Abstract: In this paper, we solve Sine-Gordon equation using finite difference method and variable separable method. Numerical solution of kink soliton, antikink soliton, kink-kink collision, kink-antikink collision and breather are calculated using finite difference scheme. The results obtained by numerical method are compared with the exact solution to prove the accuracy.

Keywords: Hyperbolic partial differential equation, Wave equation, Sine-Gordon equation, Finite difference method, Kink collision, Anti-Kink collision, Breathers.

1 Introduction

The general second order linear partial differential equation is solved by many analytical and numerical techniques [6]. All these type of equations are part of one or the other real world problems. Originally, almost all mathematical modelling of real world problem are non-linear.But there are some which are solved by using numerical techniques, these techniques are for understanding and solving mathematical problems by converting them into basic algebraic equations. Almost all numerical methods involve large number of arithmetical operations, which can be handled very easily due to the availability of digital computers. Here we restrict ourselves to one of the celebrated equation called as Sine-Gordon equation. It is a non-linear hyperbolic partial differential [2, 3] equation in $1 + 1$ dimension, involving the D'Alembert operator and the sine of the unknown function.It was first introduced by Edmond Bour in 1862 in the course of study of surfaces of constant negative curvature as the Gauss-Codazzi equation for surfaces of curvature. It was rediscovered by Frenkel and Kontorona in 1939 in the study of crystal dislocations. This equation attracted a lot of attention in the $1970s$ due to the presence of soliton solutions.

An interesting feature of Sine-Gordon equation is the existence of soliton and multi-soliton solution. [1, 5].Here we are studying one soliton solution, two soliton solution, which arises from the possibilities of coupled kink and anti-kink behavior called as breather. Breathers are of two types, standing breather and moving breather.

In mathematics and physics, a soliton is a self-reinforcing solitary wave packet, that maintains its shape while it propagates at a constant velocity. Solitons are the solutions of non-linear dispersive partial differential equations. The soliton phenomenon was first described in 1834 by John Scott Russell. He discovered a solitary wave in the union Canal in Scotland. He reproduced the phenomenon in a wave tank and named it as the "Wave of translation".

A kink is a soliton that brings in one vacuum state, $u = 2k\pi$ as $x \rightarrow \infty$ and ends in the next higher vacuum state, $u = 2(k+1)\pi$ as $x \rightarrow \infty$. Similarly an Anti-kink begins in a higher state

to the left and ends up in lower state to the right. Two kink repel each other when they come in contact. When a kink and Anti-kink collide, they temporarily combine and each emerges in the same shape as before, at the next lower vacuum state.

Sine-Gordon equation [4] has applications in the propagation of waves on a liquid membrane, one dimensional models for elementary particles, self-induced transparency of short optical pulses, domain walls in ferro-electric and ferromagnetic materials, the propagation of crystal effects and propagation of fluxons in a long Josephson junction. The huge success of devices using Josephson functions or mechanical transmission lines has been a result of the discovery of high temperature superconductors in the 1980s and also mechanical trasmission line, $u(x, t)$ describes an angle of rotation of the pendulums.

2   Method of solution

2.1   Numerical Scheme of Sine-Gordon equation

Consider an initial value problem for the Sine-Gordon equation

$$u_{tt} - u_{xx} + \sin(u) = 0, \tag{1}$$

on the interval $x \in [a, b]$ with initial conditions

$$u(x, 0) = f(x), \quad u_t(x, 0) = g(x), \tag{2}$$

and boundary conditions

$$u_x(a, t) = 0, \quad u_x(b, t) = 0. \tag{3}$$

Applying Explicit finite difference method [9, 10, 11] to equation (1), we get

$$u_{i,j+1} = -u_{i,j-1} + 2(1 - \alpha^2)u_{i,j} + \alpha^2(u_{i+1,j} + u_{i-1,j} - \Delta t^2 \sin(u_{i,j}), \tag{4}$$

where $\alpha = \dfrac{\Delta t}{\Delta x}$, $i = 0, \ldots, M$ and $t = 0, \ldots T$.

Applying second initial condition, we get

$$u_{i,-1} = u_{i,1} - 2\Delta t g(x_i) + \delta(\Delta t^2). \tag{5}$$

Substituting equation (5) in (4), and replacing $u_{i,j+1}$ by $u_{i,1}$ and $u_{i,j-1}$ by $u_{i,-1}$, we get

$$u_{i,1} = \Delta t g(x_i) + (1 - \alpha^2)u_i + \frac{\alpha^2}{2}(u_{i+1} + u_{i-1}) - \frac{\Delta t^2}{2} \sin(u_i) - \frac{\delta}{2}(\Delta t^2). \tag{6}$$

Since δ is a very small value hence it is neglected and replacing $u_{i+1} = f(x_{i+1})$, $u_{i-1} = f(x_{i-1})$ and $u_i = f(x_i)$ in RHS, we get

$$u_{i,1} = \Delta t g(x_i) + (1 - \alpha^2)f(x_i) + \frac{\alpha^2}{2}(f(x_{i+1}) + f(x_{i-1})) - \frac{\Delta t^2}{2} \sin(f(x_i)). \tag{7}$$

Applying boundary conditions to equation (5), we get

$$u_x(a, t) = 0 \Leftrightarrow u_{-1,j} = u_{1,j},$$

$$u_x(b,t) = 0 \Leftrightarrow u_{M+1,j} = u_{M,j}. \tag{8}$$

On simplifying equation (7) to matrix form, we get

$$u_1 = \Delta t \gamma + A u_0 - \frac{\Delta t^2}{2}\beta_1. \tag{9}$$

where

$$\gamma = (g(a), g(x_1), \ldots, g(x_{M-1}), g(b))^T,$$
$$\beta_1 = (\sin(u_{0,0}), \sin(u_{0,1}), \ldots, \sin(u_{0,M-1}), \sin(u_{0,M}))^T,$$

$$A = \begin{bmatrix} 1-\alpha^2 & \alpha^2 & 0 & \ldots & 0 \\ \frac{\alpha^2}{2} & 1-\alpha^2 & \frac{\alpha^2}{2} & \ldots & 0 \\ 0 & \frac{\alpha^2}{2} & 1-\alpha^2 & \ldots & 0 \\ \ldots & \ldots & \ldots & \ldots & \ldots \\ 0 & \ldots & \ldots & \alpha^2 & 1-\alpha^2. \end{bmatrix}$$

Clearly A is a $M+1 \times M+1$ tridiagonal square matrix. Equation (4) can also be written as

$$u_{j+1} = -u_{j-1} + B u_j - \Delta t^2 \beta. \tag{10}$$

where $j = 1, 2, \ldots, T-1$, $\beta = (\sin(u_{j,0}), \sin(u_{j,1}), \ldots, \sin(u_{j,M-1}), \sin(u_{j_M}))^T$ and B is a square matrix defined by $B = 2A$.

Applying explicit scheme to equation (1) and solving in the interval $[-L, L]$ with boundary conditions and following parameters.
- Taking Space interval $L = 20$.
- Space discretization step as $\Delta x = 0.2$.
- Time discretization step as $\Delta t = 0.1$.
- Amount of time steps as $T = 100$.
- Velocity of the Kink as $C = 0.2$.

The initial condition for the Kink is given by,

$$f(x) = 4 \arctan\left(\exp\left(\frac{x}{\sqrt{1-c^2}}\right)\right), \tag{11}$$

$$g(x) = -2\frac{c}{\sqrt{1-c^2}}\left[\operatorname{sech}\left(\frac{x}{\sqrt{1-c^2}}\right)\right]. \tag{12}$$

The initial condition for the Anti-Kink is given by,

$$f(x) = 4 \arctan\left(\exp\left(-\frac{x}{\sqrt{1-c^2}}\right)\right), \tag{13}$$

$$g(x) = -2\frac{c}{\sqrt{1-c^2}}\left[\operatorname{sech}\left(\frac{x}{\sqrt{1-c^2}}\right)\right]. \tag{14}$$

The initial condition for the Kink-Kink is given by,

$$f(x) = 4 \arctan\left(\exp\left(\frac{x+\frac{L}{2}}{\sqrt{1-c^2}}\right)\right) + 4 \arctan\left(\exp\left(\frac{x-\frac{L}{2}}{\sqrt{1-c^2}}\right)\right), \tag{15}$$

$$g(x) = -2\frac{c}{\sqrt{1-c^2}}. \operatorname{sech}\left(\frac{x+\frac{L}{2}}{\sqrt{1-c^2}}\right) + 2\frac{c}{\sqrt{1-c^2}}. \operatorname{sech}\left(\frac{x-\frac{L}{2}}{\sqrt{1-c^2}}\right). \tag{16}$$

The initial condition for the Kink-AntiKink is given by,

$$f(x) = 4\arctan\left(\exp\left(\frac{x+\frac{L}{2}}{\sqrt{1-c^2}}\right)\right) + 4\arctan\left(\exp\left(-\frac{x-\frac{L}{2}}{\sqrt{1-c^2}}\right)\right), \tag{17}$$

$$g(x) = -2\frac{c}{\sqrt{1-c^2}}. \operatorname{sech}\left(\frac{x+\frac{L}{2}}{\sqrt{1-c^2}}\right) - 2\frac{c}{\sqrt{1-c^2}}. \operatorname{sech}\left(\frac{x-\frac{L}{2}}{\sqrt{1-c^2}}\right). \tag{18}$$

The initial condition for breather is given by,

$$f(x) = 0, \tag{19}$$

$$g(x) = 4\sqrt{1-c^2}. \operatorname{sech}(x\sqrt{1-c^2}). \tag{20}$$

2.2   The solution of the Sine-Gordon equation by separation of variables

Consider an initial value problem for the Sine-Gordon equation [7]

$$u_{xx} - u_{tt} = \sin u. \tag{21}$$

Consider a transformation,

$$v(x,t) = \tan\left(\frac{1}{4}u\right), \tag{22}$$

then,

$$u_{xx} = \frac{(1+v^2)4v_{xx} - 4v_x(2v)v_x}{(1+v^2)^2}, \tag{23}$$

$$u_{tt} = \frac{(1+v^2)4v_{tt} - 4v_t(2v)v_t}{(1+v^2)^2}, \tag{24}$$

and using the trigonometric identity

$$\sin u = \frac{4v(1-v^2)}{(1+v^2)^2}. \tag{25}$$

Substituting equation (23), (24) and (25) in (21), we get

$$(1+v^2)(v_{xx} - v_{tt} - v) - 2v(v_x^2 - v_t^2 - v^2) = 0. \tag{26}$$

Let us consider the separation of variables in the form

$$v(x,t) = \tan\left(\frac{1}{4}u\right) = \frac{\phi(x)}{\psi(t)}. \tag{27}$$

Since, $v(x,t) = \frac{\phi(x)}{\psi(t)}$, we get

$$v_x = \frac{\phi_x}{\psi}, \quad v_t = \frac{-\phi\psi_t}{\psi^2}. \tag{28}$$

$$v_{xx} = \frac{\phi_{xx}}{\psi}, \quad v_{tt} = \frac{-\phi\psi\psi_{tt} + 2\phi\psi_t^2}{\psi^3}. \tag{29}$$

Substituting equation (28) and (29) in (26), we get

$$(\phi^2 + \psi^2)\left(\frac{\phi_{xx}}{\phi} + \frac{\psi_{tt}}{\psi}\right) - 2(\phi_x^2 + \psi_t^2) = \phi^2 - \psi^2. \tag{30}$$

Differentiating equation (30) with respect to x, we get

$$\frac{1}{\phi\phi_x}(\phi^2 + \psi^2)\left(\frac{\phi_{xx}}{\phi}\right)_x + 2\left(\frac{\psi_{tt}}{\psi} - 1\right) - 2\frac{\phi_{xx}}{\phi} = 0. \tag{31}$$

Differentiating equation (30) with respect to t, we get

$$\frac{1}{\psi\psi_t}(\phi^2 + \psi^2)\left(\frac{\psi_{tt}}{\psi}\right)_t + 2\left(\frac{\phi_{xx}}{\phi} + 1\right) - 2\frac{\psi_{tt}}{\psi} = 0. \tag{32}$$

Equation (28) can be rewritten as,

$$v_{xx}v = \frac{\phi_{xx}}{\phi}, \quad -\left[\frac{v_{tt}}{v} + \frac{2v_t\psi_t}{v\psi}\right] = \frac{\psi_{tt}}{\psi}. \tag{33}$$

Substituting equation (33) in (31), we get

$$\frac{1}{\phi\phi_x}\left(\frac{\phi_{xx}}{\phi}\right)_x = \frac{2\left[\frac{v_{tt}}{v} + \frac{2v_t\psi_t}{v\psi} + v_{xx}v + 1\right]}{\psi^2(v^2 + 1)}. \tag{34}$$

Substituting equation (33) in (32), we get

$$\frac{1}{\psi\psi_t}\left(\frac{\psi_{tt}}{\psi}\right)_t = \frac{-2\left[\frac{v_{tt}}{v} + \frac{2v_t\psi_t}{v\psi} + v_{xx}v + 1\right]}{\psi^2(v^2 + 1)}. \tag{35}$$

If $\dfrac{2\left[\frac{v_{tt}}{v} + \frac{2v_t\psi_t}{v\psi} + v_{xx}v + 1\right]}{\psi^2(v^2 + 1)} = -4k^2$, then equations (34) and (35) become

$$\frac{1}{\phi\phi_x}\left(\frac{\phi_{xx}}{\phi}\right)_x = -4k^2$$

$$-\frac{1}{\psi\psi_t}\left(\frac{\psi_{tt}}{\psi}\right)_t = -4k^2$$

Therefore, we get

$$\frac{1}{\phi\phi_x}\left(\frac{\phi_{xx}}{\phi}\right)_x = -\frac{1}{\psi\psi_t}\left(\frac{\psi_{tt}}{\psi}\right)_t = -4k^2 \tag{36}$$

and $-4k^2$ is a separation constant.

Integrating equation (36) with respect to x gives

$$\Rightarrow \phi_x\phi_{xx} = -4k^2\frac{\phi^3}{2}\phi_x + a\phi\phi_x. \tag{37}$$

Integrating again with respect to x, we obtain

$$\phi_x^2 = -k^2\phi^4 + a\phi^2 + b. \tag{38}$$

Similarly, integrating (36) twice with respect to t, we get

$$\psi_t^2 = k^2\psi^4 + c\psi^2 + d. \tag{39}$$

where a, b, c and d are integrating constants.

Substituting $a - c = 1$ and $b + d = 0$ and setting $a = m^2$ and $b = n^2$ in equation (38) and (39), we get

$$\phi_x^2 = -k^2\phi^4 + m^2\phi^2 + n^2 \ and \ \psi_t^2 = k^2\psi^4 + (m^2 - 1)\psi^2 - n^2, \tag{40}$$

where m and n are integrating constants.

However, we solve these equations for the following special cases of interest:

Case 1: $k = n = 0$ and $m > 1$

Equation (40) becomes

$$\phi_x = \pm m\phi, \quad \psi_t = \pm\sqrt{m^2 - 1}\psi. \tag{41}$$

The exact solution of equation (38) and (39) is given by,

$$\phi(x) = a_1\exp(\pm mx), \quad \psi(t) = a_2\exp(\pm\sqrt{m^2 - 1}t), \tag{42}$$

where a_1 and a_2 are integrating constants.

Substituting equation (42) in (27), we get

$$u(x,t) = 4\tan^{-1}\left[\alpha\exp\left(\pm\frac{x \pm ut}{\sqrt{1 - u^2}}\right)\right]. \tag{43}$$

where $\alpha = \dfrac{a_1}{a_2}$ and $u = \dfrac{\sqrt{m^2 - 1}}{m}$ are constants.

Equation (43) can be rewritten as,

$$u(x,t) = 4\tan^{-1}[\alpha\exp\{m(x - ut)\}]. \tag{44}$$

Equation (44) represents the soliton solution of Sine-Gordon equation.

Equation (43) can also be written as

$$u(x,t) = 4\cot^{-1}\left[\frac{1}{\alpha}\exp\{m(x - ut)\}\right]. \tag{45}$$

For $\alpha = 1$, the above equation represents anti-soliton solution.

Furthermore, u_x and u_t also represent solitary wave solutions given by,

$$u_x(x,t) = \pm 2m\sec[m(x \pm ut) + \log\alpha], \tag{46}$$

$$u_t(x,t) = \pm 2m\sqrt{m^2 - 1}\sec[m(x \pm ut) + \log\alpha]. \tag{47}$$

Case 2: $k \neq 0$, $n = 0$ and $m^2 < 1$

Consider,

$$u(x,t) \backsim -4\tan^{-1}\left[\frac{m}{\sqrt{1-m^2}}\cdot\frac{\sin(\omega t + a_2)}{\cosh(mx + a_1)}\right]. \tag{48}$$

where $m = \sqrt{1 - m^2} = mu$. This is known as breather solution of Sine-Gordon equation and it also represents a pulse-type structure of a soliton.

In case of $m \ll 1$, m corresponds to a small amplitude breather solution.

Retaining the first term of equation (48) and by expanding the inverse tangent function for small m, we get

$$u(x,t) \sim 2im\sec(mx)\exp\left[i\left(1 - \frac{m^2}{2}\right)t\right] + c.c. \tag{49}$$

$$u(x,t) = A(x,t)\exp(it), \tag{50}$$

where $A(x,t)$ satisfies the $(1+1)$ dimensional non-linear Schrodinger equation.

$$2iA_t - A_{xx} - |A|^2 A = 0, \tag{51}$$

where the term $A_{tt} = O(m^4)$, which is neglected.

Finally, more general solutions of equation (43) can be found in terms of elliptic functions.

3   Results and Discussion

The Sine Gordon equation which is converted into matrix form usively. Space time representation of the numerical solution of kink-kink collision and kink-antikink colling finite difference method. From the converted matrix and from the initial conditions of kink, anti-kink and breathers we have found the numerical solutions for each initial conditions. Numerical solution of kink soliton and Anti-kink soliton moving with velocity $c = 0.2$ is plotted in figure 1 and 2 respectision are shown in figure 3 and 4. Numerical solution of breather oscillating with the frequency $\omega = 0.2$ is plotted in figure 5 and breather solution for amplitude $m = 0.8$ is plotted in figure 6.
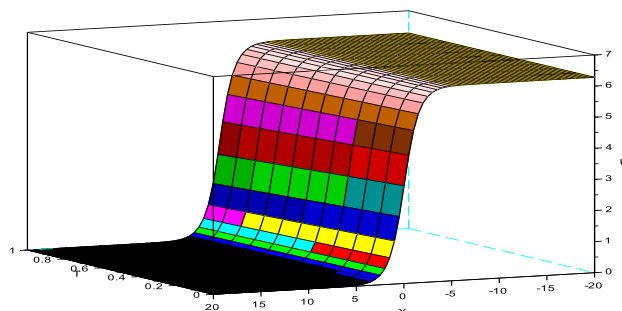
Figure 1: Numerical solution of Kink soliton moving with velocity $c = 0.2$
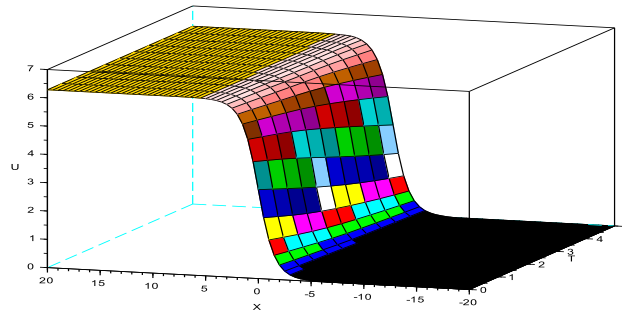
Figure 2: Numerical solution of Anti-Kink soliton moving with velocity $c = 0.2$
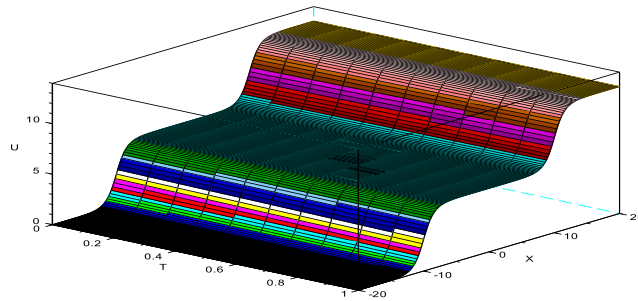
Figure 3: Numerical solution of kink-kink collision
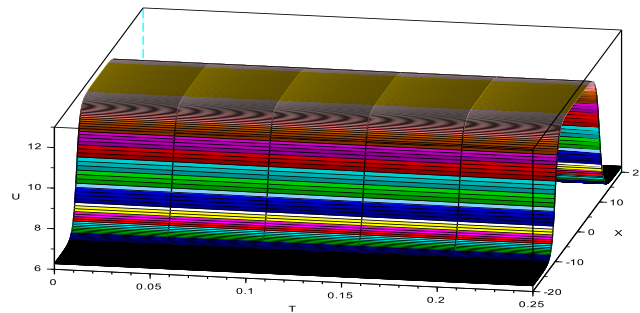
Figure 4: Numerical solution of kink-antikink collision
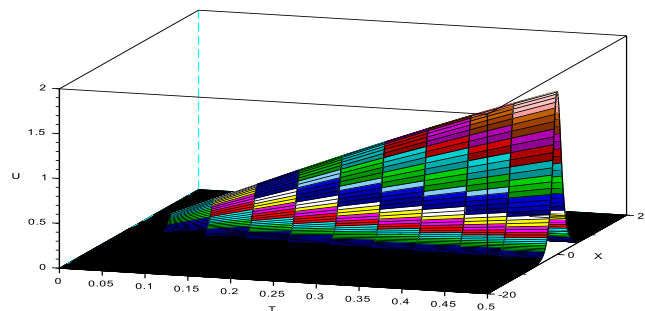
Figure 5: Numerical solution of breather oscillating with the frequency ω=0.2
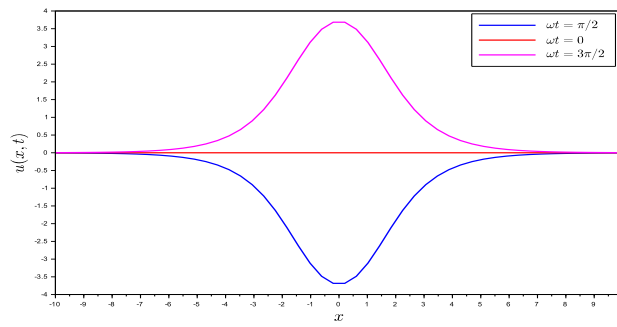
Figure 6: Solution of breather for $m = 0.8$

References

[1] P.L. Sachdev, *Nonlinear ordinary differential equations and their applications*, Marcel Dekker, Inc, 1991.

[2] G.F. Simmons, *Differential equations with applications and history notes*, TATA McGraw-Hill, 1990.

[3] C.S. Asha, *Solutions of initial and boundary value problems*, M.Phil thesis, 2007.

[4] L. Debnath, *Nonlinear partial differential equations for scientists and engineers*, Birkhauser, 1997.

[5] S.J. Farlow, *An introduction to differential equations and their applications*, Dover, 1994.

[6] G.M. Murphy, *Introductory methods of numerical analysis*, PHI, 2013.

[7] R.L. Burden, J. Douglas Faires, *Numerical analysis*, Cengage Learning, 9th edition, 2013.

[8] M.K. Jain, S.R.K. Iyengar, R.K. Jain, *Computational methods for partial differential equations*, New Age International Publishers, 2007.

[9] M.K Jain, S.R.K. Iyengar, R.K. Jain, *Numerical analysis*, New Age International Publishers, 2007.

[10] S.S. Sastry, *Introductory methods of numerical analysis*, PHI, 5th edition, 2013.

The Differential Transform Method to Partial Differential Equations

M. Bhavya[1], H.V. Gangamani[2] and L.N. Achala[3]

[1,2,3]P. G. Department of Mathematics and Research Centre in Applied Mathematics

M. E. S. College of Arts, Commerce and Science

15th cross, Malleswaram, Bangalore - 560003.

Email ID: [1]bhavya130995@gmail.com, [2]gangahv@gmail.com, [3]anargund1960@gmail.com

Abstract: Differential Transform is a semi-analytical method to find the solution of various equations such as Boundary Value Problems, Algebraic equations, linear and Non-linear partial Differential equations and Integral equations. We have applied this method to obtain an approximate solution to non-linear partial differential equations by converting into an ordinary differential equation using a wave variable. We have compared the Differential transform Method with other solutions to illustrate the accuracy obtained this method. We have also applied reduced differential transform method to solve Klein Gordon equation which plays an important role in plasma physics, fluid dynamics and chemical kinematics to understand the this technique which is powerful and effective.

Keywords: Wave variations, Nonlinear partial differential equation.

1   Introduction

The concept of Differential Transform(DT) was first introduced by Zhou [4] in solving linear and nonlinear initial value problems in electrical circuit analysis. The Differential Transform Method is the alternative way to find the Taylore series solution for the given differential equation and this method always coincides with the Taylor explanation of the exact solution because it has small error. Differential Transform Method is the semi-analytical method used to find the solution of various equations such as boundary value problems, algebraic equations, partial differential equations, integral equations etc... This method provides the accurate values. The main advantage of this method is that, it can be applied to various types of linear and nonlinear differential and integral equations [8] which are homogeneous or inhomogeneous with constant or with variable coefficients.

1.1   Definitions

- **Taylore polynomial**:
  A Taylore polynomial of degree n is defined by

$$P_n(x) = \sum_{k=0}^{n} (f^{(k)}(c))(x - c)^k \tag{1}$$

- **Differential Transform**:
  suppose the function $f(x)$ is continuously differentiable on the interval $(x_0 - r, x_0 + r)$ then the differential transform of the function $f(x)$ for the kth derivative is defined as

follows

$$F(k) = \frac{1}{k!}\left[\frac{d^k f(x)}{dx^k}\right]_{x=x_0} \tag{2}$$

where $f(x)$ is the original function and $F(k)$ is the transformed function.

- **Inverse differential transform**:
  The inverse differential transform of $F(x)$ is defined as

$$f(x) = \sum_{k=0}^{\infty}(x - x_0)^k F(k) \tag{3}$$

2   Riccati's Equation

The Riccati differential equation is named after the Italian nobleman count Francesco Riccati (1676-1754)[4]. The applications of this equation can be found in optimal control, diffusion problems, network synthesis, functional mathematics, Stochastic realization theory etc.. This equation is one of the simplest nonlinear ordinary differential equation, which plays an important role in the solution of nonlinear integrable partial differential equations.Thus Riccati equation plays an important role in the solution of various nonlinear systems.
The General form of the Riccati equation with variable coefficients is given by:

$$\frac{dy}{dx} + P(x)y(x) + Q(x)y^2 = R(x) \tag{4}$$

2.1   Solution of the Riccati equation with variable co-efficients using DTM

The Riccati equation with variable coefficients is given by

$$\frac{dy}{dx} = p(x) + q(x)y + r(x)y^2 \tag{5}$$

$$y(0) = g(x) \tag{6}$$

where $p(x), q(x), r(x)$ and $g(x)$ are functions of x.
Applying Differential Transform to equation(5), we get

$$DT[\tfrac{dy}{dx}] = DT[p(x) + q(x)y + r(x)y^2]$$

$$(k + 1)T(k + 1) = P(k) + \sum_{l=0}^{k}Q(l)T(k - l) + \sum_{m=0}^{k-s}R(s)Y(m)T(k - s - m) \tag{7}$$

where $P(x), Q(x), R(x)$ and $T(x)$ are the differential transforms of $p(x), q(x), r(x)$ and $y(x)$ respectively.

2.1.1 Problem 1

$p(x) = 3$, $q(x) = -3x^2$, $r(x) = -1$ and $g(x) = 1$

then the Riccati equation takes the form

$$\frac{dy}{dx} = 3 + 3x^2 y(x) - xy^2(x) \tag{8}$$

with initial condition $y(0) = 1$
Applying Differential Transform to (8) we get

$$DT[\frac{dy}{dx}] = DT[3 + 3x^2 y(x) - xy^2(x)] \tag{9}$$

$$DT[\frac{dy}{dx}] = DT[3] + 3DT[x^2 y(x)] + DT[xy^2(x)]$$

$$(k+1)T(k+1) = 3\delta(k) + 3\sum_{l=0}^{k}\delta(l-2)T(k-l) + \sum_{s=0}^{k}\sum_{m=0}^{k-s}\delta(s-1)T(m)T(k-s-m) \tag{10}$$

The inverse differential transform of $y(x)$ is

$$y(x) = \sum_{k=0}^{\infty} T(k)x^k \tag{11}$$

using the initial condition $y(0) = 1$ in equation (11), we get

$$T(0) = 1 \tag{12}$$

For $k = 0$ in equation (10), we get
$$T(1) = 3 \tag{13}$$

For $k = 1$ in equation (10), we get

$$2T(2) = \delta(1) + 3\delta(1) + 3\sum_{l=0}^{1}\delta(l-2)T(1-l) + \sum_{s=0}^{1}\sum_{m=0}^{1-s}\delta(s-1)T(m)T(1-s-m)$$

$$T(2) = -\frac{1}{2} \tag{14}$$

For $k = 2$ in equation (10), we get

$$3T(3) = 3\delta(2) + 3\sum_{l=0}^{2}\delta(l-2)T(2-l) + \sum_{s=0}^{2}\sum_{m=0}^{2-s}\delta(s-1)T(m)T(2-s-m)$$

$$T(3) = -1 \tag{15}$$

For $k = 3$ in equation (10), we get

$$4T(4) = 3\delta(3) + 3\sum_{l=0}^{3}\delta(l-2)T(3-l) + \sum_{s=0}^{3}\sum_{m=0}^{3-s}\delta(s-1)T(m)T(3-s-m)$$

For $k = 4$ in equation (10), we get

$$5T(5) = 3\delta(4) + 3\sum_{l=0}^{4} \delta(l-2)T(4-l) + \sum_{s=0}^{4}\sum_{m=0}^{4-s} \delta(s-1)T(m)T(4-s-m)$$

$$T(5) = \frac{7}{10} \tag{16}$$

similarly, for $k = 5$,6, 7, 8, 9, 10 ...,we get

$$T(6) = \tfrac{3}{8},\, T(7) = \tfrac{-9}{20},\, T(8) = \tfrac{-9}{20},\, T(9) = \tfrac{9}{20} \cdots$$

From equation (11), we get

$$y(x) = 1 + 3x - \frac{1}{2}x^2 - x^3 + \frac{1}{4}x^4 + \frac{7}{10}x^5 + \frac{3}{8}x^6 - \frac{9}{20}x^7 - \frac{9}{20}x^8 + \frac{133}{2520}x^9 + \frac{2099}{5600}x^{10} + - \cdots \tag{17}$$

2.2   General solution of Riccati's equation

Let W(x) be the dependent variable in equation (4) then

$$y(x) = \frac{W'(x)}{Q(x)W(x)} \tag{18}$$

differentiating equation (18) w.r.t x, we get

$$y'(x) = \frac{W''(x)}{Q(x)W(x)} - \frac{Q'(x)W'(x)}{Q^2(x)W(x)} - \frac{Q(x)W^2(x)}{Q^2(x)W^2(x)} \tag{19}$$

substituting equations (18) and (19) in equation (4),we get

$$W''(x) + \left[P(x) - \frac{Q'(x)}{q(x)} \right] W'(x) - R(x)q(x)W(x) = 0 \tag{20}$$

Thus we get a second order linear differential equation to be solved by a particular method and its general solution is given by

$$W(x) = c_1 W_1(x) + c_2 W_2(x) \tag{21}$$

where c_1 and c_2 are arbitrary constant to be determined.
Substituting equation (21) in equation (18), we get

$$y(x) = \frac{W_1'(x) + CW_2'(x)}{Q(x)\left[W_1(x) + CW_2(x)\right]}, C = \frac{c_2}{c_1} \tag{22}$$

consider the above example

$$\frac{dy}{dx} = 3 + 3x^2 y(x) - xy^2(x) \tag{23}$$

comparing equation (23) with equation (4), we get

$P(x) = 3,\, Q(x) = -3x^2,\, R(x) = -1$

Substituting these values in equation (18), we get

$$y(x) = \frac{W'(x)}{Q(x)W(x)} \tag{24}$$

$$y'(x) = \frac{W''(x)}{xW(x)} - \frac{W'(x)}{x^2 W(x)} - \frac{x(W')^2(x)}{x^2 W^2(x)} \tag{25}$$

using equation (24) and equation (25),equation (24) can be transformed into a second order linear differential equation of the form[10],

$$xW''(x) - (1 + 3x^3)W'(x) - 3x^2 W(x) = 0 \tag{26}$$

Applying Frobenious series solution method to equation (26), we get

$$W(x) = x^2 c_0 \{1 + \frac{4}{5}x^3 + \frac{1}{2}x^6 + \frac{8}{33}x^9 \ldots\} \tag{27}$$

and from equation (24), we get

$$Y(x) = 1 + \frac{\{2 + 4x^4 + 4x^7 + \frac{4}{3}x^9 + \ldots\}}{\{x^2 + \frac{4}{5}x^5 + \frac{1}{2}x^8 + \frac{8}{33}x^{11} \ldots\}} \tag{28}$$
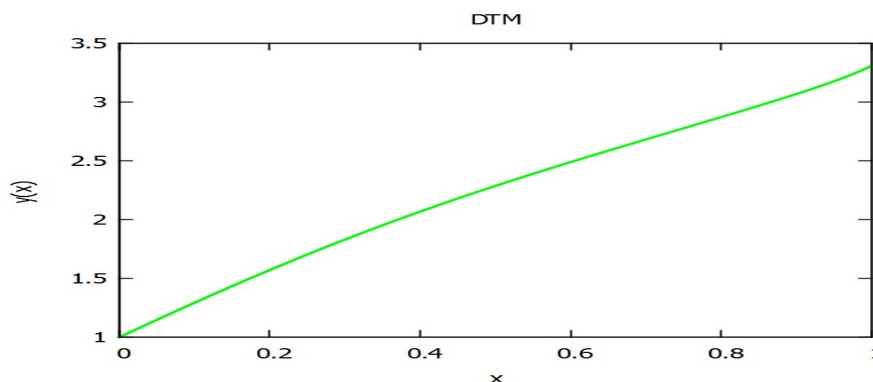
Figure 1: Graph plotted using Maxima
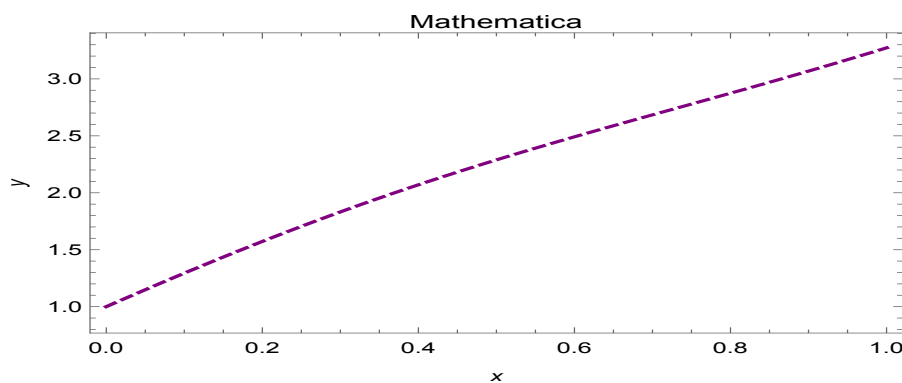
Figure 2: Graph plotted using Mathematica
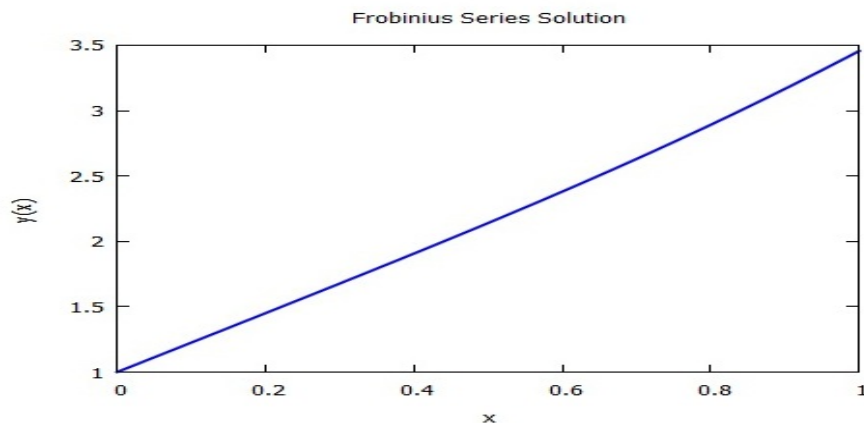
Figure 3: Graph plotted using Maxima

2.2.1 Problem 2

$p(x) = x^5 + 1$, $q(x) = -2x^4$, $r(x) = x^3$ and $g(x)$

then the Riccati equation takes the form

$$\frac{dy}{dx} = 1 + x^5 - 2x^4 y(x) + x^3 y^2(x) \tag{29}$$

with initial condition $y(0) = 0$
Applying Differential Transform to (29) we get

$$DT[\frac{dy}{dx}] = DT[1 + x^5 - 2x^4 y(x) + x^3 y^2(x)] \tag{30}$$

$$DT[\tfrac{dy}{dx}] = DT[1 + x^5] - 2DT[x^4 y(x)] + DT[x^3 y^2(x)]$$

$$(k+1)T(k+1) = \delta(k) + \delta(k-5) - 2\sum_{l=0}^{k}\delta(l-4)T(k-l) + \sum_{s=0}^{k}\sum_{m=0}^{k-s}\delta(s-3)T(m)T(k-s-m) \tag{31}$$

The inverse differential transform of y(x) is

$$y(x) = \sum_{k=0}^{\infty} T(k)x^k \tag{32}$$

using the initial condition $y(0) = 0$ in equation 32,we get

$$T(0) = 0 \tag{33}$$

For $k = 0$ in equation (31), we get

$$T(1) = 0 \tag{34}$$

For $k = 1$ in equation (31), we get

$$2T(2) = \delta(1) + \delta(1-5) - 2\sum_{l=0}^{1}\delta(l-4)T(1-l) + \sum_{s=0}^{1}\sum_{m=0}^{1-s}\delta(s-3)T(m)T(1-s-m) \tag{35}$$

$$T(2) = 0 \tag{35}$$

For k=2 in equation (31), we get

$$3T(3) = \delta(2) + \delta(2-5) - 2\sum_{l=0}^{2}\delta(l-4)T(2-l) + \sum_{s=0}^{2}\sum_{m=0}^{2-s}\delta(s-3)T(m)T(2-s-m)$$

$$T(3) = 0 \tag{36}$$

For k=3 in equation (31), we get

$$4T(4) = \delta(3) + \delta(3-5) - 2\sum_{l=0}^{3}\delta(l-4)T(3-l) + \sum_{s=0}^{3}\sum_{m=0}^{3-s}\delta(s-3)T(m)T(3-s-m)$$

$$T(4) = 0 \tag{37}$$

For k=4 in equation (31), we get

$$4T(4) = \delta(4) + \delta(4-5) - 2\sum_{l=0}^{4}\delta(l-4)T(4-l) + \sum_{s=0}^{4}\sum_{m=0}^{4-s}\delta(s-3)T(m)T(4-s-m)$$

$$T(4) = 0 \tag{38}$$

similarly, for $k = 5, 6, 7, 8, \ldots$, we get

$$T(5) = T(6) = T(7) = T(8) = T(9) = T(10) = \ldots = 0$$

From equation (32), we get

$$y(x) = x \tag{39}$$

comparing equation (23) with equation (4), we get

$$P(x) = -3x^2, Q(x) = -x^3, R(x) = 3$$

Substituting these values in equation (18), we get

$$y(x) = \frac{W'(x)}{Q(x)W(x)} \tag{40}$$

$$y'(x) = \frac{W''(x)}{xW(x)} - \frac{W'(x)}{x^2W(x)} - \frac{x(W')^2(x)}{x^2W^2(x)} \tag{41}$$

using equation (40) and equation (41), equation (40) can be transformed into a second order linear differential equation of the form,

$$xW''(x) + (2x^5 - 3)W'(x) - (x^4 + x^9)W(x) = 0 \tag{42}$$

Applying Frobenious series solution method [10] to equation (42), we get

$$W(x) = c_1\{x + \frac{1}{5}x^6 \ldots\} \tag{43}$$

and from equation (40), we get

$$Y(x) \approx x \tag{44}$$
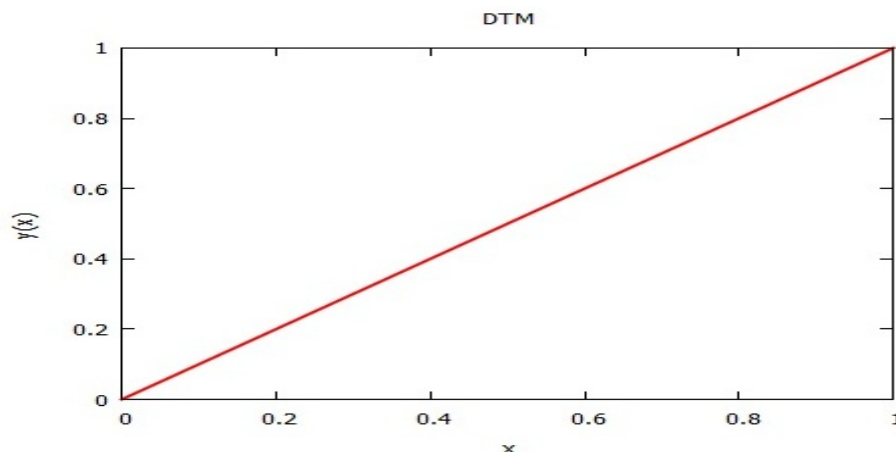
Figure 4: Graph plotted using Maxima
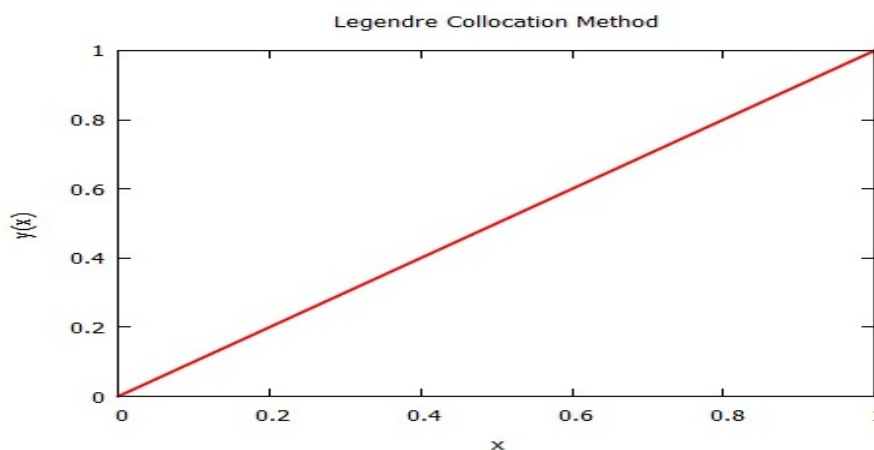
Figure 5: Graph plotted using Maxima

3   Differential Transform Method For Solving Partial Differential Equations

To solve Partial Differential Equation using DTM by a modified approach[6] we need to follow the following steps first consider a general form of nonlinear equation

$$P(u, u_t, u_x, u_{xx}, u_{xt}, u_{tt}, u_{xxx}, u_{xxt}, \ldots) = 0 \tag{45}$$

second,we introduce the wave variable

$$\zeta = \lambda(x - ct) \tag{46}$$

so that

$$u(x,t) = U(\zeta), \tag{47}$$

where $U(\zeta)$ is the localized wave function travels with speed c. Thus the PDE is converted into an ODE

$$P(U, c\lambda U^{'}, \lambda U^{'}, \lambda^2 U^{''}, c\lambda^2 U^{''}, \lambda^3 U^{'''}, c\lambda^3 U^{'''} \ldots) = 0. \tag{48}$$

Third, we apply DTM to equation (48), we get

$$U(\zeta) = \sum_{k=0}^{\infty} F(k)\alpha^k \tag{49}$$

where $F(\zeta)$ is the differential transform of $U(\zeta)$. finally, the approximate solution is

$$u_{appr}(x,t) = \sum_{k=0}^{N} F(k)(\lambda(x-ct))^k \tag{50}$$

3.1   Problem 1

Consider the nonlinear Partial Differential Equation

$$u_t = u_{xxt} - u_x - uu_x \tag{51}$$

subjected to the initial condition

$$u(x,0) = \frac{1}{\cosh^2(\frac{x}{4})} \tag{52}$$

Now using the wave variable $\zeta = \lambda(x-ct)$, ((51) and (52)) converted to the ODE

$$(1-c)U + c\lambda^2 U'' + \frac{1}{2}U^2 = 0 \tag{53}$$

subjected to the initial condition

$$U(0) = 1 \tag{54}$$

Applying the differential transform to (53) and (54), we get the following recursive formula

$$F(k+2) = \frac{1}{c\lambda^2(k+1)(k+2)}\left((c-1)F(k) - \frac{1}{2}\sum_{i=0}^{k}F(i)F(k-i)\right) \tag{55}$$

and

$$F(0) = U(0), \quad F(1) = U'(0) = a, \tag{56}$$

where a is a constant to be determined. Referring to equation (52), the approximate solution is

$$u_{appr}(x,t) = \sum_{k=0}^{8} F(k)(\lambda(x-ct))^k \tag{57}$$

Using the initial condition (52), and by Maxima software, we have

$$\begin{aligned}
u_{appr}(x,t) = {}& 1 + 0.0000492189(x - 1.33322t) - 0.062548(x - 1.33322t)^2 \\
& - 4.10262 * 10^{-6}(x - 1.33322t)^3 + 0.00260683(x - 1.33322t)^4 \\
& + 2.18047 * 10^{-7}(x - 1.33322t)^5 - 0.0000923655(x - 1.33322t)^6 \\
& - 9.47054 * 10^{-9}(x - 1.33322t)^7 + 3.00882 * 10^{-6}(x - 1.33322t)^8.
\end{aligned} \tag{58}$$

The exact solution is

$$u(x,t) = \frac{1}{\cosh^2(\frac{x}{4} - \frac{t}{3})} \tag{59}$$
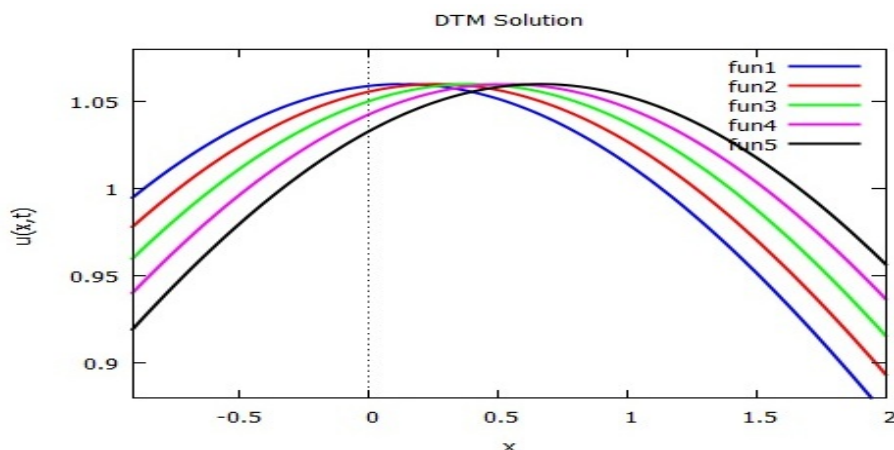
Figure 6: Graph plotted using Maxima
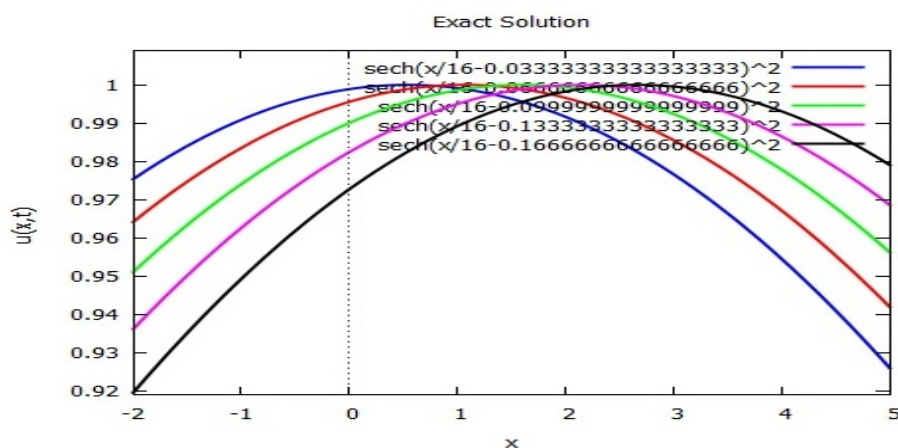
Figure 7: Graph plotted using Maxima

3.2   Problem 2

We consider the nonlinear PDE

$$u_t = u_{xx} - u^3 + u \tag{60}$$

subjected to the initial condition

$$u(x,0) = \frac{1}{1 + e^{\frac{x}{\sqrt{2}}}}, \tag{61}$$

Now using the wave variable $\zeta = \lambda(x - ct)$, (60) and (61) converted to the ODE

$$- c\lambda U' - \lambda^2 U'' + \frac{1}{2}U^3 - U = 0 \tag{62}$$

subjected to the initial condition

$$U(0) = 0.5 \tag{63}$$

Applying the differential transform to (62) and (63) , we get the following recursive formula

$$F(k+2) = -\frac{cF(k+1)}{\lambda(k+2)} - \frac{F(k)}{\lambda^2(k+1)(k+2)} + \frac{1}{\lambda^2(k+1)(k+2)} \sum_{i=0}^{k}\sum_{j=0}^{k-i} F(i)F(j)F(k-i-j)$$

$$\tag{64}$$

Referring (4), the approximate solution is

$$u_{appr}(x,t) = \sum_{k=0}^{8} F(k)(\lambda(x-ct))^k \tag{65}$$

Using the initial condition (61), and by Maxima software, we have

$$
\begin{aligned}
u_{appr}(x,t) = {} & 0.5 - 0.176469(x - 2.11966t) - 0.00047338(x - 2.11966t)^2 \\
& + 0.00768733(x - 2.11966t)^3 - 0.000171119(x - 2.11966t)^4 \\
& - 0.00028579(x - 2.11966t)^5 - 0.0000347312(x - 2.11966t)^6 \\
& + 0.0000312117(x - 2.11966t)^7 - 4.04237 * 10^{-6}(x - 2.11966t)^8.
\end{aligned}
\tag{66}
$$

The exact solution is

$$u(x,t) = \frac{1}{1 + e^{\frac{x}{\sqrt{2}} - \frac{3t}{2}}} \tag{67}$$
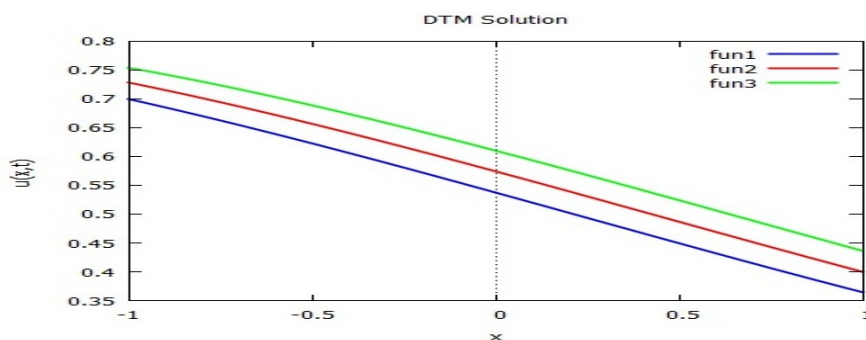
Figure 8: Graph plotted using Maxima
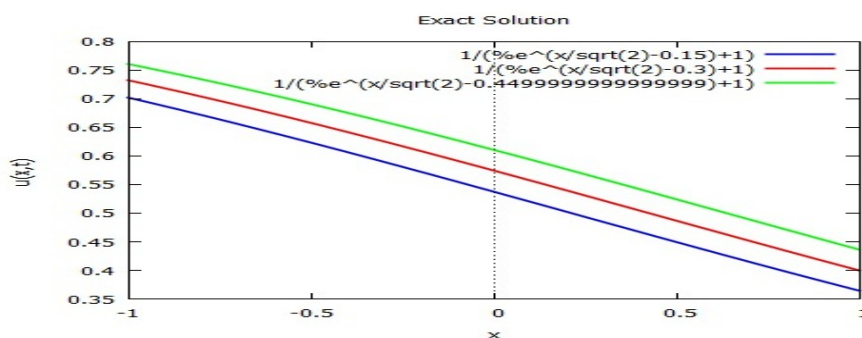
Figure 9: Graph plotted using Maxima

4   Reduced Differential Transform Method

One of the most important partial differential equations occurring in Applied Mathematics is the Klein Gordon equation[6]. It plays an important role in plasma physics, fluid dynamics and chemical kinematics.

$$u_{tt} - u_{xx} + u + Nu(x,t) = f(x,t) \tag{68}$$

subject to the initial conditions

$$u(x,0) = g(x), \quad u_t(x,0) = h(x) \tag{69}$$

4.1   Illustration of solution of Klein Gordon equation using Reduced Differential Transform Method

Consider the nonlinear Klein Gordon equation

$$u_{tt} - u_{xx} + \frac{3}{4}u - \frac{3}{2}u^3 = 0 \tag{70}$$

with initial conditions

$$u(x,0) = -sech(x) \quad u_t(x,0) = \frac{1}{2}sech(x)tanh(x) \tag{71}$$

The exact solution of equation (70) and (71) is

$$u(x,t) = -sech(x + \frac{t}{2}) \tag{72}$$

hence the transformed equation of (70)

$$\frac{(k+2)!}{k!}U_{k+2}(x) = \frac{\partial^2}{\partial x^2}U_k(x) - \frac{3}{4}U_k(x) + N_k(x) \tag{73}$$

where, $N_k(x)$ is the transformed form of $\frac{3}{2}u^3$ and the transformed initial conditions are

$$U_0(x) = -sech(x) \quad U_1(x) = \frac{1}{2}sech(x)tanh(x) \tag{74}$$

substituting (74) successively into (73) we obtain $U_k(x)$ values respectively. the $\{U_k(x)\}_{k=0}^3$ gives three term approximate solution of the problem given by

$$u(x,t) = t^3((sech(x)tanh(x)^3)/12 - (5sech(x)^3tanh(x))/12 + (sech(x)^2tanh(x))/2$$

$$+(sech(x)^2tanh(x))/2 - (sech(x)tanh(x))/16)$$
$$+t^2(-(sech(x)tanh(x)^2)/2 + sech(x)^3/2 - (3sech(x)^2)/4$$
$$+ (3sech(x))/8) + (tsech(x)tanh(x))/2 - sech(x) \tag{75}$$
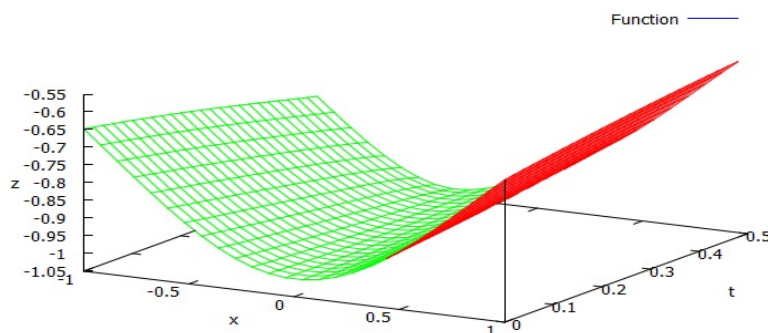
Figure 10: DTM solution plotted using Maxima
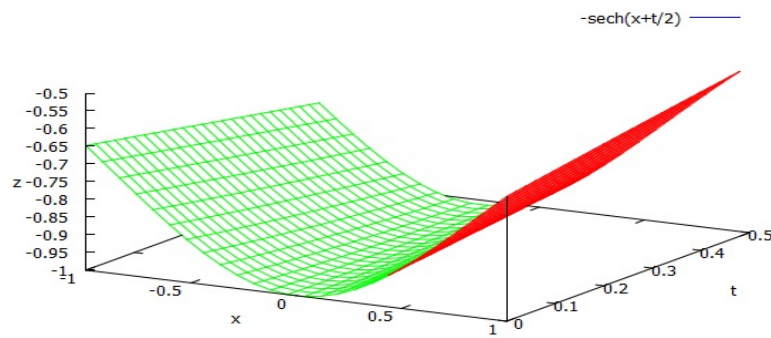
Figure 11: Exact solution plotted using Maxima
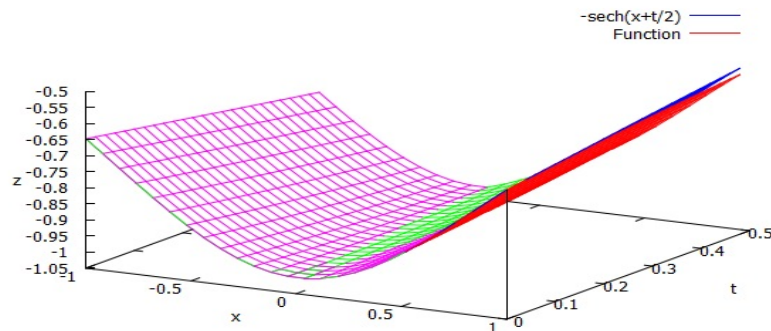
Figure 12: DTM and Exact plotted using Maxima

References

[1] W.T. Reid, *Riccati differential equations Mathematics in science and engineering*, New York: Academic Press, 1972.

[2] M.D. Raisinghania, *Advanced Differential Equations*, S. Chand and Company.

[3] Lasiecka, R. Triggiani, *Differential and algebraic Riccati equations with application to boundary/point control problems: Continuous theory and approximation theory*, Springer, 1991.

[4] S. Mukherjee, B. Roy, *Solution of Reccati equation with variable coefficient by differential transform method*, Int. J. Nonlin. Sci. (2012) 1749-3897.

[5] Y. Keskin, S. Servi, G. Oturan, *Reduced differential transform method for solving Klein Gordon equations*, Proc. World Cong. Eng. 1 (2011).

[6] M.T. Alquran, *Applying differential transform method to nonlinear partial differential equations: A modified approach*, Appl. Appl. Math. (2012) 1932-9466.

[7] J.K. Zhou, *Differential transforms and its application in electrical circuits*, Huazhong University Press, Wuhan, China, 1986.

[8] H.T. Davis, *Introduction to nonlinear differential and integral equations*, Dover, 1960.

[9] B.D. Anderson, J.B. Moore, *Optimal control-linear quadratic methods*, Prentice-Hall, New Jersey, 1999.

[10] B. Batiha, M.S.M. Noorani, I. Hashim, *Application of variation iteration method to a general Riccati equation*, Int. Math. Forum 2(56) (2007) 2759-2770.

The Method of Multiple Scales for uniformly Valid Approximation of Aperiodical Variations

B.R. Chandrika[1], H.V. Gangamani[2] and L.N. Achala[3]

[1,2,3]P. G. Department of Mathematics and Research Centre in Applied Mathematics

M. E. S. College of Arts, Commerce and Science

15th cross, Malleswaram, Bangalore - 560003.

Email ID: [1]chandrika.raju74@gmail.com, [2]gangahv@gmail.com, [3]anargund1960@gmail.com

Abstract: The method of multiple scales is significant in a variety of situations for extracting the slow time dependence of patterns. This method comprises techniques used to construct uniformly valid approximations to the solutions of perturbation problems in which the solutions depend simultaneously on widely different scale. In this report we have used classical example of linear damped oscillator since Multiple Scale method obtains solutions that evolve aperiodical on a slow-time scale is more general method involving two form of the solution.Here we have used two-time scale and derivative expansions. We have used derivative expansion method for the Duffing equation and also to the Ricatti's equation by illustrating the solutions using graphs.

Keywords: Multiple scale, Aperiodical, Two-time scale, Derivative expansion, Duffing equation, Ricatti's equation.

1   Introduction

Some natural process have more than one characteristic length or time scales associated with them, for example turbulent flows where perturbation expansion fails to recognize non-uniformity in the space/time scales [1]. Multiple-scale analysis is a global perturbation scheme that is useful in a system characterized by disparate time scales, such as weak dissipation in an oscillator. This effect could be insignificant on short time scales but it becomes important on long time scales. Classical perturbation methods generally break down because of resonances that lead to what are called as secular terms.The method of multiple scales comprises the techniques that are used to construct uniformly valid approximations to the solutions of perturbation problems [5]. In this the solution depends simultaneously on widely different scales. This is done by introducing fast-scale and slow-scale variables for an independent variable and subsequently treating these variables (fast and slow) as if they are independent. Let's begin by describing the exact solution and straight-forward expansion method for the linear damped oscillator.

1.1   The Linear Damped Oscillator

Consider the differential equation for the linear damped mass-spring system with no external forces. The equation for displacement $y(\tau)$ is [1]

$$my'' + cy' + ky = 0 \tag{1}$$

Where 'Prime' denotes the differentiation with respect to τ. If initially the mass is released from a positive displacement y_i with no initial velocity, we have the following initial conditions:

$$y(0) = y_i, \quad y'(0) = 0 \tag{2}$$

Assume here that $c \ll m, k$. Choosing y_i and $\sqrt{\frac{m}{k}}$ as the characteristic distance and characteristic time respectively, we define the following dimensionless variables.

$$x = \frac{y_i}{y} \quad t = \frac{\tau}{\sqrt{\frac{m}{k}}}$$

Under this change of variables the dimensionless form of the differential equations (1) and (2) becomes,

$$x'' + 2\varepsilon x' + x = 0 \tag{3}$$

$$x(0) = 1, \quad x'(0) = 0 \tag{4}$$

Where,

$$\varepsilon = \frac{c}{2*\sqrt{mk}} \ll 1$$

ε is a dimensionless parameter. The above equation is a linear oscillator with weak damping, where time variable has been scaled by the period of the undamped system. This is the classical example used to illustrate the method of multiple scales.

The exact solution of system equation (2) is given by

$$m^2 + 2\varepsilon m + 1 = 0$$

$$x(t) = e^{-\varepsilon t}\left[\cos\sqrt{1-\varepsilon^2}t + \frac{\varepsilon}{\sqrt{1-\varepsilon^2}}\sin\sqrt{1-\varepsilon^2}t\right] \tag{5}$$

If oscillation is undamped i.e., if $\varepsilon = 0$

$$x(t) = \cos t$$

Where both amplitude and phase of the oscillation remain constant. Equation (5) shows the change in time in both amplitude and phase with the presence of damping. The drift of the amplitude with respect to time scale is ε^{-1} and the drift of the phase with respect to time scale is ε^{-2}. Both amplitude and phase with respect to time scale are longer for the basic oscillation (5) does not have much amplitude left with respect to time as the phase as slipped. From equation (5) we can write

$$x = \cos t + O(1/\varepsilon) \quad where \quad t = O(1) \tag{6}$$

Above equation is true, but is not valid for $t = O(1/\varepsilon)$. The equation is not valid to

$$x = e^{-\varepsilon t}\cos t + O(\varepsilon) \quad where \quad t = O(1/\varepsilon) \tag{7}$$

If we consider the values of t which are $O(1/\varepsilon)$ then equation (7) is not valid. The terms of the $\varepsilon^2 t$ must be preserved in the cosine function of equation (5).
Using binomial expansion , we have

$$\sqrt{1-\varepsilon^2} = 1 - \frac{\varepsilon^2}{2} - \frac{\varepsilon^4}{8} - \frac{\varepsilon^6}{16} - \cdots \tag{8}$$

thus

$$x = e^{-\varepsilon t}\cos(1 - \frac{\varepsilon^2}{2})t + O(\varepsilon) \quad where \quad t = O(1/\varepsilon^2) \tag{9}$$

Equation (9) is uniformly valid for $t = O(1/\varepsilon^2)$.

Consider only the uniformly valid leading order expansion then the second term of equation (5) never contributes to $O(\varepsilon)$ for all t.

By straight forward expansion of equation (3) to two-term approximate solution takes the form

$$x(t) = \cos t + \varepsilon(\sin t - t\cos t) \tag{10}$$

2   The Method of Multiple Scales

Any asymptotic expansion of equation (5) must simultaneously depict both the decaying and oscillatory behaviours of the solution in order to be uniformly valid solution in order to be uniformly valid in $t = O(1/\varepsilon^k)$. Here the Poincare-Lindstedt method fails in this case. The Poincare-Lindstedt method is used to construct asymptotic approximation of periodic solutions, but it can't be used to obtain the solutions of a nonperodical, on a slow time scale. The method of multiple scales is a more general approach that involve two key tricks. The first is the idea of introducing scaled space and time coordinates to capture the slow modulation of the pattern, and treating these as separate variables in addition to the original variables that must be retained to describe the pattern state itself. This is essentially the idea of multiple scales [1]. The second is the use of what are known as solvability conditions in the formal derivation. From analytical solution (10) the functional dependence of x on t and ε is not disjoint because x depends on the combination of εt as well as on the t and ε.

Thus in place of $x = x(t; \epsilon)$, we write

$$x = \widehat{x}(t, \varepsilon t; \varepsilon)$$

We will return to the regular expansion equation (10) and rewriting it as

$$x(t) = \cos t + \varepsilon\sin t - \varepsilon t\cos t \tag{11}$$

As in the case of analytical solution, regular expansion shows that x depends on the combination of εt as well as on the individual t and ε. The trouble with the simple regular expansion is that the small damping changes both the amplitude of the oscillation on a time scale ε^{-1} and the phase of the oscillation on a time scale ε^{-2} by the slope accumulation of small effects. Thus the oscillator has three processes acting on their time scales. First, there is an basic oscillation on the time scale of 1 from the inertia causing the restoring force to over shoot the equilibrium position. Then there is a small drift in the amplitude on the time scale of ε^{-1} and finally a small drift in the amplitude on the time scale of ε^{-2} due to the small friction. We recognize these three time scales by introducing three time variables.

$$T_0 = t \text{ the fast time of the oscillation}$$
$$T_1 = \varepsilon t \text{ the slower time of the amplitude drift}$$
$$T_2 = \varepsilon^2 t \text{ even slower time of the phase drift}$$

The functions of T_0 that are combined into factors due to rapidly changing features, while the functions of T_1 and T_2 are combined into factors due to slowly changing features. Thus we have a solution of the form

$$x(t;\varepsilon) = x(T_0, T_1, T_2; \varepsilon)$$

In general, if we choose n time scales for the expansion, we have a solution of the form

$$x(t;\varepsilon) = x(T_0, T_1, T_2, \cdots, T_n; \varepsilon) \tag{12}$$

where the time scales are defined as $T_0 = t, T_1 = \varepsilon t, T_2 = \varepsilon^2 t, \cdots, T_n = \varepsilon^n t$ Thus, instead of determining x as a function of t, we determine x as a function of $T_0, T_1, \cdots, T_n$.

From the above time scale we understand that as real time t increases the fast time T_0 increases at the same rate, while the slower time T_i's increase slowly. Using the chain rule we have

$$\frac{d}{dt} = \frac{\partial}{\partial T_0}\frac{\partial T_0}{\partial t} + \frac{\partial}{\partial T_1}\frac{\partial T_1}{\partial t} + \frac{\partial}{\partial T_2}\frac{\partial T_2}{\partial t} + \cdots \tag{13}$$

$$\frac{d}{dt} = \frac{\partial}{\partial T_0} + \varepsilon\frac{\partial}{\partial T_1} + \varepsilon^2\frac{\partial}{\partial T_2} + \cdots \tag{14}$$

$$\frac{d^2}{dt^2} = \frac{\partial^2}{\partial T_0^2} + 2\varepsilon\frac{\partial^2}{\partial T_1 \partial T_0} + \varepsilon^2\left(\frac{\partial^2}{\partial T_0 \partial T_2} + \frac{\partial^2}{\partial T_1^2}\right) + \cdots \tag{15}$$

Hence (1) becomes

$$\frac{\partial^2 x}{\partial T_0^2} + 2\varepsilon\frac{\partial^2 x}{\partial T_0 \partial T_1} + \varepsilon^2\left(\frac{\partial^2 x}{\partial T_0 \partial T_2} + \frac{\partial^2 x}{\partial T_1^2}\right) + 2\varepsilon\left(\frac{\partial x}{\partial T_0} + \varepsilon\frac{\partial x}{\partial T_1} + \varepsilon^2\frac{\partial x}{\partial T_2}\right) + x + \cdots = 0 \tag{16}$$

$$x = 1 \quad, \frac{\partial x}{\partial T_0} + \varepsilon\frac{\partial x}{\partial T_1} + \varepsilon^2\frac{\partial x}{\partial T_2} + \cdots = 0 \quad for \quad T_0 = T_1 = \cdots = 0 \tag{17}$$

When $t = 0$, all $T_0, T_1, \cdots$ are zero. The benefits of introducing the multiple time variables are not yet apparent. In fact, it appears that we have made the problem harder since the original ordinary differential equation has been turned into a partial differential equation. Above said statement is true, with the experience of this method it has shown that the disadvantages of including this complications does not hold any advantages.

From pointing out to solution of equation (16) it is evident that it is not unique and that we also need to impose more conditions for uniqueness on the solution. This freedom will enable us to prevent secular terms from appearing in the expansion (at least over the time scales we are using). We now seek an asymptotic approximation for x of the form,

$$x(t) \equiv x(T_0, T_1, T_2, \cdots, T_n; \varepsilon) \sim x_0(T_0, T_1, T_2, \cdots, T_n)$$
$$+ \varepsilon x_1(T_0, T_1, T_2, \cdots, T_n) + \varepsilon^2 x_2(T_0, T_1, T_2, \cdots, T_n) \tag{18}$$

So it is understood that there are only two independent variables, t and ε, in equation (16); Since T_i's are functions of these two, and it is not independent. The principal steps in finding the coefficients x_n are carried out as though $T_0, T_1, \cdots, Tn$ and ε were independent variables. This is one of the reason why these steps cannot be justified rigorously in advance, but are merely heuristic. It must be marked that equation (16) is a generalized asymptotic expansion, since equation (18) enters both the gauges (which are just the powers of equation (18) and also through the coefficients x_n by way of T_i. Also there is no general theorem allowing the differentiation of a generalized asymptotic expansion term by term, it is nevertheless reasonable to construct the coefficients of equation (16) on the assumption that such differentiation is possible, and then to justify the resulting series by direct error estimation afterwards.

3   Description of the Method

There are three variants of the method of multiple scales. We describe them by discussing the linear damped oscillator.

$$x'' + x = -2\varepsilon x' \tag{19}$$

We choose this example because its exact solution is available for comparison with the approximate solution obtained. Because we will be able to display the different variants of the method more clearly without involving ourselves in algebra.

Let us assume a straight forward asymptotic expansion for small ε.

$$x = x_0 + \varepsilon x_1 + \varepsilon^2 x_2 + \dots \tag{20}$$

Substituting equation (2) in (1) and equating coefficients of equal powers of ε to zero lead to

$$x_0'' + x_0 = 0 \tag{21}$$

$$x_1'' + x_1 = -2x_0' \tag{22}$$

$$x_2'' + x_2 = -2x_1' \tag{23}$$

The general solution of equation (3) is

$$x_0 = a\cos(t + \phi) \tag{24}$$

Where a and ϕ are arbitrary constants. Substituting for x_0 into equation (4) and solving the resulting equation, we obtain

$$x_1 = -at\cos(t + \phi) \tag{25}$$

Substituting for x_1 in equation (5) and solving for x_2, we obtain

$$x_2 = \frac{1}{2}at^2\cos(t + \phi) + \frac{1}{2}at\sin(t + \phi) \tag{26}$$

hence, we obtain

$$x = a\cos(t + \phi) - \varepsilon at\cos(t + \phi) + \frac{1}{2}\varepsilon a[t^2\cos(t + \phi) + t\sin(t + \phi)] + O(\varepsilon^3) \tag{27}$$

Substituting equation (12) and (15) into equation (1) and equating the coefficients of equal powers of ε , we have

$$\frac{\partial^2 x_0}{\partial T_0^2} + x_0 = 0 \tag{28}$$

$$\frac{\partial^2 x_1}{\partial T_0^2} + x_1 = -2\frac{\partial x_0}{\partial T_0} - 2\frac{\partial^2 x_0}{\partial T_0 \partial T_1} \tag{29}$$

$$\frac{\partial^2 x_2}{\partial T_0^2} + x_2 = -2\frac{\partial x_1}{\partial T_0} - 2\frac{\partial^2 x_1}{\partial T_0 \partial T_1} - \frac{\partial^2 x_0}{\partial T_1^2} - 2\frac{\partial^2 x_0}{\partial T_0 \partial T_2} - 2\frac{\partial x_0}{\partial T_1} \tag{30}$$

The general solution of equation (28) is

$$x_0 = A_0(T_1, T_2)e^{iT_0} + \overline{A_0}(T_1, T_2)e^{-iT_0} \tag{31}$$

where $\bar{A}_0$ is the complex conjugate of A_0.

This solution is simply equivalent to equation (6) where a and ϕ are taken to be the functions of the slow time scales T_1 and T_2 rather than being constants.

substituting for x_0 from equation (31) into (29). we get,

$$\frac{\partial^2 x_1}{\partial T_0^2} + x_1 = -2i\left(A_0 + \frac{\partial A_0}{\partial T_1}\right)e^{iT_0} + 2i\left(\overline{A_0} + \frac{\partial \overline{A_0}}{\partial T_1}\right)e^{-iT_0} \tag{32}$$

The general solution of equation (32) is

$$x_1 = A_1(T_1, T_2)e^{iT_0} + \overline{A_1}(T_1, T_2)e^{-iT_0} - \left(A_0 + \frac{\partial A_0}{\partial T_1}\right)e^{iT_0} - \left(\overline{A_0} + \frac{\partial \overline{A_0}}{\partial T_1}\right)e^{-iT_0} \tag{33}$$

Comparing equation (33) with (31) shows that εx_1 is a small correction to x only when $\varepsilon T_0 = \varepsilon t$ is small. In order to obtain an expansion valid for times as large as $O(\varepsilon^{-1})$, the secular terms, $T_0 exp(\pm iT_0)$ in equation (33) must vanish ; i.e.,

$$A_0 + \frac{\partial A_0}{\partial T_1} = 0 \tag{34}$$

By integrating, we get

$$A_0 = a_0(T_2)e^{-T_1} \tag{35}$$

Then equation (33) becomes

$$x_1 = A_1(T_1, T_2)e^{iT_0} + \overline{A_1}(T_1, T_2)e^{-iT_0} \tag{36}$$

Using x_0 and x_1 in equation (30), we obtain

$$\frac{\partial^2 x_2}{\partial T_0^2} + x_2 = -Q(T_1, T_2)e^{iT_0} + \overline{Q_1}(T_1, T_2)e^{-iT_0} \tag{37}$$

where

$$Q(T_1, T_2) = 2iA_1 + 2i\frac{\partial A_1}{\partial T_1} - a_0 e^{-T_1} + 2i\frac{\partial a_0}{\partial T_2}e^{-T_1} \tag{38}$$

The terms on the RHS of equation (30) produce secular terms because the particular solution is

$$PI = \frac{-Q(T_1, T_2)e^{iT_0} + \overline{Q_1}(T_1, T_2)e^{-iT_0}}{D^2 + 1}$$

$$x_2 = \frac{1}{2}iQ(T_1, T_2)T_0 e^{iT_0} - \frac{1}{2}i\overline{Q_1}(T_1, T_2)T_0 e^{-iT_0} \tag{39}$$

These secular terms makes $\varepsilon^2 x_2$ the same order as εx_1 when t is as large as $O(\varepsilon^{-1})$. In order to eliminate these secular terms, Q must vanish; that is

$$A_1 + \frac{\partial A_1}{\partial T_1} = \frac{1}{2}i\left(-a_0 + 2i\frac{\partial a_0}{\partial T_2}\right)e^{-T_1} \tag{40}$$

In general, one does not need to solve for x_2 in order to arrive at equation (40). One needs only to inspect equation (36) and eliminate terms that produce secular terms.

The general solution of equation (40) is

$$A_1 = \left[a_1(T_2) + \frac{1}{2}i\left(-a_0 + 2i\frac{\partial a_0}{\partial T_2}\right)T_1\right]e^{-T_1} \tag{41}$$

Substituting for A_1 into equation (35), we obtain

$$x_1 = \left[a_1(T_2) + \frac{1}{2}i\left(-a_0 + 2i\frac{\partial a_0}{\partial T_2}\right)T_1\right]e^{-T_1}e^{iT_0} + CC \tag{42}$$

where CC is a complex conjugate of the preceding expression. However

$$x_0 = [a_0 e^{iT_0} + \overline{a_0}e^{-iT_0}]e^{-T_1} \tag{43}$$

Therefore, as $T_1 \longrightarrow \infty$, although $x_0 \quad and \quad x_1 \longrightarrow 0, \varepsilon x_1$ becomes $O(x_0)$ as t increases to $O(\varepsilon^{-2})$. Thus the expansion $x_0 + \varepsilon x_1$ breaks down for t as large as $O(\varepsilon^{-2})$ unless the coefficients of T_1 in the brackets in equation (42) vanish ; that is, unless

$$-a_0 + 2i\frac{\partial a_0}{\partial T_2} = 0 \tag{44}$$

by integrating, we get

$$a_0 = a_{00}e^{-iT_2/2} \tag{45}$$

where a_{00} is constant. Then equation (41) becomes

$$A_1 = a_1(T_2)e^{-T_1} \tag{46}$$

Therefore

$$x = e^{-T_1}a_{00}e^{i(T_0 - T_2/2)} + \overline{a_{00}}e^{-i(T_0 - T_2/2)} + \varepsilon[a_1(T_2)e^{iT_0} + \overline{a_1}(T_2)e^{-iT_0}] + O(\varepsilon^2) \tag{47}$$

The function $a_1(T_2)$ can be determined by carrying out the expansion to third order

$$a_1(T_2) = a_{11}e^{-iT_2/2} \tag{48}$$

where a_{11} is a constant.

Replace T_n by $\varepsilon^n t$ and put $a_{00} = \frac{a}{2}e^{i\phi}$ in equation (47). We get

$$x = e^{-\varepsilon t}\left\{\frac{a}{2}e^{i\phi}e^{i(t-\varepsilon^2 t/2)} + \frac{a}{2}e^{i\phi}e^{-i(t-\varepsilon^2 t/2)} + \varepsilon[a_1(\varepsilon^2 t)e^{it} + \overline{a_1}(\varepsilon^2 t)e^{-it}]\right\} + O(\varepsilon^2)$$

$$x = e^{-\varepsilon t}\frac{a}{2}\left\{e^{i(t-\varepsilon^2 t/2+\phi)} + e^{-i(t-\varepsilon^2 t/2+\phi)}\right\} + e^{-\varepsilon t}\varepsilon[a_1(\varepsilon^2 t)e^{it} + \overline{a_1}(\varepsilon^2 t)e^{-it}] + O(\varepsilon^2)$$

$$x = e^{-\varepsilon t}a\cos(t - \varepsilon^2 t/2 + \phi) + R \tag{49}$$

For linear equations such as equation (1), we may introduce the different time scales without expanding x. Thus using equation (1) in (15), we obtain

$$\left[\frac{\partial^2}{\partial T_0^2} + 2\varepsilon\frac{\partial^2}{\partial T_0 \partial T_1} + \varepsilon^2\left(\frac{\partial^2}{\partial T_1^2} + 2\frac{\partial^2}{\partial T_0 \partial T_2}\right) + \cdots\right]x + x$$

$$= -2\varepsilon \left(\frac{\partial}{\partial T_0} + \varepsilon \frac{\partial}{\partial T_1} + \varepsilon^2 \frac{\partial}{\partial T_2} + \cdots \right) x \tag{50}$$

Equating the coefficients of like powers of ε to zero yields

$$\frac{\partial^2 x}{\partial T_0^2} + x = 0 \tag{51}$$

$$2\frac{\partial^2 x}{\partial T_0 \partial T_1} = -2\frac{\partial x}{\partial T_0} \tag{52}$$

$$\frac{\partial^2 x}{\partial T_1^2} + 2\frac{\partial^2 x}{\partial T_0 \partial T_2} = -2\frac{\partial x}{\partial T_1} \tag{53}$$

The general solution of equation (51) is

$$x = A(T_1, T_2)e^{iT_0} + \overline{A}(T_1, T_2)e^{-iT_0} \tag{54}$$

Substituting into equation (51), we obtain

$$\left(\frac{\partial A}{\partial T_1} + A \right) e^{iT_0} - \left(\frac{\partial \overline{A}}{\partial T_1} + \overline{A} \right) e^{-iT_0} = 0 \tag{55}$$

Since equation (55) is valid for all T_0, the coefficients of $exp(iT_0)$ and $exp(-iT_0)$ must vanish ; that is

$$\frac{\partial A}{\partial T_1} + A = 0 \tag{56}$$

By integrating,we get

$$A = a(T_2)e^{-T_1} \tag{57}$$

Substituting equation (54) into (53) yields

$$\left(\frac{\partial^2 A}{\partial T_1^2} + 2i\frac{\partial A}{\partial T_2} + 2\frac{\partial A}{\partial T_1} \right) e^{iT_0} + CC = 0 \tag{58}$$

Thus

$$\frac{\partial^2 A}{\partial T_1^2} + 2i\frac{\partial A}{\partial T_2} + 2\frac{\partial A}{\partial T_1} = 0 \tag{59}$$

Substituting for A from equation (57) into (59) gives

$$2i\frac{\partial a}{\partial T_2} - a = 0 \tag{60}$$

Hence

$$a = a_0 e^{-iT_2/2} \tag{61}$$

where a_0 is a constant.
Therefore equation (54) becomes

$$x = a_0 e^{-T_1} e^{i(T_0 - T_2/2)} + CC \tag{62}$$

Expressing equation (62) in terms of t yields

$$x = ae^{-\varepsilon t} \cos(t - \varepsilon^2 t/2 + \phi) \tag{63}$$

Equation (63) refers to the solution of (49) given in (1).

4 Application of the Derivative-Expansion Method

The Derivative Expansion Method is a more general approach to solve a differential equation. It constructs uniformly valid approximations to the solutions of perturbation problems in which the solutions depend simultaneously on widely different scales.

5 The Duffing Equation

The second example to which we apply the derivative-expansion method is the Duffing equation

$$\frac{\partial^2 u}{\partial t^2} + \omega_0^2 u + \varepsilon u^2 = 0 \tag{64}$$

We assume that

$$u = \sum_{n=0}^{2} \varepsilon^n u_n(T_0, T_1, T_2) + O(\varepsilon^3) \tag{65}$$

Then

$$\frac{d}{dt} = D_0 + \varepsilon D_1 + \varepsilon^2 D_2 + \cdots + D_n = \frac{\partial}{\partial T_n} \tag{66}$$

Substituting equation (65) and (66) into (64) and equating coefficients of each power of ε to zero, we have

$$D_0^2 u_0 + \omega_0^2 u_0 = 0 \tag{67}$$

$$D_0^2 u_1 + \omega_0^2 u_1 = -2D_0 D_1 u_0 - u_0^2 \tag{68}$$

$$D_0^2 u_2 + \omega_0^2 u_2 = -2D_0 D_1 u_1 - 2D_0 D_2 u_0 - D_1^2 - 3u_0^2 u_1 \tag{69}$$

The solution of (65) is

$$u_0 = A(T_1, T_2)e^{i\omega_0 T_0} + \overline{A}(T_1, T_2)e^{-i\omega_0 T_0} \tag{70}$$

Equation (68) then becomes

$$D_0^2 u_1 + \omega_0^2 u_1 = -[2i\omega_0 D_1 A + 3A^2\overline{A}]e^{i\omega_0 T_0} - A^3 e^{3i\omega_0 T_0} + CC \tag{71}$$

In order that u_1/u_0 be bounded for all T_0, terms that produce secular terms must be eliminated Hence

$$2i\omega_0 D_1 A + 3A^2\overline{A} = 0 \tag{72}$$

$$D^2 u_1 + \omega_0^2 u_1 = -A^3 e^{3i\omega_0 T_0} + CC$$

and the solution for u_1 becomes

$$u_1 = B(T_1, T_2)e^{i\omega_0 T_0} + \frac{A^3}{8\omega_0^2} e^{3i\omega_0 T_0} + CC \tag{73}$$

To solve (72), we let $A = \frac{1}{2}ae^{i\phi}$ with real a and ϕ

$$\frac{\partial a}{\partial T_1} = 0 \quad , -\omega_0 \frac{\partial \phi}{\partial T_1} + \frac{3}{8}a^2 = 0 \tag{74}$$

By integrating, we get

$$u = a(T_2) \quad , \phi = \frac{3}{8\omega_0^2}a^2T_1 + \phi_0(T_2) \tag{75}$$

substituting u_0 and u_1 into equation (69)

$$D_0^2 u_2 + \omega_0^2 u_2 = -\frac{3}{8\omega_0^2}A^5 e^{5i\omega_0 T_0} + \left[\frac{-3i}{4\omega_0}D_1 A^3 - 3A^2 B - \frac{3}{4\omega_0^2}A^4\overline{A}\right]e^{3i\omega_0 T_0}$$
$$- \left[2D_1 i\omega_0 B + 2D_2 A i\omega_0 + 3D_1^2 A + 3A^2\overline{B} + 6A\overline{A}B + \frac{3}{8\omega_0^2}\overline{A}^2 A^3\right]e^{i\omega_0 T_0} + CC \tag{76}$$

$$D_0^2 u_2 + \omega_0^2 u_2 = -\frac{3}{8\omega_0^2}A^5 e^{5i\omega_0 T_0} + \left[\frac{-3i}{4\omega_0}D_1 A^3 - 3A^2 B - \frac{3}{4\omega_0^2}A^4\overline{A}\right]e^{3i\omega_0 T_0}$$
$$- Q(T_1, T_2)e^{i\omega_0 T_0} + CC \tag{77}$$

where,

$$Q(T_1, T_2) = 2D_1 i\omega_0 B + 2D_2 A i\omega_0 + 3D_1^2 A + 3A^2\overline{B} + 6A\overline{A}B + \frac{3}{8\omega_0^2}\overline{A}^2 A^3 \tag{78}$$

Secular terms are eliminated if

$$B = 0 \tag{79}$$

and

$$2i\omega_0 D_2 A = -\frac{3}{8\omega_0^2}\overline{A}^2 A^3 \tag{80}$$

With $Q = 0$, the solution of u_2, disregarding the homogeneous solution, is

$$u_2 = \frac{1}{64\omega_0^4}A^5 e^{5i\omega_0 T_0} + \frac{3}{32\omega_0^4}A^4\overline{A}e^{3i\omega_0 T_0} - \frac{3i}{32\omega_0^3}A^3 D_1 e^{3i\omega_0 T_0} + CC \tag{81}$$

Put $A = \frac{1}{2}ae^{i\phi}$ in equation (80) and separating real and imaginary parts, we get

$$\frac{\partial a}{\partial T_2} = 0 \quad , -\omega_0\frac{\partial \phi}{\partial T_2} = \frac{3}{256\omega_0^2}a^4 \tag{82}$$

By integrating we get,

$$\phi_0 = \frac{3}{256\omega_0^3}a^4 T_2 + \chi \tag{83}$$

where χ is constant

$$\phi = \frac{3}{8\omega_0}a^2 T_1 + \frac{3}{256\omega_0^3}a^4 T_2 + \chi \tag{84}$$

Substituting for u_0, u_1, u_2 into equation (65).keeping $A = \frac{1}{2}ae^{i\phi}$ and expressing the result in

terms of t

$$u = Ae^{i\omega_0 T_0} + \overline{A}e^{-i\omega_0 T_0} + \varepsilon \left(\frac{A^3}{8\omega_0^2}e^{3i\omega_0 T_0} + \frac{\overline{A}^3}{8\omega_0^2}e^{-3i\omega_0 T_0} \right)$$

$$+\varepsilon^2 \left(\frac{1}{64\omega_0^4}A^5 e^{5i\omega_0 T_0} + \frac{3}{32\omega_0^4}A^4\overline{A}e^{3i\omega_0 T_0} - \frac{3i}{32\omega_0^3}A^3 D_1 e^{3i\omega_0 T_0} \right)$$

$$+ \varepsilon^2 \left(\frac{1}{64\omega_0^4}\overline{A}^5 e^{-5i\omega_0 T_0} + \frac{3}{32\omega_0^4}\overline{A}^4 A e^{-3i\omega_0 T_0} - \frac{3i}{32\omega_0^3}\overline{A}^3 D_1 e^{-3i\omega_0 T_0} \right) \tag{85}$$

keeping $A = \frac{1}{2}ae^{i\phi}$ and expressing the result in terms of t.we get

$$u = a\cos(\omega t + \chi) + \frac{a^3\varepsilon}{32\omega_0^2} \left(1 + \frac{3a^2\varepsilon}{32\omega_0^2} - \frac{3iD_1\varepsilon}{4\omega_0^3} \right) \cos 3(\omega t + \chi)$$

$$+ \frac{a^5\varepsilon^2}{1024\omega_0^4}\cos 5(\omega t + \chi) + O(\varepsilon^3) \tag{86}$$

where
$$\omega = \omega_0 + \frac{3}{8\omega_0}a^2\varepsilon + \frac{3}{256\omega_0^3}a^4\varepsilon^2 + O(\varepsilon^3) \tag{87}$$

6   Illustration of Multiple Scale Method to Ricatti's Equation

$$y' = 3 + 3t^2 y - t\varepsilon y^2 \quad with \ \ y(0) = 1 \tag{88}$$

Substituting equation (77) in (8) and equating the coefficients of ε, we get

$$\left(\frac{\partial}{\partial T_0} + \varepsilon\frac{\partial}{\partial T_1} + \cdots \right)(y_0 + \varepsilon y_1 + \cdots) = 3 + 3(T_0 + \varepsilon T_1 + \cdots)(y_0 + \varepsilon y_1 + \cdots)$$

$$- (T_0 + \varepsilon T_1 + \cdots)\varepsilon(y_0 + \varepsilon y_1 + \varepsilon)^2 \tag{89}$$

$$\frac{\partial y_0}{\partial T_0} = 3 + 3T_0 y_0 \tag{90}$$

$$\frac{\partial y_1}{\partial T_0} - 3T_0 y_1 = 3T_1 y_0 - T_0 y_0^2 - \frac{\partial y_0}{\partial T_1} \tag{91}$$

The general solution of equation (9) is

$$y_0 = e^{\frac{3}{2}T_0} \left[\frac{\sqrt{3\pi}}{\sqrt{2}}erf\left(\frac{\sqrt{3}T_0}{\sqrt{2}} \right) + A \right] \tag{92}$$

substitute y_0 in (10) ,we get

$$y_1 = \frac{1}{2^{\frac{3}{2}}}e^{\frac{3}{2}T_0^2} \left[\frac{1}{\pi}\sqrt{2}e^{\frac{-3}{2}T_0^2} \left(\pi^{\frac{3}{2}}e^{3T_0^2}erf\left(\frac{\sqrt{3}T_0}{\sqrt{2}} \right)^2 - 2^{\frac{3}{2}}\sqrt{3}\pi T_0 e^{\frac{3}{2}T_0^2}erf\left(\frac{\sqrt{3}T_0}{\sqrt{2}} \right) - 4\sqrt{\pi} \right) \right]$$

$$\frac{1}{2^{\frac{3}{2}}}e^{\frac{3}{2}T_0^2}\left[-\frac{4}{\sqrt{3}}\left(\sqrt{\pi}e^{\frac{3}{2}T_0^2}erf\left(\frac{\sqrt{3}T_0}{\sqrt{2}} \right) - \sqrt{6}T_0 \right)\frac{2^{\frac{3}{2}}}{3}e^{\frac{3}{2}T_0^2} \right] + B \tag{93}$$
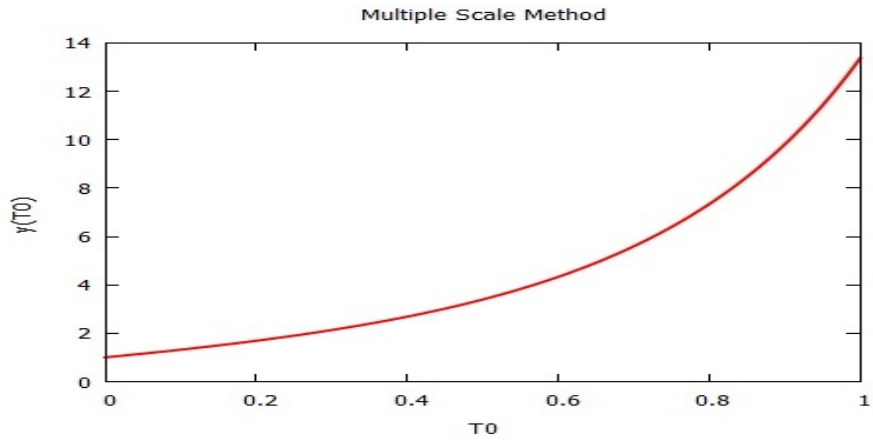
Figure 1: Variation of the Solution due to T_0
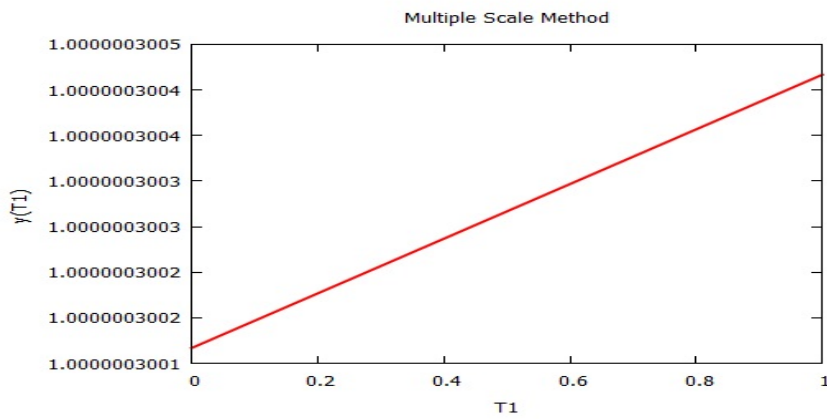
Figure 2: Variation of the Solution due to T_1
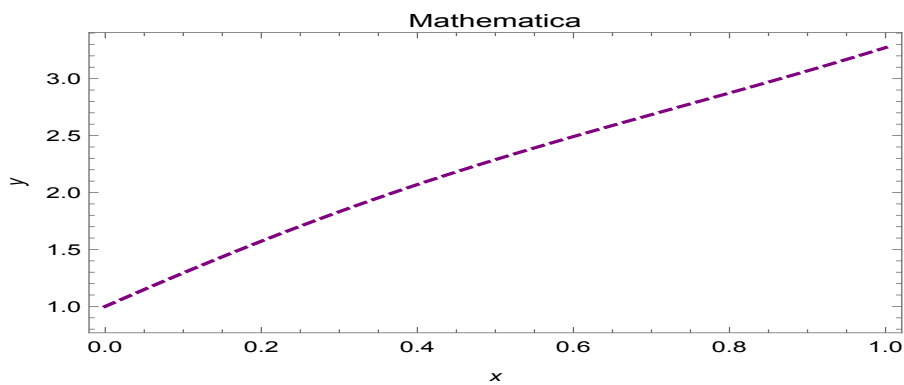
Figure 3: Graph plotted using Mathematica

References

[1] A.H. Nayfeh, *Perturbation methods*, Wiley, 1973.

[2] A. Salih, *The method of multiple scales*, Department of Aerospace Engineering, 2014.

[3] J.A. Murdock, *Perturbations theory and methods*, Wiley, 1991.

[4] J. Kevorkian, J.D. Cole, *Multiple scale and singular perturbation methods*, Springer, 1996.

[5] E.J. Hinch, *Perturbation methods*, Cambridge University Press, 1991.

[6] M.H. Holmes, *Introduction to perturbation methods*, Springer, 1995.

[7] R.S. Johnson, *Singular perturbation theory*, Springer, 2005.

[8] Y. Chen, N. Goldenfeld, Y. Oono, *Renormalization group and singular perturbations: Multiple scales, boundary layers, and reductive perturbation theory*, Phys. Rev. E, 54(1) (1996).

[9] J. Kevorkian, J.D. Cole, *Perturbation methods in applied mathematics*, Springer Verlag, 1981.

[10] W.T. Reid, *Riccati differential equations mathematics in science and engineering*, New York Academic Press, 1972.

[11] M.D. Raisinghania, *Advanced differential equations*, S.Chand and Company.

[12] Lasiecka, R. Triggiani, *Differential and algebraic Riccati equations with application to boundary/point control problems: Continuous theory and approximation theory*, Springer, 1991.

Viscous fluid flow over a stretching sheet in the boundary layer region

M.S. Dattaram[1], R.S. Sumana[2] and L.N. Achala[3]

[1,2,3]P. G. Department of Mathematics and Research Centre in Applied Mathematics

M. E. S. College of Arts, Commerce and Science

15th cross, Malleswaram, Bangalore - 560003.

Email ID: [1]datta.munikoti@gmail.com, [2]sumana.shesha@gmail.com, [3]anargund1960@gmail.com

Abstract: The mixed convection boundary layer flow of a quiescent viscous incompressible fluid over a stretching vertical heated sheet is investigated. Using appropriate similarity variables, the governing system of partial differential equations is transformed into a system of ordinary differential equations, which is then solved using power series as well as shooting method.

Keywords: Mixed convection boundary layer flow, Incompressible fluid, Stretching sheet, Power series, Shooting method.

1   Introduction

Mixed convection flows, occur when natural convection and forced convection mechanisms act together to transfer heat. This is also defined as situations where both pressure forces and buoyant forces interact. The study of heat transfer of combined free and forced convection flow has fascinated the interest of many researchers over the last few decades. Mixed convection flows arise in many transport processes both naturally and in engineering applications. They play an important role in atmospheric boundary-layer flows, heat exchangers, solar collectors, nuclear reactors and in electronic equipment. They appear in many industrial processes, such as manufacture and extraction of polymer and rubber sheets, paper production, wire drawing and glass-fiber production, melt spinning, continuous casting, etc. Mixed convection flow has many industrial applications such as heat treatment of material traveling between a feed roll and wind-up roll or conveyer belts, extrusion of steel, cooling of a large metallic plate in a bath, liquid films in condensation process and in aerodynamics, etc. In addition it should be mentioned that this type of flow plays a great role in thermal manufacturing applications and is important in establishing the temperature distribution within buildings as well as heat losses or heat loads for heating, ventilating and air conditioning systems. [4]

The aim of this paper is to study the two-dimensional mixed convection flow over a stretching sheet with boundary conditions.The governing equations are transformed into a system of nonlinear ordinary differential equations, which are then solved numerically. Representative results for the velocity and temperature profiles are presented for some values of the governing parameters.

2   Method of Solution

Consider a two dimensional mixed convection boundary layer flow of a quiescent viscous incompressible fluid over a stretching vertical heated sheet which obey the power law relations

$q_w = ax^n$ and $U_w = bx^m$ where q_w and U_w are surface heat flux and stretching velocity respectively, and a, b, m, n are constants. The rectangular coordinates (x, y) are chosen with the x-axis along the stretching sheet and the y axis normal to the plate. Two equal and opposite forces are impulsively applied along the x-axis so that the sheet is stretched, keeping the origin fixed in the fluid of ambient temperature T_∞.

The continuous stretching surface is assumed to have the velocity and temperature of the form

$$U = U_w = bx^m \tag{1}$$
$$T_w = T_\infty + q_w = T_\infty + ax^n \tag{2}$$

The governing boundary layer equations [4, 5] are given by

$$\frac{\partial u}{\partial x} + \frac{\partial v}{\partial y} = 0 \tag{3}$$

$$u\frac{\partial u}{\partial x} + v\frac{\partial v}{\partial y} = \nu\frac{\partial u^2}{\partial y^2} \pm g\beta(T - T_\infty) \tag{4}$$

$$u\frac{\partial T}{\partial x} + v\frac{\partial T}{\partial y} = \alpha\frac{\partial u^2}{\partial y^2} \tag{5}$$

and the corresponding boundary conditions are

$$\begin{aligned} u = U, \ v = 0, \ T = T_w \quad \text{at} \quad y = 0, \\ u = 0, \ T = T_\infty \quad \text{as} \quad y \to \infty, \end{aligned} \tag{6}$$

where u and v are the components of the velocity in the x and y directions, ν is the kinematic viscosity, g is the acceleration due to gravity, β is the coefficient of thermal expansion and α is the thermal diffusivity of the fluid. The last term on the right hand side of (4) indicates the influence of the thermal buoyancy force on the flow field with $+$ and $-$ sign indicating the buoyancy assisting and buoyancy opposing flow regions.

The stream function $\psi(x, y)$ is introduced such that

$$u = \frac{\partial \psi}{\partial y} \quad \text{and} \quad v = -\frac{\partial \psi}{\partial x} \tag{7}$$

Then, the equation of continuity is identically satisfied and equations (4), (5) reduce to

$$\frac{\partial \psi}{\partial y}\frac{\partial^2 \psi}{\partial x \partial y} - \frac{\partial \psi}{\partial x}\frac{\partial^2 \psi}{\partial y^2} = \nu\frac{\partial^3 \psi}{\partial y^3} \pm g\beta(T - T_\infty) \tag{8}$$

$$\frac{\partial \psi}{\partial y}\frac{\partial T}{\partial x} - \frac{\partial \psi}{\partial x}\frac{\partial T}{\partial y} = \alpha\frac{\partial u^2}{\partial y^2} \tag{9}$$

Using equation (7), the boundary conditions (6) become

$$\begin{aligned} \frac{\partial \psi}{\partial x} = 0, \ \frac{\partial \psi}{\partial y} = U, \ T = T_w \quad \text{at} \quad y = 0, \\ \frac{\partial \psi}{\partial y} = 0, \ T = T_\infty \quad \text{as} \quad y \to \infty. \end{aligned} \tag{10}$$

Now, we will convert the partial differential equations (8), (9) into ordinary differential equations. In accordance with the procedure of the law of similarity, let the velocity profile and the temperature profile be

$$u = UF(\eta), \tag{11}$$

$$T = T_\infty + (T_w - T_\infty)\theta(\eta) \tag{12}$$

where

$$\eta = y\sqrt{\frac{U}{\nu x}} = y\sqrt{\frac{b}{\nu}}x^{\frac{m-1}{2}} \tag{13}$$

is the similarity variable.

Using equations (7), (11) and (13), the stream function $\psi(x, y)$ is given by

$$\psi = \int u\, dy = \sqrt{b\nu}x^{\frac{m+1}{2}}\int F(\eta)\, d\eta = \sqrt{b\nu}x^{\frac{m+1}{2}}f(\eta) \tag{14}$$

where $f(\eta) = \int F(\eta)\, d\eta$.

The velocity components and their derivatives, and the derivatives of the temperature components are given by

$$u = \frac{\partial \psi}{\partial y} = bx^m f'(\eta), \tag{15}$$

$$v = -\frac{\partial \psi}{\partial x} = -\sqrt{b\nu}\left(\frac{m+1}{2}\right)x^{\frac{m-1}{2}}f(\eta) - b\left(\frac{m-1}{2}\right)x^{m-1}yf'(\eta), \tag{16}$$

$$\frac{\partial u}{\partial x} = \frac{\partial^2 \psi}{\partial x \partial y} = bmx^{m-1}f'(\eta) + b\sqrt{\frac{b}{\nu}}\left(\frac{m-1}{2}\right)x^{\frac{3m-3}{2}}yf''(\eta), \tag{17}$$

$$\frac{\partial u}{\partial y} = \frac{\partial^2 \psi}{\partial y^2} = b\sqrt{\frac{b}{\nu}}x^{\frac{3m-1}{2}}f''(\eta), \tag{18}$$

$$\frac{\partial^2 u}{\partial y^2} = \frac{\partial^3 \psi}{\partial y^3} = \frac{b^2}{\nu}x^{2m-1}f'''(\eta) \tag{19}$$

$$\frac{\partial T}{\partial x} = anx^{n-1}\theta(\eta) + a\sqrt{\frac{b}{\nu}}\left(\frac{m-1}{2}\right)x^{\frac{2n+m-3}{2}}y\theta'(\eta) \tag{20}$$

$$\frac{\partial T}{\partial y} = a\sqrt{\frac{b}{\nu}}x^{\frac{2n+m-1}{2}}\theta'(\eta) \tag{21}$$

$$\frac{\partial^2 T}{\partial y^2} = \frac{ab}{\nu}x^{n+m-1}\theta''(\eta) \tag{22}$$

Substituting equations (15)-(22) in equations (8), (9), we get

$$f'''(\eta) + \left(\frac{m+1}{2}\right)f(\eta)f''(\eta) - mf'^2(\eta) + \lambda\theta(\eta) = 0, \tag{23}$$

$$\frac{1}{\Pr}\theta''(\eta) + \left(\frac{m+1}{2}\right) f(\eta)\theta'(\eta) - n f'(\eta)\theta(\eta) = 0, \tag{24}$$

and the corresponding boundary conditions are

$$f(\eta) = 0, f'(\eta) = 1, \theta(\eta) = 1 \quad \text{at} \quad \eta = 0,$$
$$f'(\eta) = 0, \theta(\eta) = 0 \quad \text{as} \quad \eta \to \infty. \tag{25}$$

where $\lambda = \pm\dfrac{\mathrm{Gr}_x}{\mathrm{Re}_x^2}$, $\mathrm{Gr} = \dfrac{g\beta(T_w - T_\infty)x^3}{\nu^2}$ is the local Grashof number, $\mathrm{Re}_x = \dfrac{Ux}{\nu}$ is the local Reynold's number and $\Pr = \dfrac{\nu}{\alpha}$ is the Prandtl number.

2.1 Power Series Solution

The power series method is used to obtain power series solutions to the equations (23), (24).

We construct a series solution of the form

$$f(\eta) = \sum_{k=0}^{\infty} \frac{a_k}{k!}\eta^k = a_0 + a_1\eta + \frac{a_2}{2!}\eta^2 + \frac{a_3}{3!}\eta^3 + \frac{a_4}{4!}\eta^4 + \frac{a_5}{5!}\eta^5 + \dots \tag{26}$$

$$\theta(\eta) = \sum_{k=0}^{\infty} \frac{b_k}{k!}\eta^k = b_0 + b_1\eta + \frac{b_2}{2!}\eta^2 + \frac{b_3}{3!}\eta^3 + \frac{b_4}{4!}\eta^4 + \frac{b_5}{5!}\eta^5 + \dots \tag{27}$$

Then,

$$f'(\eta) = \sum_{k=1}^{\infty} \frac{a_k}{(k-1)!}\eta^{k-1} = a_1 + a_2\eta + \frac{a_3}{2!}\eta^2 + \frac{a_4}{3!}\eta^3 + \frac{a_5}{4!}\eta^4 + \frac{a_6}{5!}\eta^5 + \dots \tag{28}$$

$$f''(\eta) = \sum_{k=2}^{\infty} \frac{a_k}{(k-2)!}\eta^{k-2} = a_2 + a_3\eta + \frac{a_4}{2!}\eta^2 + \frac{a_5}{3!}\eta^3 + \frac{a_6}{4!}\eta^4 + \frac{a_7}{5!}\eta^5 + \dots \tag{29}$$

$$f'''(\eta) = \sum_{k=3}^{\infty} \frac{a_k}{(k-3)!}\eta^{k-3} = a_3 + c_4\eta + \frac{a_5}{2!}\eta^2 + \frac{a_6}{3!}\eta^3 + \frac{a_7}{4!}\eta^4 + \frac{a_8}{5!}\eta^5 \dots \tag{30}$$

$$\theta'(\eta) = \sum_{k=1}^{\infty} \frac{b_k}{(k-1)!}\eta^{k-1} = b_1 + b_2\eta + \frac{b_3}{2!}\eta^2 + \frac{b_4}{3!}\eta^3 + \frac{b_5}{4!}\eta^4 + \frac{b_6}{5!}\eta^5 + \dots \tag{31}$$

$$\theta''(\eta) = \sum_{k=2}^{\infty} \frac{b_k}{(k-2)!}\eta^{k-2} = b_2 + b_3\eta + \frac{b_4}{2!}\eta^2 + \frac{b_5}{3!}\eta^3 + \frac{b_6}{4!}\eta^4 + \frac{b_7}{5!}\eta^5 + \dots \tag{32}$$

Using the boundary conditions (25) in equations (26)-(28), we obtain

$$a_0 = 0, \quad a_1 = 1, \quad b_0 = 1. \tag{33}$$

Substituting equations (26)-(33) in equations (23), (24), we get

$$
(a_3 - m + \lambda) + \left\{ a_4 - \frac{1}{2}(3m-1)a_2 + \lambda b_1 \right\}\eta + \left\{ \frac{1}{2}a_5 - \frac{1}{4}(3m-1)a_2^2 - \frac{1}{2}(m-1)a_3 \right.
$$
$$
\left. + \frac{1}{2}\lambda b_2 \right\}\eta^2 + \left\{ \frac{1}{6}a_6 - \frac{1}{3}(2m-1)a_2 a_3 - \frac{1}{12}(m-3)a_4 + \frac{1}{6}\lambda b_3 \right\}\eta^3 + \left\{ \frac{1}{24}a_7 \right.
$$
$$
\left. - \frac{1}{48}(9m-7)a_2 a_4 - \frac{1}{12}(2m-1)a_3^2 + \frac{1}{12}a_5 + \frac{1}{24}\lambda b_4 \right\}\eta^4 + \cdots\cdots = 0
$$

(34)

$$
\left(\frac{1}{\mathrm{Pr}}b_2 - n \right) + \left\{ \frac{1}{\mathrm{Pr}}b_3 - na_2 - \frac{1}{2}(2n-m-1)b_1 \right\}\eta + \left\{ \frac{1}{2\mathrm{Pr}}b_4 - \frac{1}{2}na_3 \right.
$$
$$
\left. - \frac{1}{2}(n-m-1)b_2 - \frac{1}{4}(4n-m-1)a_2 b_1 \right\}\eta^2 + \left\{ \frac{1}{6\mathrm{Pr}}b_5 - \frac{1}{12}(6n-m-1)a_3 b_1 \right.
$$
$$
\left. - \frac{1}{4}(2n-m-1)a_2 b_2 - \frac{1}{6}na_4 - \frac{1}{12}(2n-3m-3)b_3 \right\}\eta^3 + \left\{ \frac{1}{24\mathrm{Pr}}b_6 \right.
$$
$$
- \frac{1}{48}(8n-m-1)a_4 b_1 - \frac{1}{12}(3n-m-1)a_3 b_2 - \frac{1}{24}(4n-3m-3)a_2 b_3 - \frac{1}{24}na_5
$$
$$
\left. - \frac{1}{24}(n-2m-2)b_4 \right\}\eta^4 + \cdots\cdots = 0
$$

(35)

Equations (34) and (35) are identities and hence all coefficients of the various powers of η must vanish identically. Thus, we have

$$
b_2 = n\mathrm{Pr},
$$
$$
a_3 = m - \lambda,
$$
$$
b_3 = \mathrm{Pr}\left[na_2 + \frac{1}{2}(2n-m-1)b_1 \right],
$$
$$
a_4 = \frac{1}{2}(3m-1)a_2 - \lambda b_1,
$$
$$
b_4 = \mathrm{Pr}\left[n\left\{ (m-\lambda) + (n-m-1)\mathrm{Pr} \right\} + \frac{1}{2}(4n-m-1)a_2 b_1 \right],
$$
$$
a_5 = \frac{1}{2}(3m-1)a_2^2 + (m-1)(m-\lambda) - \lambda n\mathrm{Pr},
$$
$$
b_5 = \frac{1}{2}\mathrm{Pr}\left[n\left\{ (3m-1) + 2(4n-3m-3)\mathrm{Pr} \right\}a_2 + \left\{ m(6n-m-1) - \lambda(7n-m-1) \right.\right.
$$
$$
\left.\left. + (2n-m-1)(2n-3m-3)\mathrm{Pr} \right\}b_1 \right],
$$
$$
a_6 = \left[\frac{1}{4}(19m^2 - 18m + 3) - \lambda\left\{ 2(2m-1) + n\mathrm{Pr} \right\} \right]a_2 - \frac{1}{2}\lambda\left\{ (m-3) \right.
$$
$$
\left. + (2n-m-1)\mathrm{Pr} \right\}b_1,
$$
$$
b_6 = \mathrm{Pr}\left[n\left\{ (m-1)(m-\lambda) - \left\{ (4m^2 - 7mn + 6n + 2m - 2) + 2\lambda(n-m-1) \right\}\mathrm{Pr} \right.\right.
$$
$$
\left. + (n-m-1)(n-2m-2)\mathrm{Pr}^2 \right\} + \frac{1}{2}n\left\{ (3m-1) + 2(4n-3m-3)\mathrm{Pr} \right\}a_2^2
$$
$$
+ \frac{1}{4}\left\{ (3m-1)(8n-m-1) + 2(12n^2 + 5m^2 - 19mn - 19n + 10m \right.
$$

$$+ 5)\mathrm{Pr}\Big\}a_2 b_1 \Big],$$

$$a_7 = \frac{1}{4}(3m-1)(9m-5)a_2^2 - \frac{1}{2}\lambda\Big\{(9m-7)+(4n-m-1)\mathrm{Pr}\Big\}a_2 b_1$$

$$+ 2(m-\lambda)\Big\{(2m^2-2m+1)-\lambda(2m-1)\Big\}+\lambda n\Big\{(2-m-\lambda)$$

$$- (n-m-1)\mathrm{Pr}\Big\}\mathrm{Pr}, \quad \ldots\ldots \tag{36}$$

Substituting equations (33) and (36) in equations (26) and (27) gives

$$f(\eta) = \eta + \frac{\alpha}{2!}\eta^2 + \frac{1}{3!}(m-\lambda)\eta^3 + \frac{1}{4!}\Big\{\frac{\alpha}{2}(3m-1)-\lambda\beta\Big\}\eta^4 + \frac{1}{5!}\Big\{\frac{\alpha^2}{2}(3m-1)$$

$$+ (m-1)(m-\lambda)-\lambda n\mathrm{Pr}\Big\}\eta^5 + \frac{1}{6!}\Big[\alpha\Big\{\frac{1}{4}(19m^2-18m+3)-\lambda(4m-2$$

$$+ n\mathrm{Pr})\Big\}-\frac{\lambda\beta}{2}\Big\{(m-3)+(2n-m-1)\mathrm{Pr}\Big\}\Big]\eta^6 + \frac{1}{7!}\Big[\frac{\alpha^2}{4}(3m-1)(9m-5)$$

$$- \frac{\lambda\alpha\beta}{2}\Big\{(9m-7)+(4n-m-1)\mathrm{Pr}\Big\}+2(m-\lambda)\Big\{(2m^2-2m+1)$$

$$- \lambda(2m-1)\Big\}+\lambda n\Big\{(2-m-\lambda)-(n-m-1)\mathrm{Pr}\Big\}\mathrm{Pr}\Big]\eta^7 + \cdots\cdots, \tag{37}$$

$$\theta(\eta) = 1 + \beta\eta + \frac{n\mathrm{Pr}}{2!}\eta^2 + \frac{\mathrm{Pr}}{3!}\Big\{n\alpha + \frac{\beta}{2}(2n-m-1)\Big\}\eta^3 + \frac{\mathrm{Pr}}{4!}\Big[n\Big\{(m-\lambda)+(n$$

$$- m-1)\mathrm{Pr}\Big\}+\frac{\alpha\beta}{2}(4n-m-1)\Big]\eta^4 + \frac{\mathrm{Pr}}{2.5!}\Big[n\alpha\Big\{(3m-1)+2(4n-3m$$

$$- 3)\mathrm{Pr}\Big\}+\beta\Big\{m(6n-m-1)-\lambda(7n-m-1)+(2n-m-1)(2n-3m$$

$$- 3)\mathrm{Pr}\Big\}\Big]\eta^5 + \frac{\mathrm{Pr}}{6!}\Big[n\Big\{(m-1)(m-\lambda)-\{(4m^2-7mn+6n+2m-2)$$

$$+ 2\lambda(n-m-1)\}\mathrm{Pr}+(n-m-1)(n-2m-2)\mathrm{Pr}^2\Big\}+\frac{\alpha^2 n}{2}\Big\{(3m-1)$$

$$+ 2(4n-3m-3)\mathrm{Pr}\Big\}+\frac{\alpha\beta}{4}\Big\{(3m-1)(8n-m-1)+2(12n^2+5m^2$$

$$- 19mn-19n+10m+5)\mathrm{Pr}\Big\}\Big]\eta^6 \tag{38}$$

where $\alpha = a_2 = f''(0)$ and $\beta = b_1 = \theta'(0)$. We have obtained the values for α and β numerically for different values of m, n, λ and Pr which is described in the next subsection.

2.2 Numerical Solution

The shooting method [6] is used to obtain numerical solutions to the equations (23), (24) along with the boundary conditions (25). Figure 1 and Figure 2 show the velocity distribution and temperature distribution respectively in the boundary layer on a stretching sheet for $\mathrm{Pr} = 1$, $\lambda = 0.1$, $n = 1$ and different values of m. The values of the functions f, f', f'', $\theta(\eta)$ and $\theta'(\eta)$ for $\mathrm{Pr} = 1$, $\lambda = 0.1$, $n = 1$ and different η, m are listed in Table 1.

Figure 1: Velocity distribution in the boundary layer on a stretching sheet for $\Pr = 1$, $\lambda = 0.1$, $n = 1$ and different m
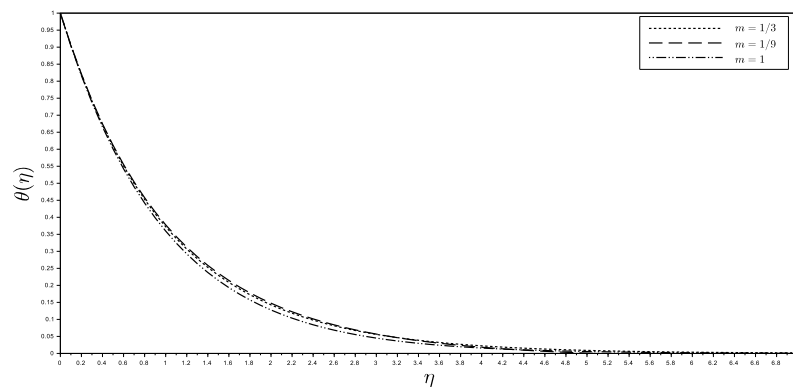
Figure 2: Temperature distribution in the boundary layer on a stretching sheet for $\Pr = 1$, $\lambda = 0.1$, $n = 1$ and different m

Table 1: The functions f, f', f'', $\theta(\eta)$ and $\theta'(\eta)$ in the boundary layer on a stretching sheet for $\Pr = 1$, $\lambda = 0.1$, $n = 1$ and different η, m

η	$f(\eta)$	$f'(\eta)$	$f''(\eta)$	$\theta(\eta)$	$\theta'(\eta)$
			$m = 1/3$		
0.0	0.000000	1.000000	-0.618315	1.000000	-0.997356
1.0	0.731920	0.505363	-0.372143	0.372330	-0.362782
2.0	1.085888	0.233451	-0.187005	0.142662	-0.134901
3.0	1.245682	0.102909	-0.085774	0.055971	-0.051915
4.0	1.315318	0.044303	-0.037681	0.022253	-0.020435
5.0	1.345107	0.018814	-0.016219	0.008905	-0.008138
6.0	1.357694	0.007896	-0.006911	0.003575	-0.003258
7.0	1.362942	0.003256	-0.002928	0.001439	-0.001308
8.0	1.365078	0.001293	-0.001236	0.000581	-0.000525
9.0	1.365898	0.000466	-0.000521	0.000236	-0.000211
10.0	1.366165	0.000117	-0.000219	0.000098	-0.000085
11.0	1.366198	-0.000029	-0.000092	0.000042	-0.000034
12.0	1.366134	-0.000091	-0.000039	0.000019	-0.000014
			$m = 1/9$		
0.0	0.000000	1.000000	-0.730527	1.000000	-0.989565
1.0	0.696825	0.450366	-0.391262	0.377821	-0.360503
2.0	0.990356	0.169970	-0.190752	0.147586	-0.137788
3.0	1.084837	0.035642	-0.090036	0.056767	-0.056799
4.0	1.084999	-0.027360	-0.041849	0.018171	-0.025038
5.0	1.041295	-0.056206	-0.018582	0.000822	-0.011462
6.0	0.978065	-0.068334	-0.006971	-0.007118	-0.005179
7.0	0.907410	-0.071981	-0.000959	-0.010573	-0.002078
8.0	0.835567	-0.071175	0.002240	-0.011766	-0.000479
9.0	0.765843	-0.067990	0.003951	-0.011781	0.000359
10.0	0.700001	-0.063547	0.004833	-0.011181	0.000790
11.0	0.638953	-0.058483	0.005233	-0.010276	0.000993
12.0	0.583113	-0.053178	0.005340	-0.009239	0.001064
			$m = 1$		
0.0	0.000000	1.000000	-0.951021	1.000000	-1.012330
1.0	0.644850	0.385371	-0.368531	0.359612	-0.370800
2.0	0.892776	0.147677	-0.142062	0.127611	-0.132671
3.0	0.987566	0.056298	-0.054407	0.045043	-0.046954
4.0	1.023647	0.021397	-0.020705	0.015884	-0.016545
5.0	1.037362	0.008147	-0.007836	0.005618	-0.005820
6.0	1.042606	0.003142	-0.002952	0.002008	-0.002046
7.0	1.044655	0.001259	-0.001109	0.000739	-0.000719
8.0	1.045504	0.000552	-0.000417	0.000293	-0.000253
9.0	1.045901	0.000285	-0.000158	0.000137	-0.000089
10.0	1.046127	0.000183	-0.000062	0.000082	-0.000031
11.0	1.046287	0.000142	-0.000026	0.000062	-0.000011
12.0	1.046419	0.000124	-0.000013	0.000055	-0.000004

3   Results and Discussion

The nonlinear ordinary differential equations (23) and (24) subject to the boundary conditions in (24) are solved using Power series method for some values of Prandtl number $\Pr$, buoyancy parameter λ and other parameters m and n. To validate the results obtained, we also have solved this system of equations using shooting method for certain values of parameters. Velocity profiles as well as temperature profiles are presented for different values of the governing parameters. The comparisons show excellent agreement between the results obtained for different values of governing parameters.

References

[1] H. Schlichting, K. Gersten, *Boundary layer theory*, Springer, 2004.

[2] J.L. Bansal, *Viscous fluid dynamics*, Oxford & IBH Publishing Co. Pvt. Ltd., 2005.

[3] R.L. Burden, J.D. Faires, *Numerical analysis*, Cengage Learning, 2012.

[4] R.Kh. Zeytounian, *Convection in fluids*, Springer, 2009.

Viscous fluid flow over a wedge

G. Singh[1], R.S. Sumana[2] and L.N. Achala[3]

[1,2,3]P. G. Department of Mathematics and Research Centre in Applied Mathematics

M. E. S. College of Arts, Commerce and Science

15th cross, Malleswaram, Bangalore - 560003.

Email ID: [1]datta.munikoti@gmail.com, [2]sumana.shesha@gmail.com, [3]anargund1960@gmail.com

Abstract: The steady boundary layer flow of a wedge submerged in an incompressible fluid of very small viscosity is investigated. Using appropriate similarity variables, the governing system of partial differential equations is transformed into an ordinary differential equation, which is then solved using power series as well as shooting method.

Keywords: Boundary layer flow, Wedge, Hartree's equation, Power series, Shooting method.

1 Introduction

A fluid may be defined as a substance in which the molecules of the substance are separated by a small gap. A fluid is also a substance that deforms continuously when subjected to stresses however small it may be constituting a flow. The theory of fluid flow (incompressible or compressible fluid) is based on the Newtonian mechanics. The concept of continuum is an idealization of continuous description of matter where the properties of matter such as density, viscosity, thermal conductivity, temperature etc. are considered as continuous function of space variables and time.

Fluid mechanics is one of the oldest branches of physics and the foundation for the understanding of many other aspects of applied sciences and engineering. It is a subject of widespread interest in almost all fields of engineering as well as biology, meteorology, physical chemistry and geophysics [1, 2, 3].

1.1 Boundary Layer Theory

As an object moves through a fluid, or as a fluid moves past an object, the molecules of the fluid near the object are disturbed and move around the object. Forces are generated between the fluid and the object. The magnitude of these forces depend on the shape of the object, the speed of the object, the mass of the fluid along the object and on two other important properties of the fluid; the viscosity, or stickiness, and the compressibility, or springiness, of the fluid. Thus if a fluid flows in the presence of an obstacle, then the obstacle will experience two types of forces,

1. drag force in the direction of motion of the fluid,

2. lift force in a direction normal to the flow direction.

These two forces are produced by tangential and normal stresses. The shearing stress i.e., the drag due to tangential stress is called friction or skin friction or viscous drag. The drag due to normal stress is called pressure drag. Thus flows constrained by solid surfaces can typically be divided into two regions as below,

1. **Boundary Layer Region:** Flows near a bounding surface with significant velocity with gradients normal to the solid body and shear stresses in this region are predominant.

2. **Potential Flow Region:** Flows far from bounding surface with negligible velocity gradients, negligible shear stresses where inertia effects are important.

1.2   Boundary layer equations

The boundary layer theory was first developed by Ludwig Prandtl in 1904. He gave a convincing explanation for motion of fluid around objects and this led to major advances in fluid dynamics. The detailed analysis of the flow within the boundary layer region is very important for many engineering problems and aerodynamics. [4]

Prandtl considered the two dimensional flow around a wedge profile submerged in an incompressible fluid of a very small viscosity. At the leading stagnation point, the thickness of the boundary layer is zero and it grows slowly towards the rear of the wedge. Within a very thin boundary layer of thickness δ a large velocity gradient exists. The equations of the continuity and momentum without body force are given by

$$\frac{\partial u}{\partial x} + \frac{\partial v}{\partial y} = 0, \tag{1}$$

$$\frac{\partial u}{\partial t} + u\frac{\partial u}{\partial x} + v\frac{\partial u}{\partial y} = -\frac{1}{\rho}\frac{\partial p}{\partial x} + \nu\left(\frac{\partial^2 u}{\partial x^2} + \frac{\partial^2 u}{\partial y^2}\right), \tag{2}$$

$$\frac{\partial v}{\partial t} + u\frac{\partial v}{\partial x} + v\frac{\partial v}{\partial y} = -\frac{1}{\rho}\frac{\partial p}{\partial y} + \nu\left(\frac{\partial^2 v}{\partial x^2} + \frac{\partial^2 v}{\partial y^2}\right), \tag{3}$$

where u and v are the components of the velocity in the x and y directions respectively, ρ is the density, p is the pressure and ν is the kinematic viscosity of the fluid.

In order to compare the order of magnitude of the individual terms, it is more advantageous to put the equations (1)-(3) in the non-dimensional form by letting

$$\begin{aligned} x^* = \frac{x}{l}, \quad y^* = \frac{y}{\delta}, \quad u^* = \frac{u}{U}, \\ v^* = \frac{v}{V}, \quad t^* = \frac{t}{l/U}, \quad p^* = \frac{p}{p_\infty}, \end{aligned} \tag{4}$$

where l, δ, U, V and p_∞ are the reference values of the corresponding quantities x, y, u, v and p.

In view of equation (4), the equations (1)-(3) become

$$\frac{\partial u^*}{\partial x^*} + \frac{Vl}{U\delta}\frac{\partial v^*}{\partial y^*} = 0, \tag{5}$$

$$\frac{\partial u^*}{\partial t^*} + u^*\frac{\partial u^*}{\partial x^*} + \frac{Vl}{U\delta}v^*\frac{\partial u^*}{\partial y^*} = -\frac{p_\infty}{\rho U^2}\frac{\partial p^*}{\partial x^*} + \frac{1}{\mathrm{Re}}\left(\frac{\partial^2 u^*}{\partial x^{*2}} + \frac{l^2}{\delta^2}\frac{\partial^2 u^*}{\partial y^{*2}}\right), \tag{6}$$

$$\frac{V}{U}\frac{\partial v^*}{\partial t^*} + \frac{V}{U}u^*\frac{\partial v^*}{\partial x^*} + \frac{V^2 L}{U^2\delta}v^*\frac{\partial v^*}{\partial y^*} = -\frac{p_\infty l}{\delta\rho U^2}\frac{\partial p^*}{\partial y^*} + \frac{1}{\mathrm{Re}}\frac{V}{U}\left(\frac{\partial^2 v^*}{\partial x^{*2}} + \frac{l^2}{\delta^2}\frac{\partial^2 v^*}{\partial y^{*2}}\right), \tag{7}$$

where $\mathrm{Re} = \dfrac{Ul}{\nu}$ is the Reynolds number.

Integrating equation (5) with respect to y^*, and using the condition $(v^*)_{y^*=1} = 1$ and $(v^*)_{y^*=0} = 0$,

$$\frac{V}{U} = -\frac{\delta}{l} \int_0^1 \frac{\partial u^*}{\partial x^*} dy^*. \tag{8}$$

Since the integral in the above equation is of order unity, $\frac{V}{U}$ is of order $\frac{\delta}{l}$. Hence $V \ll U$. By neglecting the terms of the order of δ and smaller from system of equations (5)-(7), we obtain the following equations

$$\frac{\partial u^*}{\partial x^*} + \frac{Vl}{U\delta} \frac{\partial v^*}{\partial y^*} = 0, \tag{9}$$

$$\frac{\partial u^*}{\partial t^*} + u^* \frac{\partial u^*}{\partial x^*} + \frac{Vl}{U\delta} v^* \frac{\partial u^*}{\partial y^*} = -\frac{p_\infty}{\rho U^2} \frac{\partial p^*}{\partial x^*} + \frac{1}{\text{Re}} \frac{l^2}{\delta^2} \frac{\partial^2 u^*}{\partial y^{*2}}, \tag{10}$$

$$\frac{p_\infty l}{\delta \rho U^2} \frac{\partial p^*}{\partial y^*} = 0. \tag{11}$$

Reverting the dimensional variables in equations (9)-(11), we get

$$\frac{\partial u}{\partial x} + \frac{\partial v}{\partial y} = 0, \tag{12}$$

$$\frac{\partial u}{\partial t} + u \frac{\partial u}{\partial x} + v \frac{\partial u}{\partial y} = -\frac{1}{\rho} \frac{\partial p}{\partial x} + \nu \frac{\partial^2 u}{\partial y^2}, \tag{13}$$

$$\frac{\partial p}{\partial y} = 0, \tag{14}$$

with the boundary conditions

$$\begin{aligned} u = v = 0 \quad &\text{at} \quad y = 0, \\ u = U(x,t) \quad &\text{as} \quad \frac{y}{\delta} \to \infty. \end{aligned} \tag{15}$$

The above equations describe about the unsteady two-dimensional viscous flow around a wedge profile submerged in incompressible fluid. From the equations (12)-(14), it is clear that the u, v and p are the variables to be determined. Equation (14) shows that the normal pressure gradient is negligible compared with other terms. If $U(x,t)$ is the velocity of the fluid in the potential flow then from the equation (13), we have

$$-\frac{1}{\rho} \frac{\partial p}{\partial x} = \frac{\partial U}{\partial t} + U \frac{\partial U}{\partial x}. \tag{16}$$

The system of equations (12)-(14) with (16) are collectively called as Prandtl boundary layer equations. These equations are simpler form of the Navier-Stokes equation, but the closed form solution for these equations is available only for few cases. However the study of the behavior of solutions of the boundary layer equations governing the flow field has established an important branch of theoretical fluid mechanics [4, 5].

1.3   Boundary layer flow past a wedge

A wedge is a portable inclined plane, and one of the six classical simple machines. It can be used to separate two objects or portions of an object, lift up an object, or hold an object in place. It functions by converting a force applied to its blunt end into forces perpendicular (normal) to its inclined surfaces.

Consider the steady flow around a wedge submerged in an incompressible fluid of very small viscosity. The wedge is placed along the direction of a uniform stream of velocity U_∞. Let the origin of coordinates be at the leading edge of the plate, the x-axis be along the plate and the y-axis normal to the plate. In the present case the potential flow velocity U is given by

$$U(x) = U_1 x^m \tag{17}$$

where U_1 is a constant, $m = \dfrac{\beta}{2 - \beta}$ and $\pi\beta$ is the wedge angle.

The governing boundary layer equations are given by

$$u\frac{\partial u}{\partial x} + v\frac{\partial u}{\partial y} = U\frac{dU}{dx} + \nu\frac{\partial^2 u}{\partial y^2}, \tag{18}$$

$$\frac{\partial u}{\partial x} + \frac{\partial v}{\partial y} = 0, \tag{19}$$

and the corresponding boundary conditions are

$$\begin{aligned} u = v = 0 \quad &\text{at} \quad y = 0, \\ u = U(x) \quad &\text{as} \quad y \to \infty, \end{aligned} \tag{20}$$

where u and v are the components of the velocity in the x and y directions, and ν is the kinematic viscosity.

The stream function $\psi(x, y)$ is introduced such that

$$u = \frac{\partial \psi}{\partial y} \quad \text{and} \quad v = -\frac{\partial \psi}{\partial x} \tag{21}$$

Then, the equation of continuity is identically satisfied and equation (18) reduces to

$$\frac{\partial \psi}{\partial y}\frac{\partial^2 \psi}{\partial x \partial y} - \frac{\partial \psi}{\partial x}\frac{\partial^2 \psi}{\partial y^2} = U\frac{dU}{dx} + \nu\frac{\partial^3 \psi}{\partial y^3}. \tag{22}$$

Using equation (21), the boundary conditions (20) become

$$\begin{aligned} \psi = 0, \ \frac{\partial \psi}{\partial y} = 0, \quad &\text{at} \quad y = 0, \\ \frac{\partial \psi}{\partial y} = U(x), \quad &\text{as} \quad y \to \infty. \end{aligned} \tag{23}$$

Now, we will convert the partial differential equation (22) into an ordinary differential equation. In accordance with the procedure of the law of similarity, let the velocity profile be

$$u = UF(\eta) \tag{24}$$

where

$$\eta = y\sqrt{\frac{(m+1)U}{2\nu x}} = y\sqrt{\frac{(m+1)U_1}{2\nu}}x^{\frac{m-1}{2}} \tag{25}$$

is the similarity variable.

Using equations (21), (24) and (25), the stream function $\psi(x,y)$ is given by

$$\psi = \int u\,dy = \sqrt{\frac{2U_1\nu}{m+1}}x^{\frac{m+1}{2}}\int F(\eta)\,d\eta = \sqrt{\frac{2U_1\nu}{m+1}}x^{\frac{m+1}{2}}f(\eta) \tag{26}$$

where $f(\eta) = \int F(\eta)\,d\eta$.

The velocity components and their derivatives are given by

$$u = \frac{\partial\psi}{\partial y} = U_1 x^m f'(\eta), \tag{27}$$

$$v = -\frac{\partial\psi}{\partial x} = \sqrt{\frac{(m+1)U_1\nu}{2}}x^{\frac{m-1}{2}}\left\{\left(\frac{m-1}{m+1}\right)\eta f'(\eta) - f(\eta)\right\}, \tag{28}$$

$$\frac{\partial u}{\partial x} = \frac{\partial^2\psi}{\partial x\partial y} = U_1 x^{m-1}\left\{mf'(\eta) + \left(\frac{m+1}{2}\right)\eta f''(\eta)\right\}, \tag{29}$$

$$\frac{\partial u}{\partial y} = \frac{\partial^2\psi}{\partial y^2} = U_1\sqrt{\frac{(m+1)U_1}{2\nu}}x^{\frac{3m-1}{2}}f''(\eta), \tag{30}$$

$$\frac{\partial^2 u}{\partial y^2} = \frac{\partial^3\psi}{\partial y^3} = \frac{(m+1)U_1^2}{2\nu}x^{2m-1}f'''(\eta) \tag{31}$$

Substituting equations (27)-(31) in equation (22), we get

$$f'''(\eta) + f(\eta)f''(\eta) + \frac{2m}{m+1}(1 - f'^2(\eta)) = 0, \tag{32}$$

that is,

$$f'''(\eta) + f(\eta)f''(\eta) + \beta(1 - f'^2(\eta)) = 0, \tag{33}$$

and the corresponding boundary conditions are

$$f(\eta) = 0, f'(\eta) = 0, \quad \text{at} \quad \eta = 0,$$
$$f'(\eta) = 1 \quad \text{as} \quad \eta \to \infty. \tag{34}$$

Equation (33) is a third order ordinary differential equation known as **'Hartree's equation'**. It is a particular case of the established Falkner and Skan equation. It is a non linear differential equation whose numerical solutions for different values of β, were first investigated by D. R. Hartree and later by other scientists. [5].

2 Method of Solution

2.1 Power Series Solution

The power series method is used to obtain a power series solution to the Hartree's equation (33).

We construct a series solution of the form

$$f(\eta) = \sum_{k=0}^{\infty} \frac{c_k}{k!}\eta^k = c_0 + c_1\eta + \frac{c_2}{2!}\eta^2 + \frac{c_3}{3!}\eta^3 + \frac{c_4}{4!}\eta^4 + \frac{c_5}{5!}\eta^5 + \dots \tag{35}$$

Then,

$$f'(\eta) = \sum_{k=1}^{\infty} \frac{c_k}{(k-1)!}\eta^{k-1} = c_1 + c_2\eta + \frac{c_3}{2!}\eta^2 + \frac{c_4}{3!}\eta^3 + \frac{c_5}{4!}\eta^4 + \frac{c_6}{5!}\eta^5 + \dots \tag{36}$$

$$f''(\eta) = \sum_{k=2}^{\infty} \frac{c_k}{(k-2)!}\eta^{k-2} = c_2 + c_3\eta + \frac{c_4}{2!}\eta^2 + \frac{c_5}{3!}\eta^3 + \frac{c_6}{4!}\eta^4 + \frac{c_7}{5!}\eta^5 + \dots \tag{37}$$

$$f'''(\eta) = \sum_{k=3}^{\infty} \frac{c_k}{(k-3)!}\eta^{k-3} = c_3 + c_4\eta + \frac{c_5}{2!}\eta^2 + \frac{c_6}{3!}\eta^3 + \frac{c_7}{4!}\eta^4 + \frac{c_8}{5!}\eta^5 \dots \tag{38}$$

Using the boundary conditions (34) in equations (35) and (36), we obtain

$$c_0 = 0, \quad c_1 = 0 \tag{39}$$

Substituting equations (35)-(39) in equation (33), we get

$$\begin{aligned}
&(c_3 + \beta) + c_4\eta + \frac{1}{2}\{c_5 + (1-2\beta)c_2^2\}\eta^2 + \frac{1}{6}\{c_6 + 2(2-3\beta)c_2c_3\}\eta^3 + \frac{1}{6}\{c_6+ \\
&2(2-3\beta)c_2c_3\}\eta^3 + \frac{1}{24}\{c_7 + (7-8\beta)c_2c_4 + 2(2-3\beta)c_3^2\}\eta^4 + \frac{1}{120}\{c_8 \\
&+(11-10\beta)c_2c_5 + 5(3-4\beta)c_3c_4\}\eta^5 + \frac{1}{720}\{c_9 + 4(4-3\beta)c_2c_6 \\
&+2(13-15\beta)c_3c_5 + 5(3-4\beta)c_4^2\}\eta^6 + \frac{1}{5040}\{c_{10} + 2(11-7\beta)c_2c_7 \\
&+42(1-\beta)c_3c_6 + 14(4-5\beta)c_4c_5\}\eta^7 + \cdots\cdots = 0
\end{aligned} \tag{40}$$

This is an identity and hence all coefficients of the various powers of η must vanish identically. Thus, we have

$$\begin{aligned}
c_3 = -\beta, \; c_4 = 0, \; c_5 = -(1-2\beta)c_2^2, \; c_6 = 2(2-3\beta)\beta c_2, \\
c_7 = -2(2-3\beta)\beta^2, \; c_8 = (1-2\beta)(11-10\beta)c_2^3, \\
c_9 = -2(45-113\beta+66\beta^2)\beta c_2^2, \; c_{10} = 16(2-3\beta)(8-7\beta)\beta^2 c_2, \; \dots\dots
\end{aligned} \tag{41}$$

Substituting equations (39) and (41) in equation (35) gives

$$\begin{aligned}
f(\eta) = &\frac{\alpha}{2!}\eta^2 - \frac{\beta}{3!}\eta^3 - \frac{(1-2\beta)\alpha^2}{5!}\eta^5 + \frac{2(2-3\beta)\beta\alpha}{6!}\eta^6 - \frac{2(2-3\beta)\beta^2}{7!}\eta^7 \\
&+ \frac{(1-2\beta)(11-10\beta)\alpha^3}{8!}\eta^8 - \frac{2(45-113\beta+66\beta^2)\beta\alpha^2}{9!}\eta^9 \\
&+ \frac{16(2-3\beta)(8-7\beta)\beta^2\alpha}{10!}\eta^{10} + \cdots
\end{aligned} \tag{42}$$

where $\alpha = c_2 = f''(0)$. We have obtained the value for α numerically for different values of m which is described in the next subsection.

2.2   Numerical Solution

The shooting method [6] is used to obtain a numerical solution to the Hartree's equation (33) along with the boundary conditions (34). Figure 1 shows the velocity distribution in the boundary layer on a wedge for different values of m. The values of the functions f, f' and f'' for different η and m are listed in Table 1.
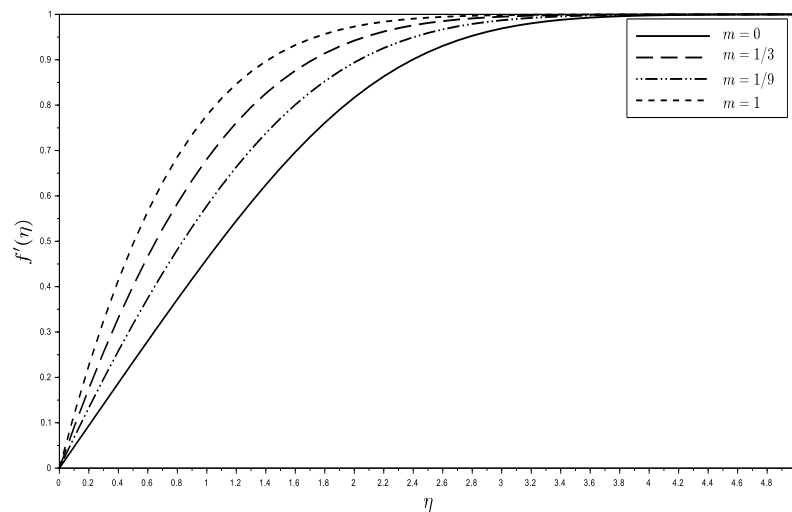
Figure 1: Velocity distribution in the boundary layer on a wedge for different m

Table 1: The functions f, f' and f'' in the boundary layer on a wedge for different η and m

η	$f(\eta)$	$f'(\eta)$	$f''(\eta)$	$f(\eta)$	$f'(\eta)$	$f''(\eta)$
	$m = 0$			$m = 1/3$		
0.0	0.000000	0.000000	0.469600	0.000000	0.000000	0.927680
0.5	0.058643	0.234227	0.465030	0.105553	0.401455	0.678817
1.0	0.232990	0.460633	0.434379	0.381092	0.681115	0.444284
1.5	0.515032	0.661474	0.361805	0.768565	0.852621	0.250801
2.0	0.886797	0.816695	0.255669	1.220038	0.942249	0.118501
2.5	1.322438	0.916808	0.147475	1.702399	0.981165	0.045854
3.0	1.795568	0.969054	0.067711	2.197079	0.994959	0.014324
3.5	2.286407	0.990709	0.024415	2.695765	0.998904	0.003579
4.0	2.783887	0.997770	0.006875	3.195501	0.999808	0.000711
4.5	3.283332	0.999575	0.001509	3.695458	0.999973	0.000112
5.0	3.783235	0.999936	0.000258	4.195453	0.999997	0.000014
5.5	4.283221	0.999992	0.000034	4.695452	1.000000	0.000001
6.0	4.783220	0.999999	0.000004	5.195452	1.000000	0.000000
6.5	5.283220	1.000000	0.000000	5.695452	1.000000	0.000000
	$m = 1/9$			$m = 1$		
0.0	0.000000	0.000000	0.686708	0.000000	0.000000	1.232587
0.5	0.081607	0.317717	0.581817	0.133586	0.494649	0.758307
1.0	0.308206	0.578203	0.456174	0.459228	0.777864	0.398014
1.5	0.648481	0.771022	0.314139	0.887330	0.916167	0.176960
2.0	1.067497	0.893982	0.181944	1.361975	0.973216	0.065827
2.5	1.532776	0.959124	0.085920	1.854430	0.992851	0.020229
3.0	2.020443	0.987106	0.032456	2.352558	0.998424	0.005079
3.5	2.516865	0.996712	0.009706	2.852174	0.999716	0.001033
4.0	3.016027	0.999328	0.002286	3.352110	0.999958	0.000169
4.5	3.515869	0.999890	0.000423	3.852102	0.999995	0.000022
5.0	4.015845	0.999986	0.000061	4.352101	1.000000	0.000002
5.5	4.515842	0.999999	0.000007	4.852100	1.000000	0.000000
6.0	5.015842	1.000000	0.000001	5.352100	1.000000	0.000000
6.5	5.515842	1.000000	0.000000	5.852100	1.000000	0.000000

3   Results and Discussion

The nonlinear ordinary differential equations (33) subject to the boundary conditions in (34) is solved using Power series method. To validate the results obtained, we also have solved this equation using shooting method for certain values of the wedge angle m. Velocity profile is presented for different values of m. The comparisons show excellent agreement between the results obtained for different values of governing parameter.

References

[1] F. Chorlton, *Textbook of fluid dynamics*, CBS Publishers & Distributors Pvt. Ltd., 2004.

[2] D.S. Chandrashekharaiah, L. Debnath, *Continuum mechanics*, Academic Press, 1994.

[3] I.G. Currie, *Fundamental mechanics of fluids*, Marcel Dekker Inc., 2003.

[4] H. Schlichting, K. Gersten, *Boundary layer theory*, Springer, 2004.

[5] J.L. Bansal, *Viscous fluid dynamics*, Oxford & IBH Publishing Co. Pvt. Ltd., 2005.

[6] R.L. Burden, J.D. Faires, *Numerical analysis*, Cengage Learning, 2012.

Study of solution of ordinary differential equations using Haar wavelets

K.D.C. Kesava[1], R.S. Sumana[2] and L.N. Achala[3]

[1,2,3]P. G. Department of Mathematics and Research Centre in Applied Mathematics

M. E. S. College of Arts, Commerce and Science

15th cross, Malleswaram, Bangalore - 560003.

Email ID: [1]kesavakumari158@gmail.com, [2]sumana.shesha@gmail.com, [3]anargund1960@gmail.com

Abstract: Ordinary differential equations arise in the modelling of many physical phenomena. In this paper, we use Haar wavelet method for the numerical solution of initial value problem and boundary value problem and its system of equations. The basic idea of Haar wavelet collocation method is to convert the ordinary differential equation into a system of algebraic equations that involve a finite number of variables. The numerical results are compared with the exact solution to prove the accuracy of the Haar wavelet method.

Keywords: Ordinary differential equations, Initial value problem, Boundary value problem, Haar wavelets, Collocation points.

1   Introduction

The term "Differential equation" was coined by Leibnitz in 1676 for a relationship between the two differentials dx and dy for the two variables x and y. A differential equation is an equation containing the derivative of one or more dependent variables with respect to one or more independent variables. If a differential equations contains only ordinary derivatives of one or more dependent variables with respect to a single independent variables, it is said to be an Ordinary Differential Equation (ODE). Ordinary Differential Equations are applicable in Newton's law of cooling, electrical circuits, modelling free mechanical oscillations, modelling forced mechanical oscillations, computer exercise or activity etc.

Wavelets are mathematical functions that decompose data into different frequency components and then each component is studied with a resolution matched to its scale. Wavelet theory is the result of a multidisciplinary effort that brought together mathematicians, physicists and engineers. This connection has created a flow of ideas that goes well beyond the construction of new bases or transforms. Wavelet theory has become an effective tool for the development of pure and applied mathematics. Wavelets are well-suited for approximating data with sharp discontinuities. Wavelet representation is more accurate and useful in data compression, noise removal, pattern classification and fast scientific computation.

In recent years, the wavelet approach for the solution of PDEs has become very popular. Multi-resolution analysis of wavelets capture local features efficiently as such enables to detect singularities, shocks, irregular structure and transient phenomena exhibited by the analyzed equations. Haar wavelets are based on the functions which were introduced by the Hungarian mathematician Alfred Haar in 1910. Haar's contribution to wavelets is very evident. The Haar wavelets are the simplest of the wavelet families [1].

Chen and Hsiao [2] recommended to expand into the Haar series the highest order derivatives appearing in the differential equation. This idea has been very prolific and it is being abundantly applied for the solution of ODEs. The wavelet coefficients appearing in the Haar series are calculated either using Collocation method or Galerkin method. Chang and Piau [3], Fazal-i-Haq and Ali [4] have solved higher order boundary value and eigenvalue problems using Haar wavelets. Lepik [5] applied the Haar wavelet method along with the segmentation technique to solve differential equations. Lepik [6] used Haar wavelets for solving higher order differential equations. Lepik [7] solved differential equations with the aid of nonuniform Haar wavelets. Dhawan et. al. [8] used wavelet based numerical scheme to solve differential equations. Hsiao and Wu [9] used Haar wavelets to solve time-varying functional differential equations. Khalid et. al. [10] solved Airy differential equation using Haar wavelets. Shi and Cao [11] applied Haar wavelets to solve eigenvalue problems of high order differential equations. Mohammadi et. al. [12] and Yousefi [13] used Legendre wavelets to solve singular ordinary differential equations and Lane-Emden type differential equations respectively.

2   Preliminaries of Haar wavelets

The Haar wavelet family for $x \in [0, 1]$ is defined as follows [1]

$$
h_i(x) = \begin{cases} 1 & \text{for } x \in [\xi_1, \xi_2) \\ -1 & \text{for } x \in [\xi_2, \xi_3) \\ 0 & \text{elsewhere} \end{cases} \tag{1}
$$

where

$$
\xi_1 = \frac{k}{m}, \quad \xi_2 = \frac{k + 0.5}{m}, \quad \xi_3 = \frac{k + 1}{m} \tag{2}
$$

In the above definition $m = 2^n, n = 0, 1, ..., J$ indicates the level of the wavelet; $k = 0, 1, ..., m - 1$ is the translation parameter. J is the maximum level of resolution. The index i in equation (1) is calculated by the formula $i = m + k + 1$. In the case of minimum values $m = 1, k = 0$ we have $i = 2$. The maximum value of i is $i = 2M = 2^{J+1}$.

For $i = 1$, $h_1(x)$ is assumed to be the scaling function which is defined as follows.

$$
h_1(x) = \begin{cases} 1 & \text{for } x \in [0, 1) \\ 0 & \text{elsewhere} \end{cases} \tag{3}
$$

In order to solve integral or differential equations of any order, we need the following integrals.

$$
p_i(x) = \int_0^x h_i(x)dx = \begin{cases} x - \xi_1 & \text{for } x \in [\xi_1, \xi_2) \\ \xi_3 - x & \text{for } x \in [\xi_2, \xi_3) \\ 0 & \text{elsewhere} \end{cases} \tag{4}
$$

$$q_i(x) = \int_0^x p_i(x)dx = \begin{cases} \dfrac{1}{2}(x - \xi_1)^2 & \text{for } x \in [\xi_1, \xi_2) \\[2mm] \dfrac{1}{4m^2} - \dfrac{1}{2}(\xi_3 - x)^2 & \text{for } x \in [\xi_2, \xi_3) \\[2mm] \dfrac{1}{4m^2} & \text{for } x \in [\xi_3, 1] \\[2mm] 0 & \text{elsewhere} \end{cases} \tag{5}$$

3   Method of Solution and Examples

3.1   Ordinary Differential Equation (Initial Value Problem)

Example 1:

$$y'' - 3y' + 2y = 6e^{-x} \tag{6}$$

with initial conditions

$$y(0) = y'(0) = 2 \tag{7}$$

The exact solution is

$$y(x) = 2e^{2x} - e^x + e^{-x} \tag{8}$$

Let the Haar Wavelet solution be in the form

$$y''(x) = \sum_{i=1}^{2M} a_i h_i(x) \tag{9}$$

Integrating equation (9) w.r.t. x from 0 to x and using equation (7) gives

$$y'(x) = 2 + \sum_{i=1}^{2M} a_i p_i(x) \tag{10}$$

Integrating equation (10) w.r.t. x from 0 to x and using equation (7) leads to

$$y(x) = 2 + 2x + \sum_{i=1}^{2M} a_i q_i(x) \tag{11}$$

Substituting equations (9), (10) and (11) in equation (6), we obtain

$$\sum_{i=1}^{2M} a_i \{h_i(x) - 3p_i(x) + 2q_i(x)\} = 2 - 4x + 6e^{-x} \tag{12}$$

The wavelet collocation points are defined as

$$x_l = \frac{l - 0.5}{2M}, \, l = 1, 2, \ldots, 2M. \tag{13}$$

Taking the collocation points $x \to x_l$ in equations (12) and (11), we get

$$\sum_{i=1}^{2M} a_i \{h_i(x_l) - 3p_i(x_l) + 2q_i(x_l)\} = 2 - 4x_l + 6e^{-x_l} \tag{14}$$

$$y(x_l) = 2 + 2x_l + \sum_{i=1}^{2M} a_i q_i(x_l) \tag{15}$$

The wavelet coefficients a_i, $i = 1, 2, \ldots, 2M$ are obtained by solving the $2M$ system of equations in (14). These coefficients are then substituted in equation (15) to obtain the Haar wavelet solution at the collocation points $x_l, l = 1, 2, \ldots, 2M$. The HWCM solution of the example with $J = 8$ is given in Table 1. Figure 1 shows the comparison of the HWCM solution with the exact solution.

3.2 Ordinary Differential Equation (Boundary Value Problem)

Example 2:

$$y'' + y = 1 \tag{16}$$

with boundary conditions

$$y(0) = 0, y(1) = 1 \tag{17}$$

The exact solution is

$$y(x) = -\cos(x) + \cot(1)\sin(x) + 1 \tag{18}$$

Let the Haar Wavelet solution be in the form

$$y''(x) = \sum_{i=1}^{2M} a_i h_i(x) \tag{19}$$

Integrating equation (19) w.r.t. x from 0 to x gives

$$y'(x) = y'(0) + \sum_{i=1}^{2M} a_i p_i(x) \tag{20}$$

Integrating equation (20) w.r.t. x from 0 to x and using equation (17) leads to

$$y(x) = xy'(0) + \sum_{i=1}^{2M} a_i q_i(x) \tag{21}$$

Putting $x = 1$ in (21) and using equation (17), we obtain

$$y'(0) = 1 - \sum_{i=1}^{2M} a_i q_i(1) \tag{22}$$

Substituting equation (22) in equations (20) and (21) we get

$$y'(x) = 1 + \sum_{i=1}^{2M} a_i[p_i(x) - q_i(1)] \tag{23}$$

$$y(x) = x + \sum_{i=1}^{2M} a_i[q_i(x) - xq_i(1)] \tag{24}$$

Substituting equations (24) and (19) in equation (16) gives

$$\sum_{i=1}^{2M} a_i\{h_i(x) + q_i(x) - xq_i(1)\} = 1 - x \tag{25}$$

The wavelet collocation points are defined as

$$x_l = \frac{l - 0.5}{2M}, \, l = 1, 2, \ldots, 2M. \tag{26}$$

Taking the collocation points $x \to x_l$ in equations (25) and (24) leads to

$$\sum_{i=1}^{2M} a_i\{h_i(x_l) + q_i(x_l) - x_l q_i(1)\} = 1 - x_l \tag{27}$$

$$y(x_l) = x_l + \sum_{i=1}^{2M} a_i[q_i(x_l) - x_l q_i(1)] \tag{28}$$

The wavelet coefficients $a_i, \, i = 1, 2, \ldots, 2M$ are obtained by solving the $2M$ system of equations in (27). These coefficients are then substituted in equation (28) to obtain the Haar wavelet solution at the collocation points $x_l, l = 1, 2, \ldots, 2M$. The HWCM solution of the example with $J = 6$ is given in Table 2. Figure 2 shows the comparison of the HWCM solution with the exact solution.

3.3 System of Ordinary Differential Equations (Initial Value Problem)

Example 3:

$$u' = v - x \tag{29}$$

$$v' = u + x \tag{30}$$

with initial conditions

$$u(0) = v(0) = 1 \tag{31}$$

The exact solutions are

$$u(x) = e^x - e^{-x} - x + 1 \tag{32}$$

$$v(x) = e^x + e^{-x} + x - 1 \tag{33}$$

Let the Haar Wavelet solutions be in the form

$$u'(x) = \sum_{i=1}^{2M} a_i h_i(x) \tag{34}$$

$$v'(x) = \sum_{i=1}^{2M} b_i h_i(x) \tag{35}$$

Integrating equations (34) and (32) w.r.t. x from 0 to x, and using equation equation (31) gives

$$u(x) = 1 + \sum_{i=1}^{2M} a_i p_i(x) \tag{36}$$

$$v(x) = 1 + \sum_{i=1}^{2M} b_i p_i(x) \tag{37}$$

Substituting equations (34) and (37) in equation (29), and equations (35) and (36) in equation (30), we get

$$\sum_{i=1}^{2M} \{a_i h_i(x) - b_i p_i(x)\} = 1 - x \tag{38}$$

$$\sum_{i=1}^{2M} \{a_i p_i(x) - b_i h_i(x)\} = -1 - x \tag{39}$$

The wavelet collocation points are defined as

$$x_l = \frac{l - 0.5}{2M}, \, l = 1, 2, \ldots, 2M. \tag{40}$$

Taking the collocation points $x \to x_l$ in equations (38), (39), (36) and (37), we obtain

$$\sum_{i=1}^{2M} \begin{bmatrix} h_i(x_l) & -p_i(x_l) \\ p_i(x_l) & -h_i(x_l) \end{bmatrix} \begin{bmatrix} a_i \\ b_i \end{bmatrix} = \begin{bmatrix} 1 - x_l \\ -1 - x_l \end{bmatrix} \tag{41}$$

$$u(x_l) = 1 + \sum_{i=1}^{2M} a_i p_i(x_l) \tag{42}$$

$$v(x_l) = 1 + \sum_{i=1}^{2M} b_i p_i(x_l) \tag{43}$$

The wavelet coefficients $a_i, b_i \, i = 1, 2, \ldots, 2M$ are obtained by solving the $4M$ system of equations in (41). These coefficients are then substituted in equation (42) and (43) to obtain the Haar wavelet solutions at the collocation points $x_l, l = 1, 2, \ldots, 2M$. The HWCM solution of the example with $J = 6$ is given in Table 3. Figure 3 shows the comparison of the HWCM solution with the exact solution.

3.4 System of Ordinary Differential Equations (Boundary Value Problem)

Example 4:

$$u'' = 2v' - 5u + 4e^x \tag{44}$$

$$v'' = 6u' + 15v + 4e^x \tag{45}$$

with boundary conditions

$$u(0) = 1, \, v(0) = 1,$$

$$u(1) = \frac{1}{2} e(e^4 + 1), \tag{46}$$

$$v(1) = \frac{1}{2} e(3e^4 - 1)$$

The exact solutions are

$$u(x) = \frac{1}{2} e^x (e^{4x} + 1) \tag{47}$$

$$v(x) = \frac{1}{2}e^x(3e^{4x} - 1) \tag{48}$$

Let the Haar Wavelet solutions be in the form

$$u''(x) = \sum_{i=1}^{2M} a_i h_i(x) \tag{49}$$

$$v''(x) = \sum_{i=1}^{2M} b_i h_i(x) \tag{50}$$

Integrating equation (49) and (50) w.r.t. x from 0 to x gives

$$u'(x) = u'(0) + \sum_{i=1}^{2M} a_i p_i(x) \tag{51}$$

$$v'(x) = v'(0) + \sum_{i=1}^{2M} b_i p_i(x) \tag{52}$$

Integrating equation (51) and (52) w.r.t. x from 0 to x, and using equation (46) leads to

$$u(x) = 1 + u'(0)x + \sum_{i=1}^{2M} a_i q_i(x) \tag{53}$$

$$v(x) = 1 + v'(0)x + \sum_{i=1}^{2M} b_i q_i(x) \tag{54}$$

Putting $x = 1$ in equations (53) and (54), and using equation (46) we get

$$u'(0) = \frac{1}{2}e(e^4 + 1) - 1 - \sum_{i=1}^{2M} a_i q_i(1) \tag{55}$$

$$v'(0) = \frac{1}{2}e(3e^4 - 1) - 1 - \sum_{i=1}^{2M} b_i q_i(1) \tag{56}$$

Substituting equation (55) in equations (51) and (53), and equation (56) in equations (52) and (54), we obtain

$$u'(x) = \frac{1}{2}e(e^4 + 1) - 1 + \sum_{i=1}^{2M} a_i[p_i(x) - q_i(1)] \tag{57}$$

$$v'(x) = \frac{1}{2}e(3e^4 - 1) - 1 + \sum_{i=1}^{2M} b_i[p_i(x) - q_i(1)] \tag{58}$$

$$u(x) = 1 + \frac{1}{2}xe(e^4 + 1) - x + \sum_{i=1}^{2M} a_i[q_i(x) - xq_i(1)] \tag{59}$$

$$v(x) = 1 + \frac{1}{2}xe(3e^4 - 1) - x + \sum_{i=1}^{2M} b_i[q_i(x) - xq_i(1)] \tag{60}$$

Substituting equations (49), (58) and (59) in equation (44), and equations (50), (57) and (60) in equation (45) gives

$$\sum_{i=1}^{2M}\{a_i[h_i(x) + 5q_i(x) - 5xq_i(1)] + b_i[-2p_i(x) + 2q_i(1)]\} = -7 + 5x + 4e^x$$
$$+e(3e^4 - 1) - \frac{5}{2}xe(e^4 + 1) \tag{61}$$

$$\sum_{i=1}^{2M}\{a_i[-6p_i(x) + 6q_i(1)] + b_i[h_i(x) - 15q_i(x) + 15xq_i(1)]\} = 9 - 15x + 4e^x$$
$$+3e(e^4 + 1) + \frac{15}{2}xe(3e^4 - 1) \tag{62}$$

The wavelet collocation points are defined as

$$x_l = \frac{l - 0.5}{2M}, \, l = 1, 2, \ldots, 2M. \tag{63}$$

Taking the collocation points $x \to x_l$ in equations (61), (62), (59) and (60), we obtain

$$\begin{bmatrix} h_i(x_l) + 5q_i(x_l) - 5x_lq_i(1) & -2p_i(x_l) + 2q_i(1) \\ -6p_i(x_l) + 6q_i(1) & h_i(x_l) - 15q_i(x_l) + 15x_lq_i(1) \end{bmatrix} \begin{bmatrix} a_i \\ b_i \end{bmatrix} =$$
$$\begin{bmatrix} -7 + 5x_l + 4e^{x_l} + e(3e^4 - 1) - \frac{5}{2}x_le(e^4 + 1) \\ 9 - 15x_l + 4e^{x_l} + 3e(e^4 + 1) + \frac{15}{2}x_le(3e^4 - 1) \end{bmatrix} \tag{64}$$

$$u(x_l) = 1 + \frac{1}{2}x_le(e^4 + 1) - x_l + \sum_{i=1}^{2M} a_i[q_i(x_l) - x_lq_i(1)] \tag{65}$$

$$v(x_l) = 1 + \frac{1}{2}x_le(3e^4 - 1) - x_l + \sum_{i=1}^{2M} b_i[q_i(x_l) - x_lq_i(1)] \tag{66}$$

The wavelet coefficients a_i, b_i $i = 1, 2, \ldots, 2M$ are obtained by solving the $4M$ system of equations in (64). These coefficients are then substituted in equation (65) and (66) to obtain the Haar wavelet solutions at the collocation points $x_l, l = 1, 2, \ldots, 2M$. The HWCM solution of the example with $J = 8$ is given in Table 4. Figure 4 shows the comparison of the HWCM solution with the exact solution.

Table 1: Comparison of HWCM solution and exact solution for $J = 8$ at different x of Example 1

x	$y(x)$	
	HWCM	Exact
0.000977	2.001957	2.001957
0.100586	2.244159	2.244159
0.200195	2.581746	2.581745
0.301758	3.044358	3.044355
0.499023	4.385975	4.385967
0.598633	5.352047	5.352035
0.698242	6.569198	6.569180
0.799805	8.126534	8.126506
0.899414	10.033808	10.033770
0.990230	12.401941	12.401887

Table 2: Comparison of HWCM solution and exact solution for $J = 6$ at different x of Example 2

x	$y(x)$	
	HWCM	Exact
0.003906	0.002516	0.002516
0.105469	0.073152	0.073152
0.207031	0.153340	0.153340
0.300781	0.235125	0.235125
0.496094	0.426184	0.426184
0.597656	0.534653	0.534653
0.699219	0.647919	0.647918
0.792969	0.755719	0.755719
0.894531	0.874894	0.874894
0.996094	0.995358	0.995358

Table 3: Comparison of HWCM solution and exact solution for $J = 6$ at different x of Example 3

x	$u(x)$		$v(x)$	
	HWCM	Exact	HWCM	Exact
0.003906	1.003906	1.003906	1.003937	1.003922
0.105469	1.105863	1.105860	1.116618	1.116618
0.207031	1.210001	1.209996	1.250063	1.250047
0.300781	1.309901	1.309893	1.391952	1.391935
0.496094	1.537309	1.537295	1.747312	1.747292
0.597656	1.670114	1.670098	1.965631	1.965609
0.699219	1.816008	1.815988	2.208397	2.208372
0.792969	1.964503	1.964479	2.455443	2.455416
0.894531	2.142887	2.142858	2.749550	2.749519
0.996094	2.342305	2.342271	3.073133	3.073097

Table 4: Comparison of HWCM solution and exact solution for $J = 8$ at different x of Example 4

x	$u(x)$		$v(x)$	
	HWCM	Exact	HWCM	Exact
0.000977	1.002935	1.002936	1.006854	1.006854
0.100586	1.379601	1.379689	1.927471	1.927429
0.200195	1.971125	1.971290	3.470632	3.470586
0.301758	2.936509	2.936743	6.105781	6.105762
0.499023	6.884791	6.885133	17.361071	17.361175
0.598633	10.883787	10.884166	29.013045	29.013238
0.698242	17.417552	17.417945	48.233120	48.233402
0.799805	28.384615	28.384982	80.704393	80.704733
0.899414	46.105713	46.105979	133.401316	133.401612
0.999023	75.202916	75.202940	220.177561	220.177563
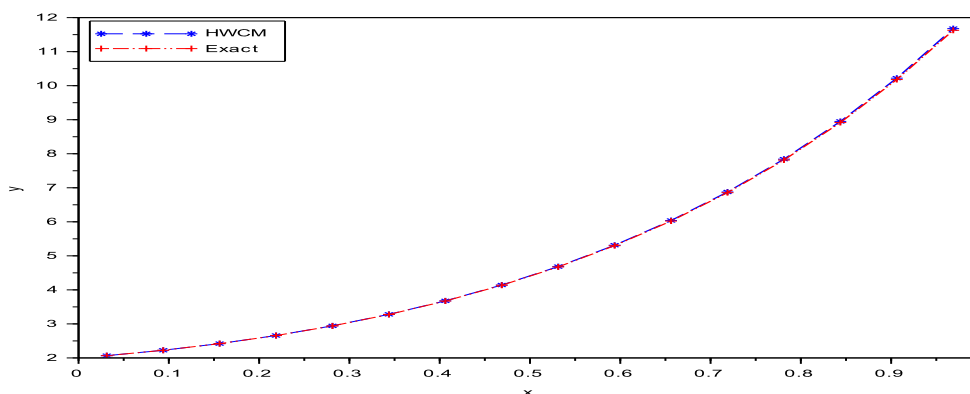
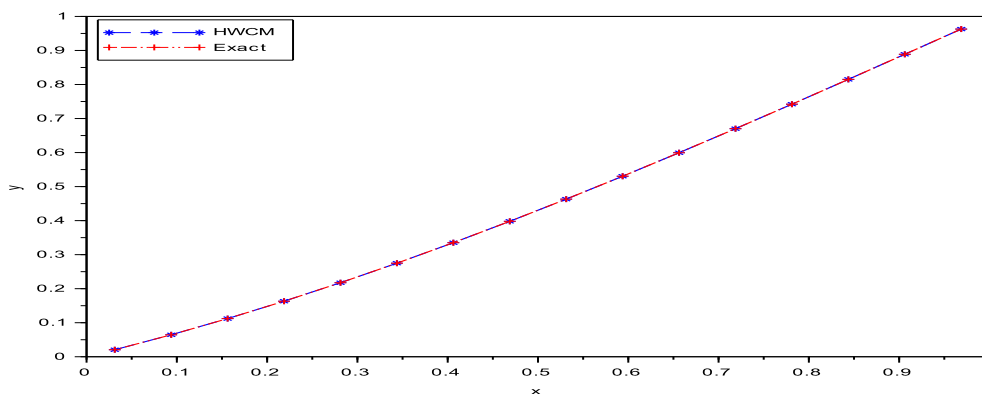**Figure 1:** Comparison of HWCM solution and exact solution of Example 1

Figure 2: Comparison of HWCM solution and exact solution of Example 2
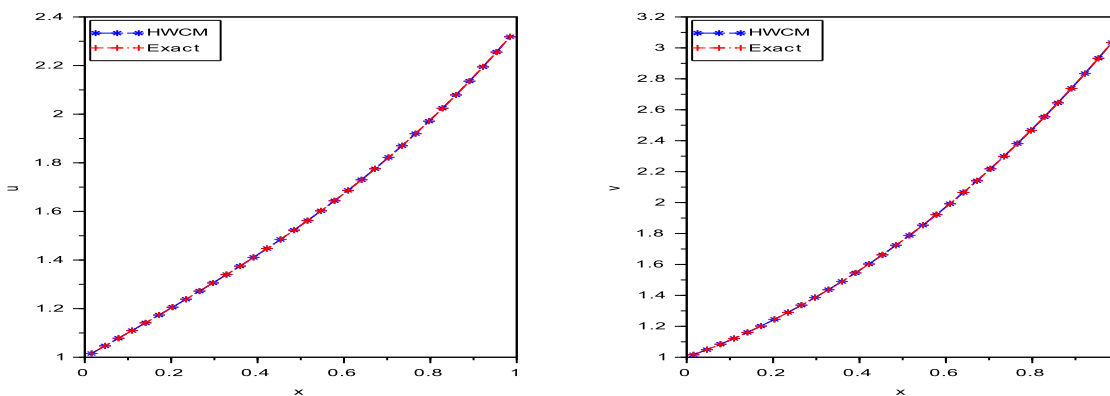

Figure 3: Comparison of HWCM solution and exact solution of Example 3
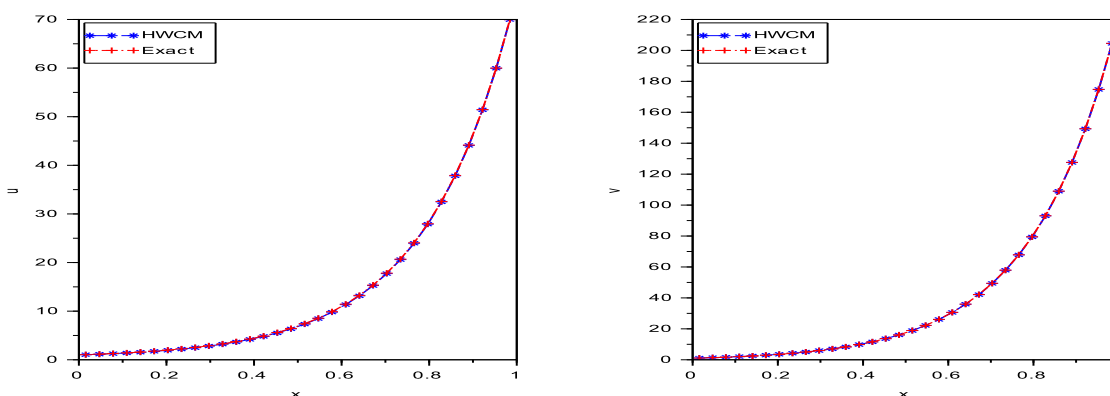

Figure 4: Comparison of HWCM solution and exact solution of Example 4

4   Conclusion

In this paper, an efficient numerical scheme based on uniform Haar wavelets is used to solve ordinary differential equations. The numerical scheme is tested for four examples. The ob-

tained numerical results are compared with the exact solutions, and are found to be in good agreement. Also,the method does not require conversion of a boundary value problem into initial value problem by using shooting like procedure and hence has higher stability. Thus the Haar wavelet method guarantees the necessary accuracy with a small number of grid points.

References

[1] U. Lepik, H. Hein, *Haar wavelets with applications*, Springer, 2014.

[2] C.F. Chen, C.H. Hsiao, *Haar wavelet method for solving lumped and distributed-parameter systems*, IEE Proc.-Control Theory Appl. 144(1) (1997) 87-94.

[3] P. Chang, P. Piau, *Haar wavelet matrices designation in numerical solution of ordinary differential equations*, Int. J. Appl. Math. 38 (2008) 164-168.

[4] Fazal-i-Haq, A. Ali, *Numerical solution of fourth-order boundary-value problems using Haar wavelets*, Appl. Math. Sci. 5 (2011) 61-64.

[5] U. Lepik, *Numerical solution of differential equations using Haar wavelets*, Math. Comput. Simul. 68 (2005) 127-143.

[6] U. Lepik, *Haar wavelet method for solving higher order differential equations*, Int. J. Math. Comput. 1 (2008) 84-94.

[7] U. Lepik, *Solving integral and differential equations by the aid of nonuniform Haar wavelets*, Appl. Math. Comput. 198 (2008) 326-332.

[8] S. Dhawan, S. Arora, S. Kumar, *Wavelet based numerical scheme for differential equations*, Int. J. Diff. Eqns. Appl. 12(2) (2013) 85-94.

[9] C. Hsiao S. Wu, *Numerical solution of time-varying functional differential equations via Haar wavelets*, Appl. Math. Comput. 188 (2007) 1049-1058.

[10] M. Khalid, M. Sultana, F. Zaidi , *Numerical solution of Airy differential equation by using Haar wavelet*, Math. Th. Model. 4(10) (2014) 142-148.

[11] Z. Shi, Y. Cao, *Application of Haar wavelet method to eigenvalue problems of high order differential equations*, Appl. Math. Model. 9 (2012) 4020-4026.

[12] F. Mohammadi, M. Hosseini, *A new Legendre wavelet operational matrix of derivative and its applications in solving the singular ordinary differential equations*, J. Franklin Inst. 348 (2011) 1787-1796.

[13] S. Yousefi, *Legendre wavelets method for solving differential equations of Lane-Emden type*, Appl. Math. Comput. 181 (2006) 1417-1422.

Mathematical modelling of Cryptography

N. Manjunatha[1], B.J. Varsha[2] and L.N. Achala[3]

[1,2,3]P. G. Department of Mathematics and Research Centre in Applied Mathematics

M. E. S. College of Arts, Commerce and Science

15th cross, Malleswaram, Bangalore - 560003.

Email ID: [1]manjunathan1794@gmail.com, [2]bjvarsha@gmail.com, [3]anargund1960@gmail.com

Abstract: Cryptography is the art of constructing and analyzing codes or messages that prevent third parties or the public from reading private messages. In this paper we encode and decode different messages using Substitution ciphers as well as Hill ciphers.

Keywords: Cryptography, Encoding, Decoding, Substitution ciphers, Hill ciphers.

1 Introduction

Mathematical Modelling is a technique which essentially consists of translating real world problems into mathematical problems, solving the mathematical problems and interpreting these solutions in the language of the real world. In other words, mathematical modelling is a method of simulating real life situations with mathematical equations to forecast their future behaviour [1].

The word Cryptography has its origin from the Greek words where *Kryptos* means "hidden" and *graphein* is "to write", meaning to write messages in secret codes [3]. Data that can be read and understood without any special measures is called *plain text*. The method of disguising the plain text in such a way as to hide its substance is called ***Encryption***. Encrypting plain text results in meaningless letters called *cipher text*. The reverse of encryption is decryption. The process of reverting the cipher texts to its original plain text is called ***Decryption***.

$$\text{Plain text} \xrightarrow{\text{Encryption}} \text{Cipher text} \xrightarrow{\text{Decryption}} \text{Plain text}$$

Encryption and decryption requires the use of some secret information, usually referred to as a **key**. The key is usually a short string of characters. Here we use the key in the form of a matrix. The matrix used for encrypting (or encoding) a message is called Encoding matrix. The matrix used to decrypt (or decode) a message is called Decoding matrix. One type of code that is difficult to break makes use of a large matrix to encode a message. The receiver of the message decodes the message using the inverse of the matrix [3] [4].

Applications of cryptography include data confidentiality and secrecy in transmissions, data integrity, authentication, military communications, electronic banking and computer passwords [5].

2 Method of Solution

2.1 Encoding a message when Enciphering matrix is known

METHOD 1: Using Substitution Ciphers

- Convert the message into the numeric code using the alpha-numerical substitution starting with $A = 1$ to $Z = 26$.
- Group the code into a sequence of 3×1 or 2×1 matrix depending on the order of the enciphering matrix. Writing all these numeric codes together we name it as matrix P.
- Find $C = AP$ where A is the enciphering matrix and P is the matrix containing numeric code corresponding to the plain text vectors.
- Finally, convert the elements in C into a string that becomes the encrypted message. Now the code has been enciphered. [3]

METHOD 2: Using Hill Ciphers

1. Convert the message into the numeric code using the alpha-numerical substitution starting with $A = 0$ to $Z = 25$.
2. Group the code into a sequence of 3×1 or 2×1 matrix depending on the order of the enciphering matrix. Writing all these numeric codes together we name it as matrix P.
3. Find $C = AP$ where A is the enciphering matrix and P is the matrix containing numeric code corresponding to the plain text vectors. If possible, replace each new vector by its residue modulo 26.
4. Finally, convert each entry in C into its corresponding position in the alphabet. Now the code has been enciphered. [5]

2.2   Decoding a message when Enciphering matrix is known

METHOD 1: Using Substitution Ciphers

- Group the given code into a sequence of 3×1 or 2×1 matrix depending on the order of the enciphering matrix. Write all these numeric codes together in a matrix and name it as C.
- Find the inverse of the enciphering matrix A i.e $A^{-1} = \dfrac{\text{adj} A}{|A|}$
- We know that $C = AP$, so compute $P = A^{-1}C$.
- Finally, convert the resultant matrix codes into their respective letters. Thus the code has been decrypted.

METHOD 2: Using Hill Cipher

1. Convert the given text into their corresponding numeric codes using Hill Cipher substitution.
2. Group the given code into a sequence of 3×1 or 2×1 matrix, depending on the order of the enciphering matrix. Write all these numeric codes together in matrix C.
3. Find the inverse of the enciphering matrix A i.e $A^{-1} = d^{-1}$ adj A where $\dfrac{1}{|A|} = \dfrac{1}{d} = d^{-1}$

   and d^{-1} is such that $d.d^{-1} \equiv 1(\text{mod } 26)$
4. Now compute $P = A^{-1}C$
5. Finally, convert the resultant matrix codes into their respective letters. Thus the code has been decrypted.

2.3   Deciphering a message when Enciphering matrix is not known using Hill Ciphers

The intercepted code or cipher text can also be deciphered without knowing the enciphering matrix. If a minimum of four letters of cipher text can be correctly matched to the plain text, then the message can be deciphered.

1. Suppose the code $c_1c_2c_3c_4$ correspond to the plain text $p_1p_2p_3p_4$ then $C_1 = \begin{bmatrix} c_1 & c_3 \\ c_2 & c_4 \end{bmatrix}$ $P_1 = \begin{bmatrix} p_1 & p_3 \\ p_2 & p_4 \end{bmatrix}$. Convert the given text into their corresponding numeric codes using Hill Cipher substitution.

2. Group the given code into a sequence of 3×1 or 2×1 matrix depending on the order of the matrix C_1. Write all these numeric codes together and name it as matrix C.

3. To find A^{-1}, we know that $P = A^{-1}C \implies A^{-1} = P_1C_1^{-1}$. To find C_1^{-1} follow the same procedure as in decoding of a message when enciphering matrix is known.

4. Now compute $P = A^{-1}C$ where C is the matrix containing the entire cipher text or code vectors.

5. At the end, convert the resultant matrix codes into their respective letters. Thus the code has been decrypted.

3   Examples and Discussion

In this section we consider a few examples to check the above explained methods of encoding and decoding.

Example 1: Encode the message " $THE\ BRITISH\ ARE\ COMING$ " using the matrix $\begin{bmatrix} 1 & 2 & 1 \\ 2 & 3 & 1 \\ -2 & 0 & 1 \end{bmatrix}$.

Solution: Assigning each alphabet to their respective numeric code and breaking the message into a sequence of 3×1 column matrices as follows, we have

$$
\begin{array}{llll}
T \to \begin{bmatrix} 20 \\ 8 \\ 5 \end{bmatrix} &
* \to \begin{bmatrix} 27 \\ 2 \\ 18 \end{bmatrix} &
I \to \begin{bmatrix} 9 \\ 20 \\ 9 \end{bmatrix} &
S \to \begin{bmatrix} 19 \\ 8 \\ 27 \end{bmatrix} \\
H \to & B \to & T \to & H \to \\
E \to & R \to & I \to & * \to
\end{array}
$$

$$
\begin{array}{llll}
A \to \begin{bmatrix} 1 \\ 18 \\ 5 \end{bmatrix} &
* \to \begin{bmatrix} 27 \\ 3 \\ 15 \end{bmatrix} &
M \to \begin{bmatrix} 13 \\ 9 \\ 14 \end{bmatrix} &
G \to \begin{bmatrix} 7 \\ 27 \\ 27 \end{bmatrix} \\
R \to & C \to & I \to & * \to \\
E \to & O \to & N \to & * \to
\end{array}
$$

Inorder to complete the last matrix, we add a space at the end of the message. Writing all the numeric codes together in the matrix P we get, $P = \begin{bmatrix} 20 & 27 & 9 & 19 & 1 & 27 & 13 & 7 \\ 8 & 2 & 20 & 8 & 18 & 3 & 9 & 27 \\ 5 & 18 & 9 & 27 & 5 & 15 & 14 & 27 \end{bmatrix}$ and the given enciphering matrix is $A = \begin{bmatrix} 1 & 2 & 1 \\ 2 & 3 & 1 \\ -2 & 0 & 1 \end{bmatrix}$

Now compute $C = AP = \begin{bmatrix} 41 & 49 & 58 & 62 & 42 & 48 & 45 & 88 \\ 69 & 78 & 87 & 89 & 61 & 78 & 67 & 122 \\ -35 & -36 & -9 & -11 & 3 & -39 & -12 & 13 \end{bmatrix}$

The columns of the above matrix transmitted in the following linear form gives the encoded message which is

$$
\begin{array}{cccccccccccc}
41, & 69, & -35, & 49, & 78, & -36, & 58, & 87, & -9, & 62, & 89, & -11 \\
42, & 61, & 3, & 48, & 78, & -39, & 45, & 67, & -12, & 88, & 95, & 13
\end{array}
$$

Thus the code had been encrypted. When the third party receives this message they will not be able to make the original message.

Example 2: Encipher the plain text "$NOANSWER$" with the enciphering matrix $\begin{bmatrix} 2 & 3 \\ 7 & 8 \end{bmatrix}$.

Solution: Converting plain text vector by Hill ciphers and breaking the message into a sequence of 2×1 column matrices, the message becomes

$$N \rightarrow \begin{bmatrix} 13 \\ 14 \end{bmatrix} \quad A \rightarrow \begin{bmatrix} 0 \\ 13 \end{bmatrix} \quad S \rightarrow \begin{bmatrix} 18 \\ 22 \end{bmatrix} \quad E \rightarrow \begin{bmatrix} 4 \\ 17 \end{bmatrix}$$

Writing all the numeric codes together in the matrix P, we get $P = \begin{bmatrix} 13 & 0 & 18 & 4 \\ 14 & 13 & 22 & 17 \end{bmatrix}$ and the

given enciphering matrix is $A = \begin{bmatrix} 2 & 3 \\ 7 & 8 \end{bmatrix}$

Now compute $C = AP = \begin{bmatrix} 68 & 39 & 102 & 59 \\ 203 & 104 & 302 & 164 \end{bmatrix} \equiv \begin{bmatrix} 16 & 13 & 24 & 7 \\ 21 & 0 & 16 & 8 \end{bmatrix}$ (mod 26)

Convert each entry in the above matrix into their respective letters.

$$\begin{bmatrix} 16 \\ 21 \end{bmatrix} \rightarrow \begin{matrix} Q \\ V \end{matrix} \begin{bmatrix} 13 \\ 0 \end{bmatrix} \rightarrow \begin{matrix} N \\ A \end{matrix} \begin{bmatrix} 24 \\ 16 \end{bmatrix} \rightarrow \begin{matrix} Y \\ Q \end{matrix} \begin{bmatrix} 7 \\ 8 \end{bmatrix} \rightarrow \begin{matrix} H \\ I \end{matrix}$$

Transmitting the entries in the linear form we get " $QVNAYQHI$ ".
Thus the code had been encrypted.

Example 3: Decode the message $71, 100, -1, 28, 43, -5, 84, 122, -11, 63, 98, -27, 69, 102,$
$-12, 88, 126, -3$ using the matrix $\begin{bmatrix} 1 & 2 & 1 \\ 2 & 3 & 1 \\ -2 & 0 & 1 \end{bmatrix}$.

Solution: The given enciphering matrix is a 3×3 matrix and hence we break the code into a

sequence of 3×1 column matrices as $C = \begin{bmatrix} 71 & 28 & 84 & 63 & 69 & 88 \\ 100 & 43 & 122 & 98 & 102 & 126 \\ -1 & -5 & -11 & -27 & -12 & -3 \end{bmatrix}$

The given enciphering matrix is $A = \begin{bmatrix} 1 & 2 & 1 \\ 2 & 3 & 1 \\ -2 & 0 & 1 \end{bmatrix}$

$\implies A^{-1} = \begin{bmatrix} 3 & -2 & -1 \\ -4 & 3 & 1 \\ 6 & -4 & -1 \end{bmatrix}$ which is the deciphering matrix

Compute $P = A^{-1}C = \begin{bmatrix} 14 & 3 & 19 & 20 & 15 & 15 \\ 15 & 12 & 19 & 15 & 18 & 23 \\ 27 & 1 & 27 & 13 & 18 & 27 \end{bmatrix}$

Now convert the codes in the above matrix into their respective letters and transmit in the linear form and we get message as

14	15	27	3	12	1	19	19	27	20	15	13	15	18	18	15	23
N	O	*	C	L	A	S	S	*	T	O	M	O	R	R	O	W

NO CLASS TOMORROW

Thus the code has been decrypted and we can observe that if A changes then the resultant matrix also changes resulting in some gibberish message.

Example 4: Decipher the code "$SAKNOXAOJX$ " with the enciphering matrix $\begin{bmatrix} 4 & 1 \\ 3 & 2 \end{bmatrix}$.

Solution: Converting the plain text vector by Hill ciphers and breaking the message into a sequence of 2×1 column matrices as follows, we obtain

$$S \rightarrow \begin{bmatrix} 19 \\ 1 \end{bmatrix} \quad K \rightarrow \begin{bmatrix} 11 \\ 14 \end{bmatrix} \quad O \rightarrow \begin{bmatrix} 15 \\ 24 \end{bmatrix} \quad A \rightarrow \begin{bmatrix} 1 \\ 15 \end{bmatrix} \quad J \rightarrow \begin{bmatrix} 10 \\ 24 \end{bmatrix}$$

Writing all the numeric codes together in the matrix C, we get $C = \begin{bmatrix} 19 & 11 & 15 & 1 & 10 \\ 1 & 14 & 24 & 15 & 24 \end{bmatrix}$

The given enciphering matrix is $A = \begin{bmatrix} 4 & 1 \\ 3 & 2 \end{bmatrix} \implies |A| = 5 = d$

$$\implies d^{-1} = (5)^{-1} \equiv 21 \ (\text{mod } 26) \quad (\because 5 \times 21 \equiv 1 \ (\text{mod } 26))$$

$\therefore \ A^{-1} = 21 \begin{bmatrix} 2 & -1 \\ -3 & 4 \end{bmatrix} = \begin{bmatrix} 42 & -21 \\ -63 & 84 \end{bmatrix} \equiv \begin{bmatrix} 16 & 5 \\ 15 & 6 \end{bmatrix} (\text{mod } 26)$, which is the deciphering matrix.

Compute $P = A^{-1}C = \begin{bmatrix} 309 & 246 & 360 & 91 & 280 \\ 291 & 249 & 369 & 105 & 294 \end{bmatrix} \equiv \begin{bmatrix} 23 & 12 & 22 & 13 & 20 \\ 5 & 15 & 5 & 1 & 9 \end{bmatrix} (\text{mod } 26)$

Convert each entry in the above matrix into their respective letters and transmit in the linear form we get the message as

23	5	12	15	22	5	13	1	20	9
W	E	L	O	V	E	M	A	T	H

WE LOVE MATH

Thus the code has been decoded.

Example 5: You intercept the message "$FBRTLWUGAJQINZTHHXTEPHBNXSW$", which you know was encoded using a linear transformation of trigraphs in the $26-$ letter alphabet $A - Z$ with numerical equivalents $0 - 25$. You also know that last three trigraphs are the senders signature "$JAMESBOND$". Find the deciphering matrix and read the message.

Solution: The cipher text $TEPHBNXSW$ corresponding to the plain text $JAMESBOND$

The matrix C_1 is made up from $TEPHBNXSW$

$$\begin{matrix} T \rightarrow \begin{bmatrix} 19 \\ 4 \\ 15 \end{bmatrix} & H \rightarrow \begin{bmatrix} 7 \\ 1 \\ 13 \end{bmatrix} & X \rightarrow \begin{bmatrix} 23 \\ 18 \\ 22 \end{bmatrix} \end{matrix} \implies C_1 = \begin{bmatrix} 19 & 7 & 23 \\ 4 & 1 & 18 \\ 15 & 13 & 22 \end{bmatrix}$$

The matrix P_1 is made up from $JAMESBOND$

$$\begin{matrix} J \rightarrow \begin{bmatrix} 9 \\ 0 \\ 12 \end{bmatrix} & E \rightarrow \begin{bmatrix} 4 \\ 18 \\ 1 \end{bmatrix} & O \rightarrow \begin{bmatrix} 14 \\ 13 \\ 3 \end{bmatrix} \end{matrix} \implies P_1 = \begin{bmatrix} 9 & 4 & 14 \\ 0 & 18 & 13 \\ 12 & 1 & 3 \end{bmatrix}$$

To find A^{-1}, compute $A^{-1} = P_1 C_1^{-1}$

Given $C_1 = \begin{bmatrix} 19 & 7 & 23 \\ 4 & 1 & 18 \\ 15 & 13 & 22 \end{bmatrix} \implies |C_1| = -1903 \equiv 21 \ (\text{mod } 26) = d$

$$\implies d^{-1} = 21^{-1} \equiv 5 \ (\text{mod } 26)$$

$\therefore C_1^{-1} = 5 \begin{bmatrix} 22 & 15 & 25 \\ 0 & 21 & 10 \\ 11 & 14 & 17 \end{bmatrix} = \begin{bmatrix} 110 & 75 & 125 \\ 0 & 105 & 50 \\ 55 & 70 & 85 \end{bmatrix} \equiv \begin{bmatrix} 6 & 23 & 21 \\ 0 & 1 & 24 \\ 3 & 18 & 7 \end{bmatrix} \ (\text{mod } 26)$

On substituting, we get $A^{-1} = \begin{bmatrix} 96 & 463 & 383 \\ 39 & 252 & 523 \\ 81 & 331 & 297 \end{bmatrix} \equiv \begin{bmatrix} 18 & 21 & 19 \\ 13 & 18 & 3 \\ 3 & 19 & 11 \end{bmatrix} \ (\text{mod } 26)$

Now we should find the full plain text message,

where $C = \begin{bmatrix} 5 & 19 & 20 & 9 & 13 & 7 & 19 & 7 & 23 \\ 1 & 11 & 6 & 16 & 25 & 7 & 4 & 1 & 18 \\ 17 & 22 & 0 & 8 & 19 & 23 & 15 & 13 & 22 \end{bmatrix}$

i.e., $P = A^{-1}C = \begin{bmatrix} 434 & 991 & 486 & 650 & 1120 & 710 & 711 & 394 & 1210 \\ 128 & 445 & 332 & 333 & 526 & 244 & 340 & 142 & 581 \\ 221 & 508 & 174 & 419 & 723 & 407 & 298 & 83 & 653 \end{bmatrix}$

$\equiv \begin{bmatrix} 18 & 3 & 18 & 0 & 2 & 8 & 9 & 4 & 14 \\ 4 & 17 & 4 & 13 & 0 & 0 & 0 & 18 & 13 \\ 13 & 14 & 18 & 3 & 21 & 17 & 12 & 1 & 3 \end{bmatrix} \ (\text{mod } 26)$

Convert each entry in the above matrix into their respective letters and transmit the entries in the linear form, we arrive at

18	4	13	3	17	14	18	4	18	0	13	3
S	E	N	D	R	O	S	E	S	A	N	D

2	0	21	8	0	17	9	0	12	4	18	1	14	13	3
C	A	V	I	A	R	J	A	M	E	S	B	O	N	D

SEND ROSES AND CAVIAR JAMES BOND

The message is now decoded. By this we can notice that knowing the entire matrix is not needed. Even if we know a few code words we can decode the message.

4 Conclusion

In this paper, we have just given an introduction to what Cryptography is. We can observe that the same plain text encrypts to different cipher text with different keys(matrices). If the recipient does not know the *right key*, they will not be able to decode the received message properly, which makes our message secure. Any classified information can be shared between two individuals or groups, so that even if others get a hold of the message they will not be able

to make out hidden meaning in it without the key.

References

[1] J.N. Kapur, *Mathematical modelling*, Wiley Eastern Ltd., 1998.

[2] G. Williams, *Linear algebra with applications*, Jones and Bartlett Publishers, Inc., pp. 85-89.

[3] V.V. Yaschenko, *Cryptography: An introduction*, American Mathematical Society, 2009.

[4] T. Koshy, *Elementary number theory with applications*, Elsevier,2007, pp. 413-454.

[5] N. Koblitz, *A course in number theory and crytography*, Springer, 1994, pp. 54-82.

Mathematical modelling of Curve fitting, Traffic flow and Electrical network

A.G. Mohankumar[1], M.S. Suguna[2] and L.N. Achala[3]

[1,2,3]P. G. Department of Mathematics and Research Centre in Applied Mathematics

M. E. S. College of Arts, Commerce and Science

15th cross, Malleswaram, Bangalore - 560003.

Email ID: [1]gmohankmr@gmail.com, [2]sugunamsb.92@gmail.com , [3]anargund1960@gmail.com

Abstract: This article consists of some examples of real world problems which can be solve using Mathematical Modelling technique. In this article we briefly discussed about Curve Fitting, Traffic flow and Electrical Network problems and also we use Gauss Jordan Elimination method to solve the examples.

Keywords: Mathematical Modelling, Curve Fitting, Traffic flow, Electrical Network and Gauss Jordan Elimination method.

1   Introduction

Mathematical Modelling is a technique which essentially consists of translating real world problems into mathematical problems, solving the mathematical problems and interpreting these solutions in the language of the real world. In other words, mathematical modelling is a method of simulating real life situations with mathematical equations to forecast their future behaviour [1]. Mathematical Modelling of large-scale systems presents its own special problems. However mathematical modellers from all disciplines - mathematics, statistics, computer science, physics, engineering, social sciences - are meeting the challenges with courage [2].

System of Linear equations arise in a wide variety of applications. A system of equations is a set of collection of equations that we deal with all together at once. In this article we will look at two application, The first application shows how to fit a polynomial function to a set of data points in the plane. The second application focuses on network and Kirchoff's law of electricity.

1.1   Gauss-Jordan Elimination Method

Carl Friedrich Gauss (1777 - 1855) was a German mathematician, generally regarded as one of the greatest mathematicians of all time for his contributions to number theory, geometry, probability theory, geodesy, planetary astronomy, the theory of functions, and potential theory. Wilhelm Jordan (1842 - 1899) was a German geodesist who conducted surveys in Germany and Africa and founded the German geodesy journal.

1. The process of Gauss-Jordan elimination involves creating an augmented matrix for given system of linear equations.
2. Derive the reduced row echelon form using row operations. This is done by creating leading 1s, then zeros above and below each leading 1, column by column starting with the first column.
3. Write the system of equations corresponding to the reduced echelon form. This system gives the solution. [3]

2   Curve Fitting

Curve fitting is the process of constructing a curve, or mathematical function, that has the best fit to a series of data points. Most of the time the curve fit will produce an equation that can be used to find points any where along the curve. In some cases, we may not be concerned about finding an equation. Instead, we may just want to use a curve fit to smooth the data and improve the appearance of our plot [3].

2.1   Applications of curve fitting

1. In Indian structures the curve fitting is used in NEO-GOTHIC architectural buildings such as University of Mumbai Library and Santhome Basilica, Chennai.
2. Analysis of the shape of the cooling tower at SIPAT thermal power plant in Bilaspur district in state of Chhattisgarh.

3   Traffic flow

Mathematical theory of traffic flow and traffic equilibrium analysis was first introduced by *Frank Knit* in $1920's$, and was refined into *Wardrop's* first and second principles of equilibrium. Current traffic models use a mixture of empirical and theoretical techniques. These models are then developed into traffic forecast, to take account of proposed local or major changes, such as increased vehicle use, changes in land use or changes in mode of transport and to identify areas of congestion where the network needs to be adjusted [4].

3.1   Applications of traffic flow problems

Traffic flow plays an important role in electrical engineering. The concept have been found to be useful in many other fields. Such as information theory and study of transportation systems. The following analysis of traffic flow through a road network during peak period illustrates how system of linear equations with many solutions can arise in practice.

Traffic congestion has a number of negative effects on humanity. These include wasting time of motorists and passengers which therefore reduce regional economic health; delays, which may result in late arrival for employment, meetings and education, resulting in loss of businesses, disciplinary action or other personal losses. Blocked traffic may interfere with the passage of emergency vehicles traveling to their destinations where they are urgently needed; wasted fuel, increasing air pollution and carbon dioxide emissions owing to increasing idling, acceleration and breaking of vehicles; wear and tear on vehicles as a result of idling in traffic and frequent accelerating and breaking, leading to more frequent repairs and replacement of car parts; stressed and frustrated motorists, encouraging road rage and reduced health of motorists [1].

4   Electrical Network

1. **Kirchhoff's First Law** (Junction rule) : At every node the sum of the incoming currents equals to sum of the outgoing currents.

2. **Kirchhoff's Second Law** (loop rule) : Around every loop the algebraic sum of all voltages is zero.

3. **Ohm's law** : For every resistor the voltage drop E, the current I and the resistance R satisfy $E = IR$. [1][3]

5   Examples and Discussions

Example 1: Find a polynomial that relates the periods of the three planets that are closest to the Sun to their mean distances from the Sun, as shown in the table. Then test the accuracy of the fit by using the polynomial to calculate the period of Mars. (In the table, the mean distance is given in astronomical units, and the period is given in years.)

Planet	Mercury	Venus	Earth	Mars
Mean distance	0.387	0.723	1.000	1.524
Period	0.241	0.615	1.000	1.881

Solution: Let us consider a quadratic polynomial function, $P(x) = a_0 + a_1 x + a_2 x^2$ to the points, (0.387,0.241), (0.723,0.615) and (1,1).
The system of linear equations obtained by substituting these points into above quadratic polynomial function is,
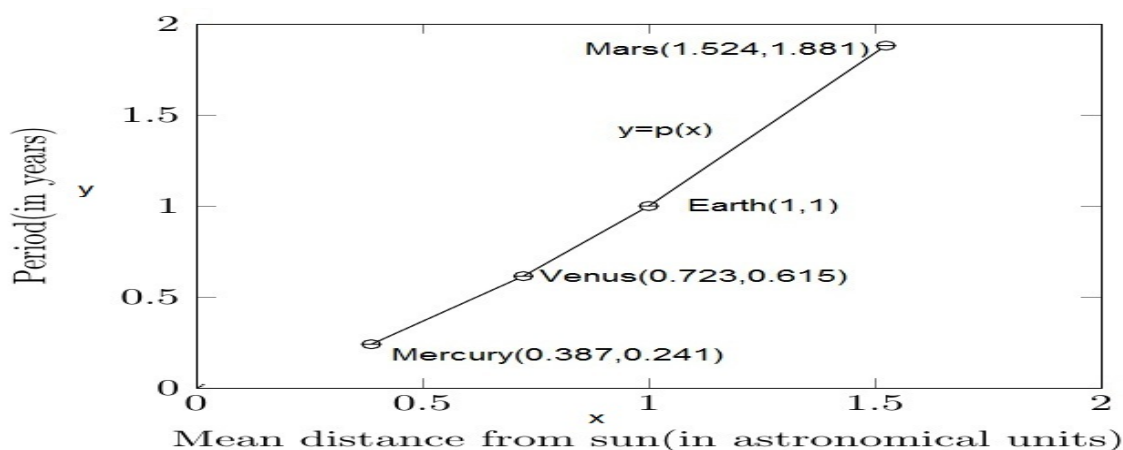
$$a_0 + 0.387a_1 + (0.387)^2 a_2 = 0.241$$
$$a_0 + 0.723a_1 + (0.723)^2 a_2 = 0.615$$
$$a_0 + a_1 + a_2 = 1$$

By solving above system of equations, we get

$$a_0 \approx -0.0634, \quad a_1 \approx 0.6119, \quad a_2 \approx 0.4515.$$
$$\therefore P(x) = -0.0634 + 0.6119x + 0.4515x^2$$

Using $P(x)$ we can evaluate the period of Mars. i.e. $P(1.524) \approx 1.918$ years.
Here the actual period of Mars is 1.881 years. Figure 1 compares the estimate with the actual period graphically.

Figure 1: Graph of Mean distance vs. Period

Example 2: Determine the polynomial $P(x) = a_0 + a_1x + a_2x^2$ whose graph passes through the points (1,4), (2,4) and (3,12).

Solution: Given $P(x) = a_0 + a_1x + a_2x^2$

at $(1, 4)$ $p(x)$ becomes $P(1) = a_0 + a_1(1) + a_2(1)^2$

$$a_0 + a_1 + a_2 = 4 \tag{1}$$

at $(2, 4)$ $p(x)$ becomes $P(2) = a_0 + a_1(2) + a_2(2)^2$
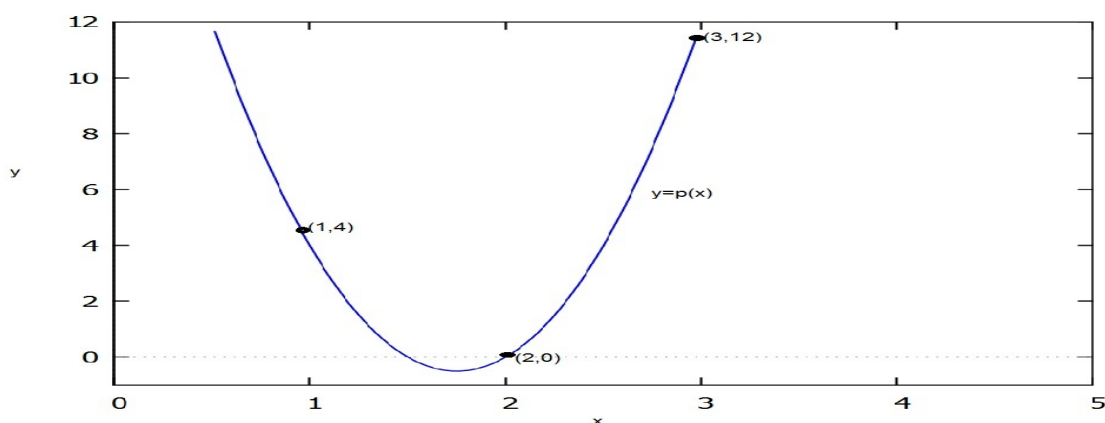
$$a_0 + 2a_1 + 4a_2 = 0 \tag{2}$$

at $(3, 12)$ $p(x)$ becomes $P(3) = a_0 + a_1(3) + a_2(3)^2$

$$a_0 + 3a_1 + 9a_2 = 12 \tag{3}$$

By solving above three equations we get

$$a_0 = 24, \quad a_1 = -28, \quad a_2 = 8$$

And we draw the points in the Figure 2 we get the polynomial equation as below, So the polynomial function is, $P(x) = 24 - 28x + 8x^2$.

Figure 2: Graph of a polynomial $P(x)$

Example 3: Determine the equation of the polynomial of degree two whose graph passes through the points (1,6), (2,3), (3,2).

Solution: Let us consider a polynomial of degree two,

$$y = a_0 + a_1x + a_2x^2 \tag{4}$$

We have 3 points (1,6), (2,3) and (3,2) and substitute x and y values in the above polynomial gives,

$$\begin{aligned} a_0 + a_1 + a_2 &= 6 \\ a_0 + 2a_1 + 4a_2 &= 3 \\ a_0 + 3a_1 + 9a_2 &= 2 \end{aligned} \tag{5}$$

We can solve above system of equations using Gauss-jordan elimination method. The augmented matrix for above is,

$$\begin{bmatrix} 1 & 1 & 1 & : & 6 \\ 1 & 2 & 4 & : & 3 \\ 1 & 3 & 9 & : & 2 \end{bmatrix}$$

$$\approx \quad \begin{matrix} R_2 \to R_2 - R_1 \\ R_3 \to R_3 - R_1 \end{matrix} \quad \begin{bmatrix} 1 & 1 & 1 & : & 6 \\ 0 & 1 & 3 & : & -3 \\ 0 & 2 & 8 & : & -4 \end{bmatrix}$$
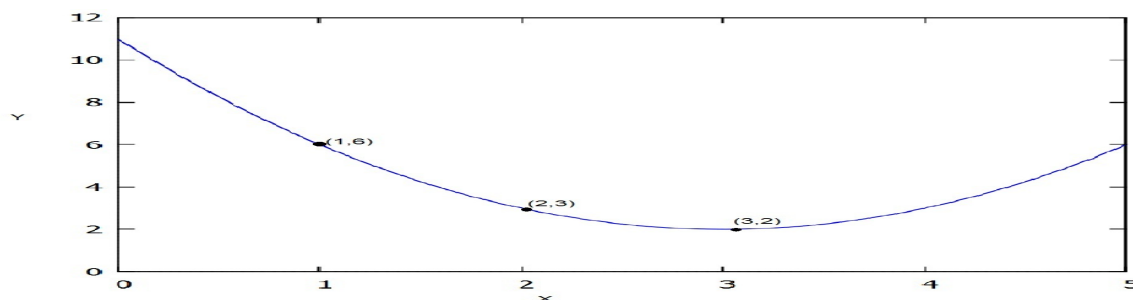
$$\approx \quad \begin{matrix} R_1 \to R_1 - R_2 \\ R_3 \to R_3 - R_2 \end{matrix} \quad \begin{bmatrix} 1 & 0 & -2 & : & 9 \\ 0 & 1 & 3 & : & -3 \\ 0 & 0 & 2 & : & 2 \end{bmatrix}$$

$$\approx \quad R_3 \to \frac{R_3}{2} \quad \begin{bmatrix} 1 & 0 & -2 & : & 9 \\ 0 & 1 & 3 & : & -3 \\ 0 & 0 & 1 & : & 1 \end{bmatrix}$$

$$\approx \quad \begin{matrix} R_1 \to R_1 + 2R_3 \\ R_2 \to R_2 - 3R_3 \end{matrix} \quad \begin{bmatrix} 1 & 0 & 0 & : & 11 \\ 0 & 1 & 0 & : & -6 \\ 0 & 0 & 1 & : & 1 \end{bmatrix}$$

From the above diagonal matrix we get, $a_0 = 11, \quad a_1 = -6, \quad a_2 = 1$.
The parabola that passes through these points is $y = 11 - 6x + x^2$, as shown in the Figure 3.

Figure 3: Graph of a polynomial $y = 11 - 6x + x^2$

Example 4: Let us consider the typical road network, A system of linear equations were used to analyze the flow of traffic for a network of 4 one-way streets. The variables x, y, z and w represent the flow of the traffic between the four intersections in the network. The data was obtained by counting the number of vehicles that traveled around the four one-way streets between the hours of 6am to 10am and 2pm to 6pm during the mid-week peak traffic hours. The arrows in the Figure 4 indicate the direction of flow of traffic in and out of the network that is measured in terms of number of vehicles per hour (vph). (Figure 4 describes the four one-way streets in Kumasi under study in the model)
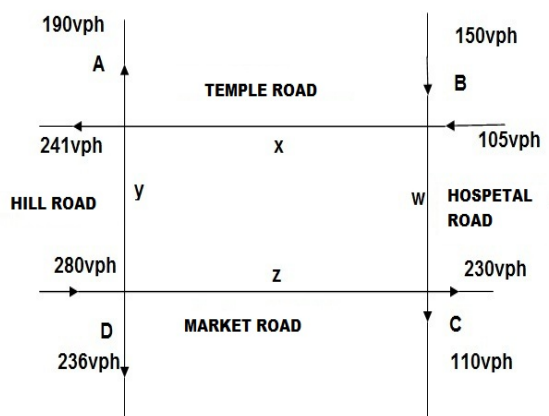
Figure 4: Diagram of the four one-way streets

Solution: Let us assume that, vehicles entering each intersection should always be equal to the number of vehicles leaving the intersection and, the streets must all be one-way with the arrows indicating the direction of traffic flow. The system of equations for the model was formulated as follows:

At intersection A:

$$\text{Traffic in} = x + y$$
$$\text{Traffic out} = 240 + 190$$
$$\text{Thus}, x + y = 431$$

At intersection B:

$$\text{Traffic in} = 150 + 105$$
$$\text{Traffic out} = x + w$$
$$\text{Thus}, x + w = 255$$

At intersection C:

$$\text{Traffic in} = z + w$$
$$\text{Traffic out} = 230 + 110$$
$$\text{Thus}, z + w = 340$$

At intersection D:

$$\text{Traffic in} = 280 + 236$$
$$\text{Traffic out} = y + z$$
$$\text{Thus}, y + z = 516$$

The constraints were written as a system of linear equations as follows:

$$
\begin{aligned}
x + y &= 431 \\
x + w &= 255 \\
z + w &= 340 \\
y + z &= 516
\end{aligned}
\tag{6}
$$

We then used the Gauss-Jordan elimination method to solve the system of equations. The augmented matrix and reduced row-echelon form of equation (1) is as follows,

$$
\left[
\begin{array}{cccc:c}
1 & 1 & 0 & 0 & 431 \\
1 & 0 & 0 & 1 & 255 \\
0 & 0 & 1 & 1 & 340 \\
0 & 1 & 1 & 0 & 516
\end{array}
\right]
\xrightarrow{\left(\text{Row operations}\right)}
\left[
\begin{array}{cccc:c}
1 & 0 & 0 & 1 & 255 \\
0 & 1 & 0 & -1 & 176 \\
0 & 0 & 1 & 1 & 340 \\
0 & 0 & 0 & 0 & 0
\end{array}
\right]
$$

The system of equations that corresponds to reduced row-echelon form is,

$$
\begin{aligned}
x + w &= 255 \\
y - w &= 176 \\
z + w &= 340
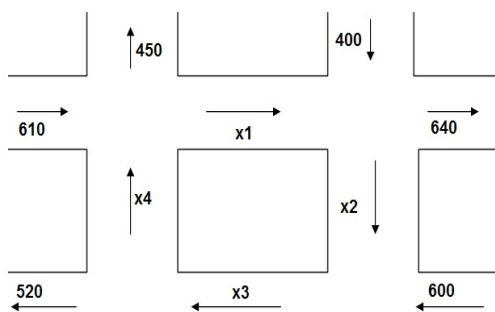\end{aligned}
\tag{7}
$$

Hence we have,

$$
\begin{aligned}
x &= 255 - w \\
y &= 176 + w \\
z &= 340 - w
\end{aligned}
\tag{8}
$$

If we take a construction limit on Labour-Asafo Interchange Rd (w) to be 100 vph, then using above equation the values of x, y, z will be,

$$x = 255 - 100, \quad y = 176 + 100, \quad z = 340 - 100$$
$$\therefore x = 155 \text{ vph}, \quad y = 276 \text{ vph}, \quad z = 240 \text{ vph}.$$

Example 5: Determine the amount of traffic between each of the four intersections in Figure 5.

Figure 5: Traffic flow between four junctions

Solution: At each intersection, the incoming traffic has to match the outgoing traffic.
Intersection $A : x_4 + 610 = x_1 + 450$
Intersection $B : x_1 + 400 = x_2 + 640$
Intersection $C : x_2 + 600 = x_3$
Intersection $D : x_3 = x_4 + 520$

$$\begin{aligned}
\therefore x_1 - x_4 &= 160 \\
x_1 - x_2 &= 240 \\
x_2 - x_3 &= -600 \\
x_3 - x_4 &= 520
\end{aligned} \tag{9}$$

The augmented matrix and reduced row-echelon form using Gauss-Jordan elimination method of equation (9) as follows,

$$\begin{bmatrix}
1 & 0 & 0 & -1 & : & 160 \\
1 & -1 & 0 & 0 & : & 240 \\
0 & 1 & -1 & 0 & : & -600 \\
0 & 0 & 1 & -1 & : & 520
\end{bmatrix} \xrightarrow{\left(\text{Row operations}\right)} \begin{bmatrix}
1 & 0 & 0 & -1 & : & 160 \\
0 & 1 & 0 & -1 & : & -80 \\
0 & 0 & 1 & -1 & : & 680 \\
0 & 0 & 0 & 0 & : & 0
\end{bmatrix}$$

The system of equations that corresponds to this reduced row-echelon form is,

$$\begin{aligned}
x_1 - x_4 &= 160 \\
x_2 - x_4 &= -80 \\
x_3 - x_4 &= 680
\end{aligned} \tag{10}$$

Let $x_4 = t$ in equation (10) then, $x_1 = t + 160, \quad x_2 = t - 160, \quad x_3 = t + 680$
Where t is a real number, so this system has a infinitely many solutions. If we could control the amount of flow along x_4.
For instance, letting $t = 100$. then,

$$x_1 = 260, \quad x_2 = 20, \quad x_3 = 780, \quad x_4 = 100$$

Example 6: Determine the currents I_1, I_2, I_3, I_4, I_5 and I_6 for the electrical network shown in the Figure 6.
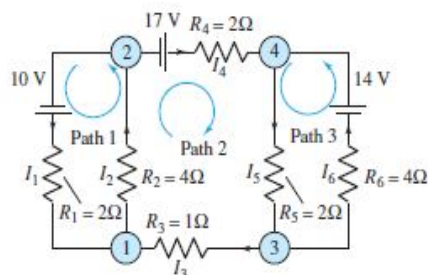
Figure 6: Electrical network

Solution: Applying Kirchhoff's first law to the four junctions in Figure 6, then

Junction 1: $I_1 + I_3 = I_2$
Junction 2: $I_1 + I_4 = I_2$
Junction 3: $I_3 + I_6 = I_5$
Junction 4: $I_4 + I_6 = I_5$

Applying Kirchhoff's second law to the three paths produces in Figure 6, then

Path 1: $2I_1 + 4I_2 = 10$
Path 2: $4I_2 + I_3 + 2I_4 + 2I_5 = 17$
Path 3: $2I_5 + 4I_6 = 14$

Now we have the following system of linear equations with variables I_1, I_2, I_3, I_4, I_5 and I_6.

$$
\begin{aligned}
I_1 - I_2 + I_3 &= 0 \\
I_1 - I_2 + I_4 &= 0 \\
I_3 - I_5 + I_6 &= 0 \\
I_4 - I_5 + I_6 &= 0 \\
2I_1 + 4I_2 &= 10 \\
4I_2 + I_3 + 2I_4 + 2I_5 &= 17 \\
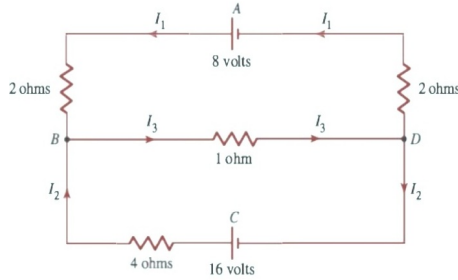2I_5 + 4I_6 &= 14
\end{aligned}
\tag{11}
$$

The augmented matrix for equation (11) is,

$$
\begin{bmatrix}
1 & -1 & 1 & 0 & 0 & 0 & : & 0 \\
1 & -1 & 0 & 1 & 0 & 0 & : & 0 \\
0 & 0 & 1 & 0 & -1 & 1 & : & 0 \\
0 & 0 & 0 & 1 & -1 & 1 & : & 0 \\
2 & 4 & 0 & 0 & 0 & 0 & : & 10 \\
0 & 4 & 1 & 2 & 2 & 0 & : & 17 \\
0 & 0 & 0 & 0 & 2 & 4 & : & 14
\end{bmatrix}
\tag{12}
$$

Using Gauss-Jordan elimination method we have the solution,i.e.

$$I_1 = 1 \text{ amp}, \quad I_2 = 2 \text{ amp}, \quad I_3 = 1 \text{ amp}, \quad I_4 = 1 \text{ amp}, \quad I_5 = 3 \text{ amp}, \quad I_6 = 2 \text{ amp}$$

Example 7: Determine the currents through each branch of the electrical network shown in the Figure 7.

Figure 7: Electrical network

Solution: Let currents in the various branches of the circuit (Figure 7) be I_1, I_2 and I_3. Kirchhoff's law refers to junctions & closed paths. There are 2 junctions in this circuit, namely the points B & D and there are three closed paths, namely $ABDA$, $CBDC$, and $ABCDA$. Apply Kirchhoff's laws to the junctions & paths.

At junctions,

$$\text{Junction B} : I_1 + I_2 = I_3$$
$$\text{Junction D} : I_3 = I_1 + I_2$$

The equations result in a single linear equation, $I_1 + I_2 - I_3 = 0$

At paths,

$$\text{path } ABDA : 2I_1 + I_3 + 2I_1 = 8$$
$$\text{path } CBDC : 4I_2 + I_3 = 16$$

$\therefore$ We have

$$
\begin{aligned}
I_1 + I_2 - I_3 &= 0 \\
4I_1 + I_3 &= 8 \\
4I_2 + I_3 &= 16
\end{aligned}
\tag{13}
$$

The augmented matrix and reduced row-echelon form of equation (13) using Gauss-Jordan elimination method as follows,

$$
\begin{bmatrix}
1 & 1 & -1 & : & 0 \\
4 & 0 & 1 & : & 8 \\
0 & 4 & 1 & : & 16
\end{bmatrix}
\xrightarrow{\left(\text{Row operations}\right)}
\begin{bmatrix}
1 & 0 & 0 & : & 1 \\
0 & 1 & 0 & : & 3 \\
0 & 0 & 1 & : & 4
\end{bmatrix}
$$

From matrix of reduced row-echelon form, we have

$$
\begin{aligned}
I_1 &= 1 \text{ amps} \\
I_2 &= 3 \text{ amps} \\
I_3 &= 4 \text{ amps}
\end{aligned}
$$

6 Conclusion

In this article we consider the linear system in real life problems like Curve Fitting, Traffic Flow and Electrical Network. Linear systems are the collection of linear equations. Hence here we use the Mathematical Modelling Technique to solve the linear system of equations with Gauss Jordan Elimination Method with this we get exact solutions.

References

[1] J.N. Kapur, *Mathematical modelling*, Wiley Eastern Ltd., 1998.

[2] A.C. Fowler, *Mathematical models in applied sciences*, Cambridge University Press, 1997.

[3] G. Williams, *Linear algebra with applications*, Jones and Bartlett Publishers Inc., 2001, pp. 85-89.

[4] I.K. Adu, D.K. Boah, V. Tulasi, *Application of system of linear equation to traffic flow*, Int. J. Cont. Math. Sci. Vol.9(14), 2014, pp. 653-660.

Study of solution of Integro Differential Equations using Haar wavelets

R. Kumar[1], R.S. Sumana[2] and L.N. Achala[3]

[1,2,3]P. G. Department of Mathematics and Research Centre in Applied Mathematics

M. E. S. College of Arts, Commerce and Science

15th cross, Malleswaram, Bangalore - 560003.

Email ID: [1]rrajeshjangir@gmail.com, [2]sumana.shesha@gmail.com, [3]anargund1960@gmail.com

Abstract: Integro-differential equations arise in the mathematical modelling of many physical phenomena. In this paper, we use Haar wavelet method for the numerical solution of Fredholm integro-differential equation, Volterra integro-differential equation, system of Fredholm integro-differential equations and system of Volterra integro-differential equations. The basic idea of Haar wavelet collocation method is to convert the integro-differential equation into a system of algebraic equations that involves a finite number of variables. The numerical results are compared with the exact solution to prove the accuracy of the Haar wavelet method.

Keywords: Fredholm integro-differential equation,, Volterra integro-differential equation, Haar wavelets, Collocation points.

1   Introduction

An integro-differential equation is an equation that involves both integrals and derivatives of a function. In other words, an integro-differential equation is a combination of differential and Fredholm-Volterra integral equations. Integro-differential equations play an important role in many branches of linear and nonlinear functional analysis and their applications in the theory of engineering, mechanics, physics, chemistry, astronomy, biology, economics, potential theory and electrostatics. The mentioned integro-differential equations are usually difficult to solve analytically, so a numerical method is required.

In the recent years, wavelets have been widely used to solve differential equations. Alfred Haar, a Hungarian mathematician introduced Haar wavelets in 1910. The Haar wavelets consist of piecewise constant functions and are therefore the simplest orthonormal wavelets with a compact support. An advantage of these wavelets is the possibility to integrate them analytically arbitrary times. They are the simplest possible wavelets and are often known as a first order Daubechies wavelet which are conceptually simple, fast, memory efficient and exactly reversible [1]. Sumana and Achala [2] have given a brief report on Haar wavelets. Chen and Hsiao [3] recommended to expand into the Haar series the highest order derivatives appearing in the differential equation. This idea has been very prolific and it is being abundantly applied for the solution of differential equations. The wavelet coefficients appearing in the Haar series are calculated either using Collocation method or Galerkin method.

Cattani [4] applied the Shannon wavelets for solving integro-differential equations. Sayed and Aziz [5] compared Adomian decomposition method and wavelet-Galerkin method for solving integro-differential equations. Lepik [6] solved nonlinear integro-differential equations using Haar wavelet method. Maleknejad et. al. [7] solved linear integro-differential equations

system by using rationalized Haar functions method. Mishra et. al. [8] presented numerical solution of integro-differential equations using Haar wavelet algorithm. Siraj-ul-Islam et. al. [9, 10] used Haar wavelets to solve linear integro-differential equations and higher order nonlinear integro-differential equations. Sekar and Jaisankar [11] used single-term Haar wavelet series to solve nonlinear integro-differential equations. Aminikhah and Hossein [12] used Chebyshev wavelets to solve nonlinear system of integro-differential equations. Kajania and Vencheh [13] solved linear integro-differential equations, and Meng et. al. [14] solved fractional integro-differential equations using Legendre wavelets.

2   Preliminaries of Haar wavelets

The Haar wavelet family for $x \in [0, 1]$ is defined as follows [1]

$$h_i(x) = \begin{cases} 1 & \text{for } x \in [\xi_1, \xi_2) \\ -1 & \text{for } x \in [\xi_2, \xi_3) \\ 0 & \text{elsewhere} \end{cases} \tag{1}$$

where

$$\xi_1 = \frac{k}{m}, \quad \xi_2 = \frac{k + 0.5}{m}, \quad \xi_3 = \frac{k + 1}{m} \tag{2}$$

In order to solve integral or differential equations of any order, we need the following integral.

$$p_i(x) = \int_0^x h_i(x)dx = \begin{cases} x - \xi_1 & \text{for } x \in [\xi_1, \xi_2) \\ \xi_3 - x & \text{for } x \in [\xi_2, \xi_3) \\ 0 & \text{elsewhere} \end{cases} \tag{3}$$

In the above definition $m = 2^n, n = 0, 1, ..., J$ indicates the level of the wavelet; $k = 0, 1, ..., m - 1$ is the translation parameter. J is the maximum level of resolution. The index i in equation (1) is calculated by the formula $i = m + k + 1$. In the case of minimum values $m = 1, k = 0$ we have $i = 2$. The maximum value of i is $i = 2M = 2^{J+1}$.

For $i = 1$, $h_1(x)$ is assumed to be the scaling function which is defined as follows.

$$h_1(x) = \begin{cases} 1 & \text{for } x \in [0, 1) \\ 0 & \text{elsewhere} \end{cases} \tag{4}$$

3   Method of Solution and Examples

3.1   Fredholm integro-differential equation

Example 1:

$$y'(x) + 2xy(x) = 2x^4 + 2x^3 + 3x^2 - \frac{17}{12} + \int_0^1 (x + t)y'(t)dt \tag{5}$$

with initial condition

$$y(0) = 0 \tag{6}$$

The exact solution is

$$y(x) = x^2(1 + x) \tag{7}$$

Let the Haar wavelet solution be in the form

$$y'(x) = \sum_{i=1}^{2M} a_i h_i(x) \tag{8}$$

Integrating equation (8) w.r.t. x from 0 to x and using equation (6) gives

$$y(x) = \sum_{i=1}^{2M} a_i p_i(x) \tag{9}$$

Substituting equations (8) and (9) in equation (5) leads to

$$\sum_{i=1}^{2M} a_i[h_i(x) + 2x p_i(x) - G_i(x)] = 2x^4 + 2x^3 + 3x^2 - \frac{17}{12} \tag{10}$$

where

$$G_i(x) = \int_0^1 (x + t) h_i(t) dt \tag{11}$$

Solving $G_i(x)$, we obtain

$$G_i(x) = \begin{cases} x + \dfrac{1}{2}, & \text{if } i = 1 \\[2mm] -\dfrac{1}{4m^2}, & \text{if } i > 1 \end{cases} \tag{12}$$

The wavelet collocation points are defined as

$$x_l = \frac{l - 0.5}{2M}, \, l = 1, 2, \ldots, 2M. \tag{13}$$

Taking $x \to x_l$ in equations (10) and (9), we get

$$\sum_{i=1}^{2M} a_i[h_i(x_l) + 2x_l p_i(x_l) - G_i(x_l)] = 2x_l^4 + 2x_l^3 + 3x_l^2 - \frac{17}{12} \tag{14}$$

$$y(x_l) = \sum_{i=1}^{2M} a_i p_i(x_l) \tag{15}$$

The wavelet coefficients a_i, $i = 1, 2, \ldots, 2M$ are obtained by solving the $2M$ system of equations in (14). These coefficients are then substituted in equation (15) to obtain the Haar wavelet solution at the collocation points $x_l, l = 1, 2, \ldots, 2M$. The HWCM solution of the example with $J = 6$ is given in Table 1. Figure 1 shows the comparison of the HWCM solution with the exact solution.

3.2   Volterra integro-differential equation

Example 2:

$$y'(x) + y(x) = \int_0^x e^{t-x} y(t) dt \tag{16}$$

with initial condition

$$y(0) = 1 \tag{17}$$

The exact solution is

$$y(x) = e^{-x} \cosh(x) \tag{18}$$

Let the Haar wavelet solution be in the form

$$y'(x) = \sum_{i=1}^{2M} a_i h_i(x) \tag{19}$$

Integrating equation (19) w.r.t. x from 0 to x and using equation (17), we get

$$y(x) = 1 + \sum_{i=1}^{2M} a_i p_i(x) \tag{20}$$

Substituting equations (19) and (20) in equation (16), we obtain

$$\sum_{i=1}^{2M} a_i [h_i(x) - p_i(x) - G_i(x)] = -e^{-x} \tag{21}$$

where

$$G_i(x) = \int_0^x e^{t-x} p_i(t) dt \tag{22}$$

Solving $G_i(x)$ for $i = 1$ leads to

$$G_i(x) = x - 1 + e^{-x} \tag{23}$$

Solving $G_i(x)$ for $i > 1$ gives

$$G_i(x) = \begin{cases} 0 & \text{if } x \in [0, \xi_1) \\ e^{\xi_1 - x} + x - \xi_1 - 1, & \text{if } x \in [\xi_1, \xi_2) \\ e^{\xi_1 - x} - 2e^{\xi_2 - x} - x + \xi_3 + 1, & \text{if } x \in [\xi_2, \xi_3) \\ e^{\xi_1 - x} + e^{\xi_3 - x} - 2e^{\xi_2 - x}, & \text{if } x \in [\xi_3, 1] \end{cases} \tag{24}$$

The wavelet collocation points are defined as

$$x_l = \frac{l - 0.5}{2M}, \, l = 1, 2, \ldots, 2M. \tag{25}$$

Taking $x \to x_l$ in equations (21) and (20),we obtain

$$\sum_{i=1}^{2M} a_i [h_i(x_l) - p_i(x_l) - G_i(x_l)] = -e^{-x_l} \tag{26}$$

$$y(x_l) = 1 + \sum_{i=1}^{2M} a_i p_i(x_l) \tag{27}$$

The wavelet coefficients a_i, $i = 1, 2, \ldots, 2M$ are obtained by solving the $2M$ system of equations in (26). These coefficients are then substituted in equation (27) to obtain the Haar wavelet solution at the collocation points x_l, $l = 1, 2, \ldots, 2M$. The HWCM solution of the example with $J = 3$ is given in Table 2. Figure 2 shows the comparison of the HWCM solution with the exact solution.

3.3   System of Fredholm integro-differential equations

Example 3:

$$2\pi u(x) = 2\pi \cos(2\pi x)[1 + \sin(2\pi x)] + \int_0^1 [\cos(2\pi t)\sin(4\pi x)u'(t) - \sin(4\pi x + 2\pi t)v'(t)]dt \tag{28}$$

$$v'(x) = \cos(2\pi x)[2\pi - \sin(2\pi x)] - \int_0^1 [\cos(4\pi x)\sin(2\pi t)u(t) + \cos(4\pi x + 2\pi t)v(t)]dt \tag{29}$$

with initial condition

$$u(0) = 1, v(0) = 0 \tag{30}$$

The exact solutions are

$$u(x) = \cos(2\pi x) \tag{31}$$

$$v(x) = \sin(2\pi x) \tag{32}$$

Let the Haar wavelet solutions be in the form

$$u'(x) = \sum_{i=1}^{2M} a_i h_i(x) \tag{33}$$

$$v'(x) = \sum_{i=1}^{2M} b_i h_i(x) \tag{34}$$

Integrating equations (33) and (34) w.r.t. x from 0 to x, and using equation (30) gives

$$u(x) = 1 + \sum_{i=1}^{2M} a_i p_i(x) \tag{35}$$

$$v(x) = \sum_{i=1}^{2M} b_i p_i(x) \tag{36}$$

Substituting equations (33), (34), (35) and (36) in equations (28) and (29) leads to

$$\sum_{i=1}^{2M} \{a_i[2\pi p_i(x) - \sin(4\pi x)G_{1i}(x)] + b_i[H_{1i}(x)]\} = -2\pi + 2\pi \cos(2\pi x)(1 + \sin(2\pi x)) \tag{37}$$

$$\sum_{i=1}^{2M} \{a_i[\cos(4\pi x)G_{2i}(x)] + b_i[h_i(x) + H_{2i}(x)]\} = \cos(2\pi x)(2\pi - \sin(2\pi x)) \tag{38}$$

where

$$G_{1i}(x) = \int_0^1 \cos(2\pi t)h_i(t)dt \tag{39}$$

$$G_{2i}(x) = \int_0^1 \sin(2\pi t)p_i(t)dt \tag{40}$$

$$H_{1i}(x) = \int_0^1 \sin(4\pi x + 2\pi t)h_i(t)dt \tag{41}$$

$$H_{2i}(x) = \int_0^1 \cos(4\pi x + 2\pi t)p_i(t)dt \tag{42}$$

Solving $G_{1i}(x)$, $G_{2i}(x)$, $H_{1i}(x)$ and $H_{2i}(x)$ we obtain

$$G_{1i}(x) = \begin{cases} 0 & \text{if } i = 1 \\ \dfrac{1}{2\pi}[2\sin(2\pi\xi_2) - \sin(2\pi\xi_1) - \sin(2\pi\xi_3)], & \text{if } i > 1 \end{cases} \tag{43}$$

$$G_{2i}(x) = \begin{cases} -\dfrac{1}{2\pi}, & \text{if } i = 1 \\ \dfrac{1}{4\pi^2}[2\sin(2\pi\xi_2) - \sin(2\pi\xi_1) - \sin(2\pi\xi_3)], & \text{if } i > 1 \end{cases} \tag{44}$$

$$H_{1i}(x) = \begin{cases} 0, & \text{if } i = 1 \\ \dfrac{1}{2\pi}[-2\cos(4\pi x + 2\pi\xi_2) + \cos(4\pi x + 2\pi\xi_1) + \cos(4\pi x + 2\pi\xi_3)], & \text{if } i > 1 \end{cases} \tag{45}$$

$$H_{2i}(x) = \begin{cases} \dfrac{\sin(4\pi x)}{2\pi}, & \text{if } i = 1 \\ \dfrac{1}{4\pi^2}[2\cos(4\pi x + 2\pi\xi_2) - \cos(4\pi x + 2\pi\xi_1) - \cos(4\pi x + 2\pi\xi_3)], & \text{if } i > 1 \end{cases} \tag{46}$$

The wavelet collocation points are defined as

$$x_l = \frac{l - 0.5}{2M}, \quad l = 1, 2, \ldots, 2M. \tag{47}$$

Taking $x \to x_l$ in equations (37), (38), (39) and (36), we get

$$\sum_{i=1}^{2M} \begin{bmatrix} 2\pi p_i(x_l) - \sin(4\pi x_l)G_{1i}(x_l) & H_{1i}(x_l) \\ \cos(4\pi x_l)G_{2i}(x_l) & h_i(x_l) + H_{2i}(x_l) \end{bmatrix} \begin{bmatrix} a_i \\ b_i \end{bmatrix} = \\ \begin{bmatrix} -2\pi + 2\pi\cos(2\pi x_l)(1 + \sin(2\pi x_l)) \\ \cos(2\pi x_l)(2\pi - \sin(2\pi x_l)) \end{bmatrix} \tag{48}$$

$$u(x_l) = 1 + \sum_{i=1}^{2M} a_i p_i(x_l) \tag{49}$$

$$v(x_l) = \sum_{i=1}^{2M} b_i p_i(x_l) \tag{50}$$

The wavelet coefficients $a_i, b_i,\ i = 1, 2, \ldots, 2M$ are obtained by solving the $4M$ system of equations in (48). These coefficients are then substituted in equations (49) and (50) to obtain the Haar wavelet solution at the collocation points $x_l, l = 1, 2, \ldots, 2M$. The HWCM solution of the example with $J = 5$ is given in Table 3. Figure 3 shows the comparison of the HWCM solution with the exact solution.

3.4   System of Volterra integro differential equation

Example 4:

$$u'(x) = 1 + x + x^2 - v(x) - \int_0^x [u(t) + v(t)]dt \tag{51}$$

$$v'(x) = -1 - x + u(x) - \int_0^x [u(t) - v(t)]dt \tag{52}$$

with initial condition

$$u(0) = 1, v(0) = -1 \tag{53}$$

The exact solutions are

$$u(x) = x + e^x \tag{54}$$

$$v(x) = x - e^x \tag{55}$$

Let the Haar wavelet solutions be in the form

$$u'(x) = \sum_{i=1}^{2M} a_i h_i(x) \tag{56}$$

$$v'(x) = \sum_{i=1}^{2M} b_i h_i(x) \tag{57}$$

Integrating equations (56) and (57) w.r.t. x from 0 to x, and using equation (53), we obtain

$$u(x) = 1 + \sum_{i=1}^{2M} a_i p_i(x) \tag{58}$$

$$v(x) = -1 + \sum_{i=1}^{2M} b_i p_i(x) \tag{59}$$

Substituting equations (56), (57), (58) and (59) in equations (51) and (52), we get

$$\sum_{i=1}^{2M} a_i [h_i(x) + G_i(x)] + \sum_{i=1}^{2M} b_i [p_i(x) + G_i(x)] = 2 + x + x^2 \tag{60}$$

$$\sum_{i=1}^{2M} a_i [h_i(x) - G_i(x)] + \sum_{i=1}^{2M} b_i [G_i(x) - p_i(x)] = -3x \tag{61}$$

where

$$G_i(x) = \int_0^x p_i(t)dt \tag{62}$$

Solving $G_i(x)$ for $i = 1$ gives

$$G_i(x) = \frac{x^2}{2} \tag{63}$$

Solving $G_i(x)$ for $i > 1$ leads to

$$
G_i(x) = \begin{cases}
0, & \text{if } x \in [0, \xi_1) \\[2mm]
\dfrac{(x - \xi_1)^2}{2}, & \text{if } x \in [\xi_1, \xi_2) \\[2mm]
(\xi_2 - \xi_1)^2 - \dfrac{(\xi_3 - x)^2}{2}, & \text{if } x \in [\xi_2, \xi_3) \\[2mm]
(\xi_2 - \xi_1)^2, & \text{if } x \in [\xi_2, 1]
\end{cases} \tag{64}
$$

The wavelet collocation points are defined as

$$
x_l = \frac{l - 0.5}{2M}, \ l = 1, 2, \ldots, 2M. \tag{65}
$$

Taking $x \to x_l$ in equations (60), (61), (58) and (59), we get

$$
\sum_{i=1}^{2M} \begin{bmatrix} h_i(x_l) + G_i(x_l) & p_i(x_l) + G_i(x_l) \\ h_i(x_l) - G_i(x_l) & G_i(x_l) - p_i(x_l) \end{bmatrix} \begin{bmatrix} a_i \\ b_i \end{bmatrix} = \begin{bmatrix} 2 + x_l + x_l^2 \\ -3x_l \end{bmatrix} \tag{66}
$$

$$
u(x_l) = 1 + \sum_{i=1}^{2M} a_i p_i(x_l) \tag{67}
$$

$$
v(x_l) = -1 + \sum_{i=1}^{2M} b_i p_i(x_l) \tag{68}
$$

The wavelet coefficients $a_i, b_i, \ i = 1, 2, \ldots, 2M$ are obtained by solving the $4M$ system of equations in (66). These coefficients are then substituted in equations (67) and (68) to obtain the Haar wavelet solution at the collocation points $x_l, l = 1, 2, \ldots, 2M$. The HWCM solution of the example with $J = 4$ is given in Table 4. Figure 4 shows the comparison of the HWCM solution with the exact solution.

Table 1: Comparison of HWCM solution and exact solution for $J = 6$ at different x of Example 1

x	$y(x)$	
	HWCM	Exact
0.003906	0.000030	0.000015
0.035156	0.001292	0.001279
0.074219	0.005927	0.005917
0.152344	0.026749	0.026744
0.207031	0.051736	0.051735
0.402344	0.226995	0.227012
0.605469	0.588516	0.588552
0.855469	1.357825	1.357881
0.957031	1.792399	1.792462
0.996094	1.980465	1.980529

Table 2: Comparison of HWCM solution and exact solution for $J = 3$ at different x of Example 2

x	$y(x)$	
	HWCM	Exact
0.031250	0.970615	0.969706
0.156250	0.866488	0.865807
0.281250	0.785405	0.784891
0.406250	0.722264	0.721873
0.531250	0.673096	0.672795
0.656250	0.634809	0.634573
0.781250	0.604994	0.604805
0.843750	0.592661	0.592490
0.906250	0.581778	0.581622
0.968750	0.572174	0.572031

Table 3: Comparison of HWCM solution and exact solution for $J = 5$ at different x of Example 3

x	$u(x)$		$v(x)$	
	HWCM	Exact	HWCM	Exact
0.007813	0.998815	0.998795	0.049028	0.049068
0.101563	0.803400	0.803208	0.595209	0.595699
0.210938	0.243075	0.242980	0.969222	0.970031
0.304688	-0.337017	-0.336890	0.940759	0.941544
0.507813	-0.998776	-0.998795	-0.049028	-0.049068
0.710938	-0.242886	-0.242980	-0.969282	-0.970031
0.804688	0.336762	0.336890	-0.940816	-0941544
0.914063	0.857552	0.857729	-0.573698	-0.514103
0.976563	0.989118	0.989177	-0.146613	-0.146730
0.992188	0.998776	0.998795	-0.049028	-0.049028

Table 4: Comparison of HWCM solution and exact solution for $J = 4$ at different x of Example 4

| x	$u(x)$		$v(x)$	
	HWCM	Exact	HWCM	Exact
0.015625	1.031498	1.031373	-1.000244	-1.000123
0.203125	1.291769	1.291618	-1.010485	-1.010368
0.359375	1.868733	1.868529	-1.087390	-1.087279
0.515625	2.190540	2.190310	-1.159170	-1.159060
0.609375	2.538549	2.538292	-1.257153	-1.257042
0.713125	2.916248	2.915963	-1.384827	-1.384713
0.828125	3.327590	3.327277	-1.546148	-1.546027
0.890625	3.436195	3.435875	-1.592247	-1.592125
0.953125	3.547255	3.546928	-1.640803	-1.640678
0.984375	3.660848	3.660514	-1.691891	-1.691764
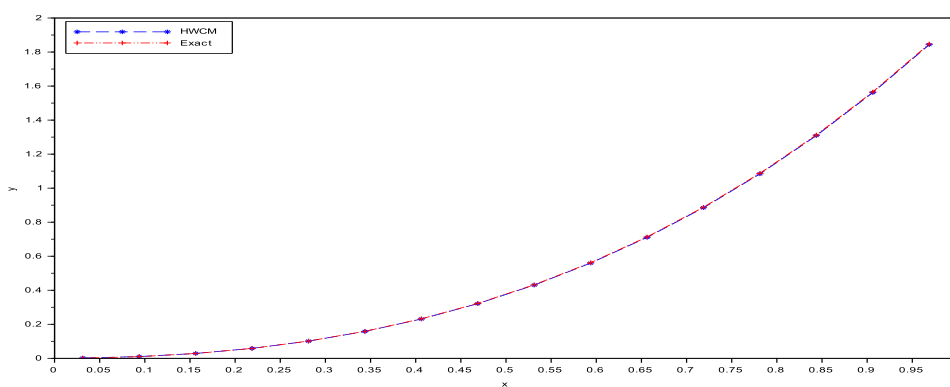
Figure 1: Comparison of HWCM solution and exact solution of Example 1
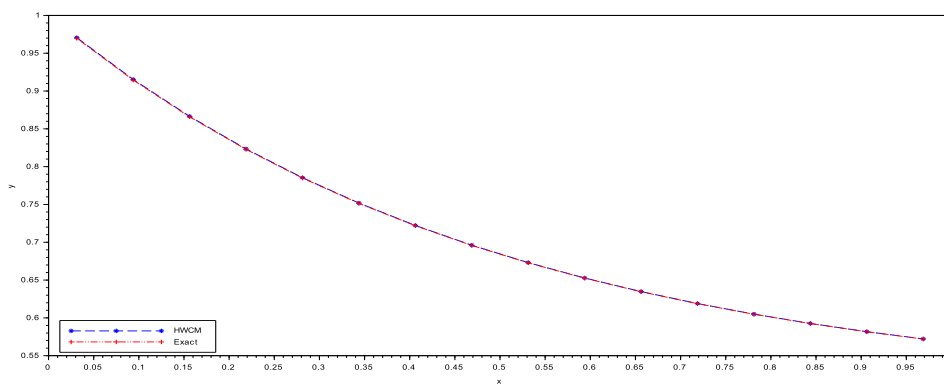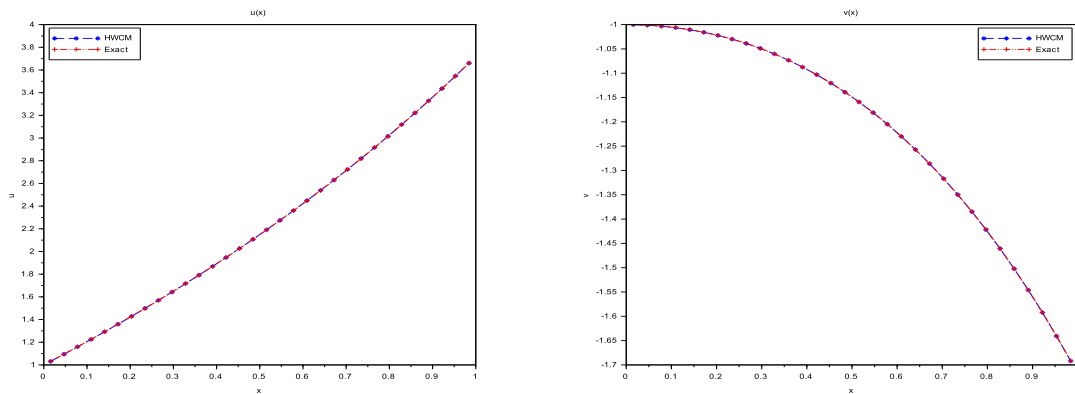

Figure 2: Comparison of HWCM solution and exact solution of Example 2
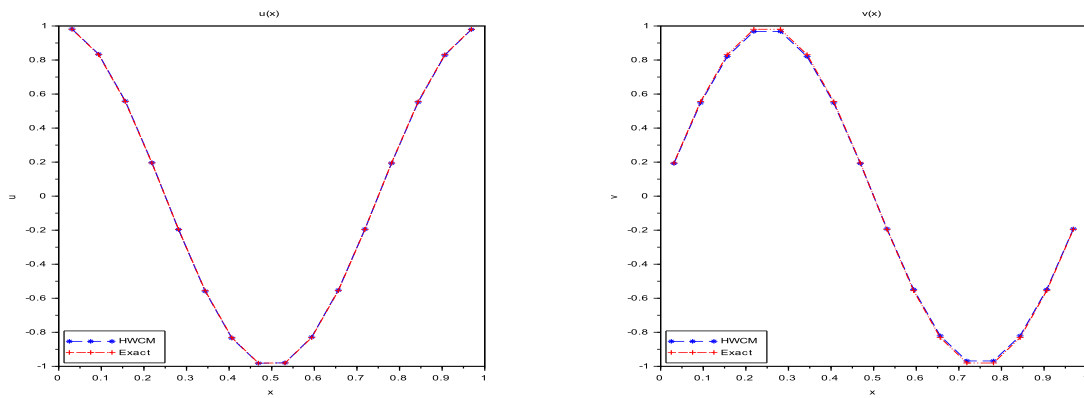
Figure 3: Comparison of HWCM solution and exact solution of Example 3

Figure 4: Comparison of HWCM solution and exact solution of Example 4

4   Conclusion

In this paper, an efficient numerical scheme based on uniform Haar wavelets is used to solve Fredholm integro-differential equation, Volterra integro-differential equation, system of Fredholm integro-differential equations and system of Volterra integro-differential equations. The numerical scheme is tested for four examples. The obtained numerical results are compared with the exact solutions, and are found to be in good agreement. Thus the Haar wavelet method guarantees the necessary accuracy with a small number of grid points.

References

[1] U. Lepik, H. Hein, *Haar wavelets with applications*, Springer, 2014.

[2] R.S. Sumana, L.N. Achala, *A short report on different wavelets and their structures*, Int. J. Res. Engg. Sci. 4(2) (2016) 31-35.

[3] C.F. Chen, C.H. Hsiao, *Haar wavelet method for solving lumped and distributed-parameter systems*, IEE Proc.-Control Theory Appl. 144(1) (1997) 87-94.

[4] C. Cattani, *Shannon wavelets for the solution of integro-differential equations*, Math. Prob. Engg. 2010 (2010).

[5] S. El-Sayed, M. Abdel-Aziz, *A comparison of Adomian's decomposition method and wavelet-Galerkin method for solving integro-differential equations*, Appl. Math. Comput. 136 (2003) 151-159.

[6] U. Lepik, *Haar wavelet method for nonlinear integro-differential equations*, Appl. Math. Comp. 176 (2006) 324-333.

[7] K. Maleknejad, F. Mirzaee, S. Abbasbandy, *Solving linear integro-differential equations system by using rationalized Haar functions method*, Appl. Math. Comput. 155 (2004) 317-328.

[8] V. Mishra, H. Kaur, R.C. Mittal, *Haar wavelet algorithm for solving certain differential, integral and integro-differential equations*, Int. J. Appl. Math Mech. 8(6) (2012) 69-82.

[9] Siraj-ul-Islam, I. Aziz, M. Fayyaz, *A new approach for numerical solution of integro-differential equations via Haar wavelets*, Int. J. Comp. Math. 90(9) (2013) 1971-1989.

[10] Siraj-ul-Islam, I. Aziz, A.S. Al-Fhaid, *An improved method based on Haar wavelets for numerical solution of nonlinear integral and integro-differential equations of first and higher orders*, J. Comp. Appl. Math. 260 (2014) 449-469.

[11] S. Sekar, C. Jaisankar, *Numerical strategies for the nonlinear integro-differential equations using single-term Haar wavelet series*, Appl. Math. Sci. 8(51) (201) 2547-2554.

[12] H. Aminikhah, S. Hossein, *Numerical solution of nonlinear system of integro-differential equations using Chebyshev wavelets*, J. Appl. Math. Stat. Inf. 11(2) (2015) 15-34.

[13] M.T. Kajania, A.H. Vencheh, *Solving linear integro-differential equation with Legendre wavelets*, Int. J. Comp. Math. 81(6) (2004) 719-726.

[14] Z. Meng, L. Wang, H. Li, Wei Zhang, *Legendre wavelets method for solving fractional integro-differential equations*, Int. J. Comp. Math. 92(6) (2015) 1275-1291.

Study of solution of Volterra integral equation and system of Volterra integral equations using Haar wavelets

S. Savitha[1], R.S. Sumana[2] and L.N. Achala[3]

[1,2,3]P. G. Department of Mathematics and Research Centre in Applied Mathematics

M. E. S. College of Arts, Commerce and Science

15th cross, Malleswaram, Bangalore - 560003.

Email ID: [1]savathreya10@gmail.com, [2]sumana.shesha@gmail.com, [3]anargund1960@gmail.com

Abstract: Volterra integral equations arise in the mathematical modelling of many physical phenomena. In this paper, we use Haar wavelet method for the numerical solution of Volterra and system of Volterra integral equations. The basic idea of Haar wavelet collocation method is to convert the integral equation into a system of algebraic equations that involves a finite number of variables. The numerical results are compared with the exact solution to prove the accuracy of the Haar wavelet method.

Keywords: Volterra integral equation, System of Volterra integral equations, Haar wavelets, Collocation points.

1   Introduction

An integral equation is an equation in which an unknown function appears under an integral sign. The types of integral equations are Fredholm Integral Equation and Volterra Integral Equation. Volterra integral equations have applications in mathematical physics, chemistry, electrochemistry, semi-conductors, scattering theory, seismology, heat conduction, metallurgy, fluid flow, chemical reaction, population dynamics etc.

In the recent years, wavelets have been widely used to solve differential equations. Alfred Haar, a Hungarian mathematician introduced Haar wavelets in 1910. The Haar wavelets consist of piecewise constant functions and are therefore the simplest orthonormal wavelets with a compact support. An advantage of these wavelets is the possibility to integrate them analytically arbitrary times. They are the simplest possible wavelets and are often known as a first order Daubechies wavelet which are conceptually simple, fast, memory efficient and exactly reversible [1]. Sumana and Achala [2] have given a brief report on Haar wavelets.

Lepik [3] applied Haar wavelets to solve nonlinear Fredholm integral equations. Linear Volterra integral equations were solved using Haar wavelets by Rabbani [4]. Reihani [5] used rationalized Haar function method for solving Fredholm and Volterra integral equations. Mirzaee [6] gave the numerical computational solution of system of linear Volterra integral equations using Haar wavelets. Shahsavaran [7] used Haar wavelet collocation method to solve Volterra integral equations with weakly singular kernel. Babolian and Shahsavaran [8] solved nonlinear Fredholm integral equations of the second kind using Haar wavelets. Derili et. al. [9] applied two-dimensional Haar wavelets to solve two-dimensional Fredholm integral equations. Biazar and Ebrahimi [10], and Yousefi and Razzaghi [11] solved nonlinear integral equations using Chebyshev wavelets and Legendre wavelets respectively.

2   Preliminaries of Haar wavelets

The Haar wavelet family for $x \in [0, 1]$ is defined as follows [1]

$$h_i(x) = \begin{cases} 1 & \text{for } x \in [\xi_1, \xi_2) \\ -1 & \text{for } x \in [\xi_2, \xi_3) \\ 0 & \text{elsewhere} \end{cases} \tag{1}$$

where

$$\xi_1 = \frac{k}{m}, \quad \xi_2 = \frac{k + 0.5}{m}, \quad \xi_3 = \frac{k + 1}{m} \tag{2}$$

In the above definition $m = 2^n, n = 0, 1, ..., J$ indicates the level of the wavelet; $k = 0, 1, ..., m - 1$ is the translation parameter. J is the maximum level of resolution. The index i in equation (1) is calculated by the formula $i = m + k + 1$. In the case of minimum values $m = 1, k = 0$ we have $i = 2$. The maximum value of i is $i = 2M = 2^{J+1}$.

For $i = 1$, $h_1(x)$ is assumed to be the scaling function which is defined as follows.

$$h_1(x) = \begin{cases} 1 & \text{for } x \in [0, 1) \\ 0 & \text{elsewhere} \end{cases} \tag{3}$$

3   Method of Solution and Examples

3.1   Volterra integral equation

Example 1:

$$y(x) = 1 + x^2 + \int_0^x \left(\frac{1 + x^2}{1 + t^2} \right) y(t) dt \tag{4}$$

The exact solution is

$$y(x) = e^x(1 + x^2) \tag{5}$$

Let the Haar wavelet solution be in the form

$$y(x) = \sum_{i=1}^{2M} a_i h_i(x) \tag{6}$$

Substituting equation (6) in equation (4), we obtain

$$\sum_{i=1}^{2M} a_i \{h_i(x) - G_i(x)\} = 1 + x^2 \tag{7}$$

where $G_i(x)$ is given by

$$G_i(x) = \int_0^x \frac{1 + x^2}{1 + t^2} h_i(t) dt \tag{8}$$

Solving $G_i(x)$ for $i = 1$ leads to

$$G_i(x) = (1 + x^2) \tan^{-1}(x) \tag{9}$$

Solving $G_i(x)$ for $i > 1$ gives

$$G_i(x) = \begin{cases} 0, & \text{for } x \in [0, \xi_1) \\[2mm] (1+x^2)(\tan^{-1}(x) - \tan^{-1}(\xi_1)), & \text{for } x \in [\xi_2, \xi_3) \\[2mm] (1+x^2)(2\tan^{-1}(\xi_2) - \tan^{-1}(\xi_1) - \tan^{-1}(x)), & \text{for } x \in [\xi_2, \xi_3) \\[2mm] (1+x^2)(2\tan^{-1}(\xi_2) - \tan^{-1}(\xi_1) - \tan^{-1}(\xi_3)), & \text{for } x \in [\xi_3, 1) \end{cases} \tag{10}$$

The wavelet collocation points are defined as

$$x_l = \frac{l - 0.5}{2M}, \ l = 1, 2, \ldots, 2M. \tag{11}$$

Taking the collocation points $x \to x_l$ in equations (7) and (6), we get

$$\sum_{i=1}^{2M} a_i \{h_i(x_l) - G_i(x_l)\} = 1 + x_l^2 \tag{12}$$

$$y(x_l) = \sum_{i=1}^{2M} a_i h_i(x_l) \tag{13}$$

The wavelet coefficients a_i, $i = 1, 2, \ldots, 2M$ are obtained by solving the $2M$ system of equations in (12). These coefficients are then substituted in equation (13) to obtain the Haar wavelet solution at the collocation points $x_l, l = 1, 2, \ldots, 2M$. The HWCM solution of the example with $J = 8$ is given in Table 1. Figure 1 shows the comparison of the HWCM solution with the exact solution.

3.2   System of Volterra integral equation

Example 2:

$$u(x) = \frac{1}{18}x + \frac{17}{36} + \int_0^1 \left(\frac{x+t}{3}\right)(u(t) + v(t))dt \tag{14}$$

$$v(x) = x^2 - \frac{19}{12}x + 1 + \int_0^1 xt(u(t) + v(t))dt \tag{15}$$

The exact solutions are

$$u(x) = x + 1 \tag{16}$$

$$v(x) = x^2 + 1 \tag{17}$$

Let the Haar wavelet solutions be in the form

$$u(x) = \sum_{i=1}^{2M} a_i h_i(x) \tag{18}$$

$$v(x) = \sum_{i=1}^{2M} b_i h_i(x) \tag{19}$$

Substituting equations (18) and (19) in equations (14) and (15) gives

$$\sum_{i=1}^{2M}\{a_i[h_i(x) - G_i(x)] - b_iG_i(x)\} = \frac{1}{18}x + \frac{17}{36} \tag{20}$$

$$\sum_{i=1}^{2M}\{b_i[h_i(x) - H_i(x)] - a_iH_i(x)\} = x^2 - \frac{19}{12}x + 1 \tag{21}$$

where

$$G_i(x) = \int_0^1 \left(\frac{x+t}{3}\right) h_i(t)dt \tag{22}$$

$$H_i(x) = \int_0^1 xth_i(t)dt \tag{23}$$

Solving $G_i(x)$ and $H_i(x)$, we get

$$G_i(x) = \begin{cases} \dfrac{1}{3}\left(x + \dfrac{1}{2}\right), & \text{for } i = 1 \\[2ex] \dfrac{1}{6}\left(2\xi_2^2 - \xi_1^2 - \xi_3^2\right), & \text{for } i > 1 \end{cases} \tag{24}$$

$$H_i(x) = \begin{cases} \dfrac{x}{2}, & \text{for } i = 1 \\[2ex] \dfrac{x}{2}\left(2\xi_2^2 - \xi_1^2 - \xi_3^2\right), & \text{for } i > 1 \end{cases} \tag{25}$$

The wavelet collocation points are defined as

$$x_l = \frac{l - 0.5}{2M}, \, l = 1, 2, \ldots, 2M. \tag{26}$$

Taking the collocation points $x \to x_l$ in equations (20), (21), (18) and (19), we obtain

$$\sum_{i=1}^{2M} \begin{bmatrix} h_i(x_l) - G_i(x_l) & -G_i(x_l) \\ -H_i(x_l) & h_i(x_l) - H_i(x_l) \end{bmatrix} \begin{bmatrix} a_i \\ b_i \end{bmatrix} = \begin{bmatrix} \frac{1}{18}x_l + \frac{17}{36} \\ x_l^2 - \frac{19}{12}x_l + 1 \end{bmatrix} \tag{27}$$

$$u(x_l) = \sum_{i=1}^{2M} a_ih_i(x_l) \tag{28}$$

$$v(x_l) = \sum_{i=1}^{2M} b_ih_i(x_l) \tag{29}$$

The wavelet coefficients $a_i, b_i, \, i = 1, 2, \ldots, 2M$ are obtained by solving the $4M$ system of equations in (27). These coefficients are then substituted in equations (28) and (29) to obtain the Haar wavelet solution at the collocation points $x_l, l = 1, 2, \ldots, 2M$. The HWCM solution of the example with $J = 7$ is given in Table 2. Figure 2 shows the comparison of the HWCM solution with the exact solution.

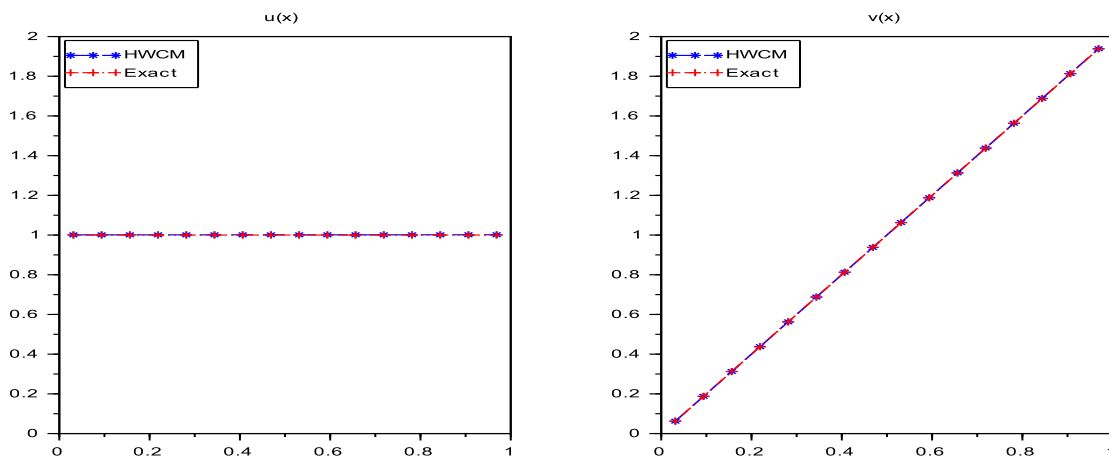**Table 1:** Comparison of HWCM solution and exact solution for $J = 8$ at different x of Example 1

x	$y(x)$	
	HWCM	Exact
0.000977	1.000978	1.000978
0.041992	1.044726	1.044725
0.122070	1.146670	1.146669
0.254883	1.374137	1.374136
0.354492	1.604588	1.604586
0.444336	1.867346	1.867344
0.559570	2.297856	2.297854
0.684570	2.912192	2.912188
0.758789	3.365339	3.365334
0.874023	4.227293	4.227287
0.999023	5.425964	5.425956

Table 2: Comparison of HWCM solution and exact solution for $J = 7$ at different x of Example 2

x	$u(x)$		$v(x)$	
	HWCM	Exact	HWCM	Exact
0.001953	1.001950	1.001953	1.000004	1.000004
0.044922	1.044919	1.044922	1.002018	1.002018
0.123047	1.123044	1.123047	1.015139	1.015141
0.263672	1.263668	1.263672	1.069521	1.069523
0.345703	1.345699	1.345703	1.119508	1.119511
0.443359	1.443355	1.443359	1.196564	1.196568
0.560547	1.560542	1.560547	1.314208	1.314213
0.650391	1.650386	1.650391	1.423002	1.423008
0.775391	1.775385	1.775391	1.601224	1.601231
0.849609	1.849604	1.849609	1.721829	1.721836
0.998047	1.998041	1.998047	1.996089	1.996098
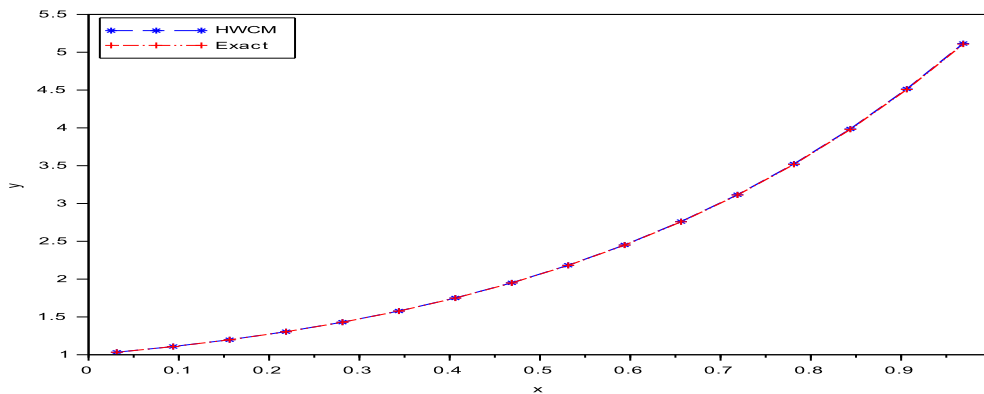
Figure 1: Comparison of HWCM solution and exact solution of Example 1

Figure 2: Comparison of HWCM solution and exact solution of Example 2

4   Conclusion

In this paper, an efficient numerical scheme based on uniform Haar wavelets is used to solve Volterra and system of Volterra integral equations. The numerical scheme is tested for two example. The obtained numerical results are compared with the exact solutions, and are found to be in good agreement. Thus the Haar wavelet method guarantees the necessary accuracy with a small number of grid points.

References

[1] U. Lepik, H. Hein, *Haar wavelets with applications*, Springer, 2014.

[2] R.S. Sumana, L.N. Achala, *A short report on different wavelets and their structures*, Int. J. Res. Engg. Sci. 4(2) (2016) 31-35.

[3] U. Lepik, E. Tamme, *Solution of nonlinear Fredholm integral equations via the Haar wavelet method*, Proc. Estonian Acad. Sci. Phys. Math. 56 (2007) 17-27.

[4] M. Rabbani, K. Maleknejad, N. Aghazadeh, R. Mollapourasl, *Computational projection method for solving Fredholm integral equation*, Appl. Math. Comput. 191 (2007) 140-143.

[5] M. Reihani, Z. Abadi, *Rationalized Haar functions method for solving Fredholm and Voltera integral equations*, J. Comput. Appl. Math. 200 (2007) 12-20.

[6] F. Mirzaee, *Numerical computational solution of the linear Volterra integral equations system via rationalized Haar functions*, J. King Saud Univ. Sci. 22 (2010) 265-268.

[7] A. Shahsavaran, *Haar wavelet method to solve Volterra integral equations with weakly singular kernel by collocation method*, Appl. Math. Sci. 5(65) (2011) 3201-3210.

[8] E. Babolian, A. Shahsavaran, *Numerical solution of nonlinear Fredholm integral equations of the second kind using Haar wavelets*, J. Comput. Appl. Math. 225 (2009) 7-95.

[9] H.A. Derili, S. Sohrabi, A. Arzhang1, *Two-dimensional wavelets for numerical solution of integral equations*, Math. Sci. 6(5) (2012).

[10] J. Biazar, H. Ebrahimi, *Chebyshev wavelets approach for nonlinear systems of Volterra integral equations*, Comp. Math. Appl. 63 (2012) 608-616.

[11] S. Yousefi, M. Razzaghi, *Legendre wavelets method for the nonlinear Volterra-Fredholm integral equations*, Math. Comput. Simul. 70 (2005) 1-8.

Solution of one-dimensional parabolic partial differential equations using Haar wavelet method

M. Tejuswini[1], R.S. Sumana[2] and L.N. Achala[3]

[1,2,3]P. G. Department of Mathematics and Research Centre in Applied Mathematics

M. E. S. College of Arts, Commerce and Science

15th cross, Malleswaram, Bangalore - 560003.

Email ID: [1]9tejuswini3@gmail.com, [2]sumana.shesha@gmail.com, [3]anargund1960@gmail.com

Abstract: Parabolic partial differential equations arise in the mathematical modelling of many physical phenomena. In this paper, we use Haar wavelet method for the numerical solution of one dimensional homogeneous and inhomogeneous heat equation. The basic idea of Haar wavelet collocation method is to convert the partial differential equation into a system of algebraic equations that involves a finite number of variables. The numerical results are compared with the exact solution to prove the accuracy of the Haar wavelet method.

Keywords: Parabolic partial differential equations, One-dimensional heat equation, Inhomogeneous one-dimensional heat equation, Haar wavelets, Collocation points.

1   Introduction

A differential equation that contains partial unknown multivariable functions and their partial derivatives is called partial differential equation (PDE). Partial differential equations are used to formulate problems involving functions of several variables, and are either solved by hand, or used to create a relevant computer model. Partial differential equations can also be used to describe a wide variety of phenomena such as sound, heat, electrostatics, electrodynamics, fluid flow, elasticity, or quantum mechanics. Just as ordinary differential equations often model one-dimensional dynamical systems, partial differential equations often model multidimensional systems.

The Haar wavelet [1] is the principal known wavelet and was proposed in 1909 by Alfred Haar. The Haar wavelet is likewise the least complex conceivable wavelet. Over the recent decades, wavelets by and large have picked up a respectable status because of their applications in different disciplines and in that capacity have numerous examples of overcoming adversity. Prominent effects of their studies are in the fields of signal and image processing, numerical analysis, differential and integral equations, tomography, and so on. A standout amongst the best utilizations of wavelets has been in image processing. The FBI has built up a wavelet based algorithm for fingerprint compression. Wavelets have the capability to designate functions at different levels of resolution, which permits building up a chain of approximate solutions of equations. Compactly supported wavelets are localized in space, wherein solutions can be refined in regions of sharp variations/transients without going for new grid generation, which is the basic methodology in established numerical schemes. Sumana and Achala [2] have given a brief report on Haar wavelets.

Chen and Hsiao [3] recommended to expand into the Haar series the highest order derivatives appearing in the differential equation. This idea has been very prolific and it is being

abundantly applied for the solution of PDEs. The wavelet coefficients appearing in the Haar series are calculated either using Collocation method or Galerkin method. Lepik [4] applied Haar wavelets to solve evolution equations. Shi et. al. [5] solved wave equation using Haar wavelets. Ram Jiwari [6] used Haar wavelets to solve Burgers equation. Hariharan et. al. [7, 8, 9, 10, 11] applied Haar wavelets to solve Cahn-Allen Equation, Fisher's equation, FitzHugh-Nagumo equation, Klein-Gordon equation, Sine-Gordon equation and some nonlinear parabolic equations. Dhawan et. al. [12] solved heat equation using Haar wavelets. Lepik [13] used two-dimensional Haar wavelets to solve diffusion equation and Poisson equation. Wang and Zhao [14] solved two-dimensional Burgers equation using two-dimensional Haar wavelets. Celik [15, 16] used Haar wavelets to solve magnetohydrodynamic flow equations and generalized Burgers-Huxley equation. Bujurke et. al. [17] applied wavelet-multigrid method to solve elliptic partial differential equations. Kumar and Pandit [18] used a composite numerical scheme based on Haar wavelets for the numerical simulation of coupled Burgers equation.

2 Preliminaries of Haar wavelets

The Haar wavelet family for $x \in [0, 1]$ is defined as follows [1]

$$
h_i(x) = \begin{cases} 1 & \text{for } x \in [\xi_1, \xi_2) \\ -1 & \text{for } x \in [\xi_2, \xi_3) \\ 0 & \text{elsewhere} \end{cases} \tag{1}
$$

where

$$
\xi_1 = \frac{k}{m}, \quad \xi_2 = \frac{k + 0.5}{m}, \quad \xi_3 = \frac{k + 1}{m} \tag{2}
$$

In the above definition $m = 2^n, n = 0, 1, ..., J$ indicates the level of the wavelet; $k = 0, 1, ..., m - 1$ is the translation parameter. J is the maximum level of resolution. The index i in equation (1) is calculated by the formula $i = m + k + 1$. In the case of minimum values $m = 1, k = 0$ we have $i = 2$. The maximum value of i is $i = 2M = 2^{J+1}$.

For $i = 1$, $h_1(x)$ is assumed to be the scaling function which is defined as follows.

$$
h_1(x) = \begin{cases} 1 & \text{for } x \in [0, 1) \\ 0 & \text{elsewhere} \end{cases} \tag{3}
$$

In order to solve PDEs of any order, we need the following integrals.

$$
p_i(x) = \int_0^x h_i(x)dx = \begin{cases} x - \xi_1 & \text{for } x \in [\xi_1, \xi_2) \\ \xi_3 - x & \text{for } x \in [\xi_2, \xi_3) \\ 0 & \text{elsewhere} \end{cases} \tag{4}
$$

$$q_i(x) = \int_0^x p_i(x)dx = \begin{cases} \dfrac{1}{2}(x - \xi_1)^2 & \text{for } x \in [\xi_1, \xi_2) \\[2mm] \dfrac{1}{4m^2} - \dfrac{1}{2}(\xi_3 - x)^2 & \text{for } x \in [\xi_2, \xi_3) \\[2mm] \dfrac{1}{4m^2} & \text{for } x \in [\xi_3, 1] \\[2mm] 0 & \text{elsewhere} \end{cases} \tag{5}$$

2.1 Function approximation

Any function $f(x)$ which is square integrable on $(0, 1)$ can be expressed as an infinite sum of Haar wavelets as

$$f(x) = \sum_{i=1}^{\infty} a(i)h_i(x), \tag{6}$$

where

$$a(i) = \int_0^1 f(x)h_i(x)dx. \tag{7}$$

If $f(x)$ is approximated as piecewise constant during each subinterval, then equation (6) will be terminated at finite terms, i.e.

$$f(x) = \sum_{i=1}^{2M} a(i)h_i(x), \tag{8}$$

where the wavelet coefficients $a(i)$, $i = 1, 2, \ldots, 2M$ are to be determined.

3 Method of solution

3.1 One dimensional heat equation

Consider the one-dimensional heat equation

$$\frac{\partial u}{\partial t} = c\frac{\partial^2 u}{\partial x^2}, \quad 0 \leq x \leq 1, t \geq 0 \tag{9}$$

with initial and boundary conditions

$$u(x, 0) = f(x), \ 0 \leq x \leq 1 \tag{10}$$

$$u(0, t) = g_1(t), \ t \geq 0 \tag{11}$$

$$u(1, t) = g_2(t), \ t \geq 0 \tag{12}$$

Divide the interval $[0, T]$ into N equal parts of length $\Delta t = \frac{T}{N}$ and denote $t_s = (s-1)\Delta t$, $s = 1, 2, 3 \ldots N$

Let the Haar wavelet solution be in the form

$$\dot{u}''(x, t) = \sum_{i=1}^{2M} a_s(i)h_i(x) \tag{13}$$

Integrating equation (13) w.r.t. t in the limits $[t_s, t]$, we get

$$u''(x,t) = (t - t_s) \sum_{i=1}^{2M} a_s(i) h_i(x) + u''(x, t_s) \tag{14}$$

Integrating equation (14) w.r.t. x in the limits $[0, x]$, we obtain

$$u'(x,t) = (t - t_s) \sum_{i=1}^{2M} a_s(i) p_i(x) + u'(x, t_s) + u'(0, t) - u'(0, t_s) \tag{15}$$

Integrating equation (15) w.r.t. x in the limits $[0, x]$, we arrive at

$$u(x,t) = (t - t_s) \sum_{i=1}^{2M} a_s(i) q_i(x) + u(x, t_s) + u(0, t) - u(0, t_s) + x[u'(0, t) - u'(0, t_s)] \tag{16}$$

Differentiating equation (16) w.r.t. t gives

$$\dot{u}(x,t) = (t - t_s) \sum_{i=1}^{2M} a_s(i) q_i(x) + \dot{u}(0, t) + x\dot{u}'(0, t) \tag{17}$$

Using equation (11) in equations (16) and (17), we get

$$u(x,t) = (t - t_s) \sum_{i=1}^{2M} a_s(i) q_i(x) + u(x, t_s) + g_1(t) - g_1(t_s) + x[u'(0, t) - u'(0, t_s)] \tag{18}$$

$$\dot{u}(x,t) = \sum_{i=1}^{2M} a_s(i) q_i(x) + \dot{g}_1(t) + x\dot{u}'(0, t) \tag{19}$$

Putting $x = 1$ in equations (18) and (19), and using equation (12) gives

$$u'(0,t) - u'(0, t_s) = -(t - t_s) \sum_{i=1}^{2M} a_s(i) q_i(1) + g_2(t) - g_2(t_s) - g_1(t) + g_1(t_s) \tag{20}$$

$$\dot{u}'(0,t) = -\sum_{i=1}^{2M} a_s(i) q_i(1) + \dot{g}_2(t) - \dot{g}_1(t) \tag{21}$$

Substituting equation (20) in equations (15) and (20), and equation (21) in equation (19), we have

$$u'(x,t) = (t - t_s) \sum_{i=1}^{2M} a_s(i)[p_i(x) - q_i(1)] + u'(x, t_s) + g_2(t) - g_2(t_s) - g_1(t) + g_1(t_s) \tag{22}$$

$$u(x,t) = (t - t_s) \sum_{i=1}^{2M} a_s(i)[q_i(x) - xq_i(1)] + u(x, t_s) + x[g_2(t) - g_2(t_s)] \\ +(1 - x)[g_1(t) - g_1(t_s)] \tag{23}$$

$$\dot{u}(x,t) = \sum_{i=1}^{2M} a_s(i)[q_i(x) - xq_i(1)] + x\dot{g}_2(t) + (1 - x)\dot{g}_1(t) \tag{24}$$

Substituting equations (14) and (24) in equation (9), we obtain

$$\sum_{i=1}^{2M} a_s(i)[q_i(x) - xq_i(1) - c(t - t_s)h_i(x)] = cu''(x, t_s) - x\dot{g}_2(t) - (1-x)\dot{g}_1(t) \quad (25)$$

The wavelet collocation points are defined as,

$$x_l = \frac{l - 0.5}{2M}, \quad l = 1, 2, \ldots, 2M \quad (26)$$

Taking $x \to x_l$, $t \to t_{s+1}$ in equations (25), (23) and (14) gives

$$\sum_{i=1}^{2M} a_s(i)[q_i(x_l) - x_l q_i(1) - c(\Delta t)h_i(x_l)] = cu''(x_l, t_s) - x_l \dot{g}_2(t_{s+1}) - (1-x_l)\dot{g}_1(t_{s+1}) \quad (27)$$

$$u(x_l, t_{s+1}) = \Delta t \sum_{i=1}^{2M} a_s(i)[q_i(x_l) - x_l q_i(1)] + u(x_l, t_s) + x_l[g_2(t_{s+1}) - g_2(t_s)]$$
$$+ (1 - x_l)[g_1(t_{s+1}) - g_1(t_s)] \quad (28)$$

$$u''(x_l, t_{s+1}) = \Delta t \sum_{i=1}^{2M} a_s(i)h_i(x_l) + u''(x_l, t_s) \quad (29)$$

Using the initial conditions (10), we have

$$\begin{aligned} u(x_l, 0) &= f(x_l) \\ u'(x_l, 0) &= f'(x_l) \\ u''(x_l, 0) &= f''(x_l) \end{aligned} \quad (30)$$

The wavelet coefficients $a_s(i)$, $i = 1, 2, \ldots, 2M$ can be successively calculated from equation (27). This process is started with equation (30). These coefficients are then substituted in equations (28) and (29) to obtain the approximate solutions at different time levels.

3.2   Inhomogeneous one-dimensional heat equation

Consider the inhomogeneous one-dimensional heat equation

$$\frac{\partial u}{\partial t} = c\frac{\partial^2 u}{\partial x^2} + F(x, t), \quad 0 \le x \le 1, t \ge 0 \quad (31)$$

with initial and boundary conditions

$$u(x, 0) = f(x), \ 0 \le x \le 1 \quad (32)$$

$$u(0, t) = g_1(t), \ t \ge 0 \quad (33)$$

$$u(1, t) = g_2(t), \ t \ge 0 \quad (34)$$

Substituting (14) and (24) in (31) and taking $x \to x_l$, $t \to t_{s+1}$ in the resultant equation, we obtain

$$\sum_{i=1}^{2M} a_s(i)[q_i(x_l) - x_l q_i(1) - c(\Delta t)h_i(x_l)] = cu''(x_l, t_s) - x_l \dot{g}_2(t_{s+1}) - (1-x_l)\dot{g}_1(t_{s+1})$$
$$+ F(x_l, t_{s+1}) \quad (35)$$

4   Examples and Discussions

In this section, two examples each of one-dimensional heat equation and inhomogeneous heat equation are solved, and the efficiency and accuracy of the Haar wavelet collocation method (HWCM) are discussed. Lagrange's interpolation and cubic-spline interpolation are used to find the solution of the heat equation and inhomogeneous heat equation respectively at the indicated points.

Example 1:

$$\frac{\partial u}{\partial t} = \frac{\partial^2 u}{\partial x^2}, \ \ 0 \le x \le 1, t \ge 0,$$
$$u(x, 0) = \sin(\pi x), \ 0 \le x \le 1, \tag{36}$$
$$\left.\begin{array}{l} u(0, t) = 0 \\ u(1, t) = 0 \end{array}\right\} t \ge 0.$$

The exact solution is

$$u(x, t) = e^{-\pi^2 t} \sin(\pi x) \tag{37}$$

The HWCM solution of the example at $t = 0.1, 0.2$ with $M = 32$ and $\Delta t = 0.0001$ is given in Table 1. Figure 1 shows the comparison of the HWCM solution with the exact solution at $t = 0.1$ and $t = 0.2$. Figure 2 depicts the physical behavior of the HWCM solution in contour and 3D.

If $u_{ex}(x, t_s)$ is the exact solution (37) at $t = t_s$, we define the error estimate as

$$\mu(t_s) = \frac{1}{2M} \|u(x, t_s) - u_{ex}(x, t_s)\| \tag{38}$$

We have obtained the following error estimates for $M = 32$ and $\Delta t = 0.0001$.
  (i) $\mu(0.1) = 1.8340E - 05$ in L_2 space and $\mu(0.1) = 3.2411E - 06$ in L_∞ space.
 (ii) $\mu(0.2) = 1.7164E - 05$ in L_2 space and $\mu(0.2) = 3.0333E - 06$ in L_∞ space.

Example 2:

$$\frac{\partial u}{\partial t} = \frac{4}{\pi^2} \frac{\partial^2 u}{\partial x^2}, \ \ 0 \le x \le 4, t \ge 0,$$
$$u(x, 0) = \sin\left(\frac{\pi x}{4}\right)\left(1 + 2\cos\left(\frac{\pi x}{4}\right)\right), \ 0 \le x \le 4 \tag{39}$$
$$\left.\begin{array}{l} u(0, t) = 0 \\ u(4, t) = 0 \end{array}\right\} t \ge 0.$$

The exact solution is
$$u(x, t) = e^{-t} \sin\left(\frac{\pi x}{2}\right) + e^{-\frac{t}{4}} \sin\left(\frac{\pi x}{4}\right) \tag{40}$$

The HWCM solution of the example at $t = 0.1, 0.2$ with $M = 32$ and $\Delta t = 0.001$ is given in Table 2. Figure 3 shows the comparison of the HWCM solution with the exact solution at $t = 0.1$ and $t = 0.2$. Figure 4 depicts the physical behavior of the HWCM solution in contour

and 3D.

We have obtained the following error estimates for $M = 32$ and $\Delta t = 0.001$.
  (i) $\mu(0.1) = 4.1726E - 06$ in L_2 space and $\mu(0.1) = 7.7000E - 07$ in L_∞ space.
  (ii) $\mu(0.2) = 7.8744E - 06$ in L_2 space and $\mu(0.2) = 1.4558E - 06$ in L_∞ space.

Example 3:

$$\frac{\partial u}{\partial t} = \frac{\partial^2 u}{\partial x^2} - \pi^2 \sin(\pi x), \ \ 0 \leq x \leq 1, t \geq 0,$$
$$u(x, 0) = \sin(2\pi x), \ 0 \leq x \leq 1,$$
$$\left.\begin{array}{l} u(0, t) = 0 \\ u(1, t) = 0 \end{array}\right\} t \geq 0. \tag{41}$$

The exact solution is

$$u(x, t) = (e^{-\pi^2 t} - 1) \sin(\pi x) + e^{-4\pi^2 t} \sin(2\pi x) \tag{42}$$

The HWCM solution of the example at $t = 0.1, 0.2$ with $M = 64$ and $\Delta t = 0.0001$ is given in Table 3. Figure 5 shows the comparison of the HWCM solution with the exact solution at $t = 0.1$ and $t = 0.2$. Figure 6 depicts the physical behavior of the HWCM solution in contour and 3D.

We have obtained the following error estimates for $M = 64$ and $\Delta t = 0.0001$.
  (i) $\mu(0.1) = 1.9117E - 05$ in L_2 space and $\mu(0.1) = 2.9859E - 06$ in L_∞ space.
  (ii) $\mu(0.2) = 1.1476E - 05$ in L_2 space and $\mu(0.2) = 1.7386E - 06$ in L_∞ space.

Example 4:

$$\frac{\partial u}{\partial t} = 3\frac{\partial^2 u}{\partial x^2} + 18x, \ \ 0 \leq x \leq 1, t \geq 0,$$
$$u(x, 0) = \sin(\pi x) - x^3, \ 0 \leq x \leq 1,$$
$$\left.\begin{array}{l} u(0, t) = 0 \\ u(1, t) = 0 \end{array}\right\} t \geq 0. \tag{43}$$

The exact solution is
$$u(x, t) = e^{-3\pi^2 t} \sin(\pi x) - x^3 \tag{44}$$

The HWCM solution of the example at $t = 0.1, 0.2$ with $M = 32$ and $\Delta t = 0.0001$ is given in Table 2.4. Figure 7 shows the comparison of the HWCM solution with the exact solution at $t = 0.1$ and $t = 0.2$. Figure 8 depicts the physical behavior of the HWCM solution in contour and 3D.

We have obtained the following error estimates for $M = 32$ and $\Delta t = 0.0001$.
  (i) $\mu(0.1) = 2.7112E - 05$ in L_2 space and $\mu(0.1) = 4.7914E - 06$ in L_∞ space.
  (ii) $\mu(0.2) = 1.0788E - 05$ in L_2 space and $\mu(0.2) = 1.9066E - 06$ in L_∞ space.

Table 1: Comparison of the HWCM solution and exact solution of Example 1

x	$u(x,t)$			
	$t = 0.1$		$t = 0.2$	
	HWCM	Exact	HWCM	Exact
0.1	0.11523721	0.11517306	0.04298591	0.04292590
0.2	0.21919413	0.21907217	0.08176406	0.08164992
0.3	0.30169484	0.30152698	0.11253857	0.11238147
0.4	0.35466356	0.35446622	0.13229702	0.13211234
0.5	0.37291533	0.37270784	0.13910532	0.13891113
0.6	0.35466356	0.35446622	0.13229702	0.13211234
0.7	0.30169484	0.30152698	0.11253857	0.11238147
0.8	0.21919413	0.21907217	0.08176406	0.08164992
0.9	0.11523719	0.11517306	0.04298592	0.04292590

Table 2: Comparison of the HWCM solution and exact solution of Example 2

x	$u(x,t)$			
	$t = 0.1$		$t = 0.2$	
	HWCM	Exact	HWCM	Exact
0.1	0.83326643	0.83323743	0.77523844	0.77518392
0.2	1.43387092	1.43382431	1.33786594	1.33777785
0.3	1.64964111	1.64959382	1.54830943	1.54821999
0.4	1.45945555	1.45942494	1.38596882	1.38591080
0.5	0.97531299	0.97530991	0.95123549	0.95122942
0.6	0.39570000	0.39572476	0.42338861	0.42343508
0.7	-0.07155154	-0.07150923	-0.00917807	-0.00909845
0.8	-0.28732173	-0.28727874	-0.21962156	-0.21954059
0.9	-0.23048968	-0.23046275	-0.18734240	-0.18729180

Table 3: Comparison of the HWCM solution and exact solution of Example 3

x	$u(x,t)$			
	$t = 0.1$		$t = 0.2$	
	HWCM	Exact	HWCM	Exact
0.1	-0.18230193	-0.18250186	-0.26576365	-0.26587223
0.2	-0.35002123	-0.35036121	-0.50559235	-0.50578121
0.3	-0.48875658	-0.48913814	-0.69605935	-0.69628140
0.4	-0.58492761	-0.58524822	-0.81852041	-0.81872532
0.5	-0.62710420	-0.62729216	-0.86093885	-0.86108887
0.6	-0.60789545	-0.60793238	-0.81908259	-0.81916304
0.7	-0.52591933	-0.52584189	-0.69696897	-0.69698965
0.8	-0.38718397	-0.38706496	-0.50650197	-0.50648946
0.9	-0.20526977	-0.20518602	-0.26632583	-0.26630995

Table 4: Comparison of the HWCM solution and exact solution of Example 4

| x	$u(x,t)$			
	$t = 0.1$		$t = 0.2$	
	HWCM	Exact	HWCM	Exact
0.1	0.01509361	0.01499882	-0.00013397	-0.00017169
0.2	0.02261186	0.02243156	-0.00635272	-0.00642446
0.3	0.01513361	0.01488545	-0.02473271	-0.02483145
0.4	-0.01446897	-0.01476070	-0.06133464	-0.06145072
0.5	-0.07291999	-0.07322673	-0.12219747	-0.12231953
0.6	-0.16646897	-0.16676070	-0.21333464	-0.21345072
0.7	-0.30086639	-0.30111455	-0.34073271	-0.34083145
0.8	-0.48138814	-0.48156844	-0.51035272	-0.51042446
0.9	-0.71290637	-0.71300118	-0.72813395	-0.72817169
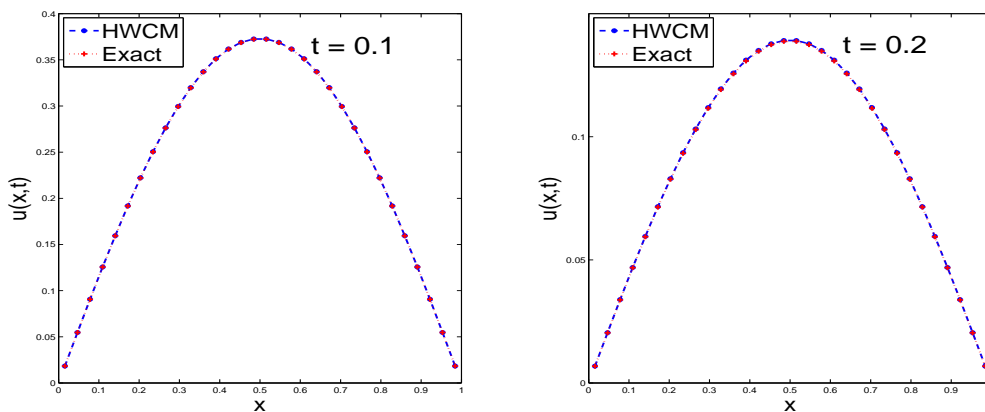
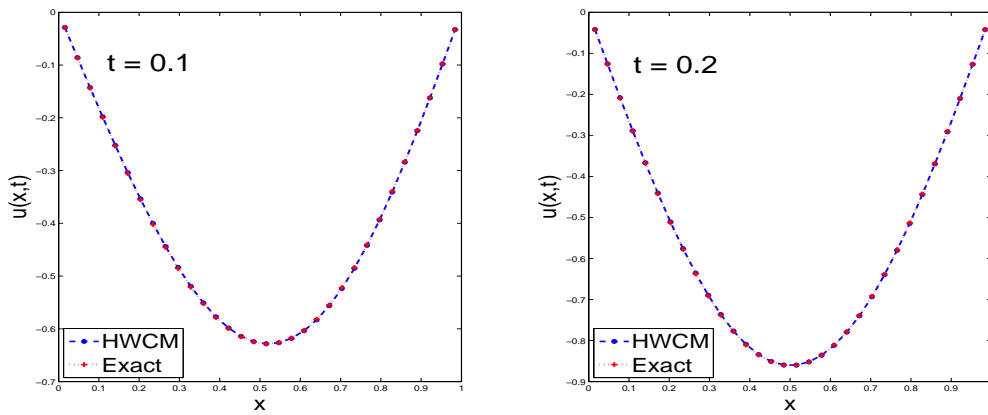**Figure 1:** Comparison of the HWCM solution and exact solution of Example 1
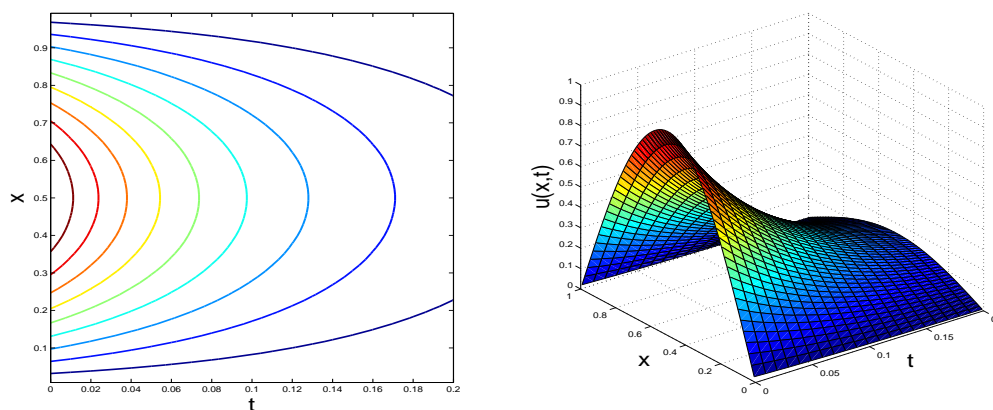
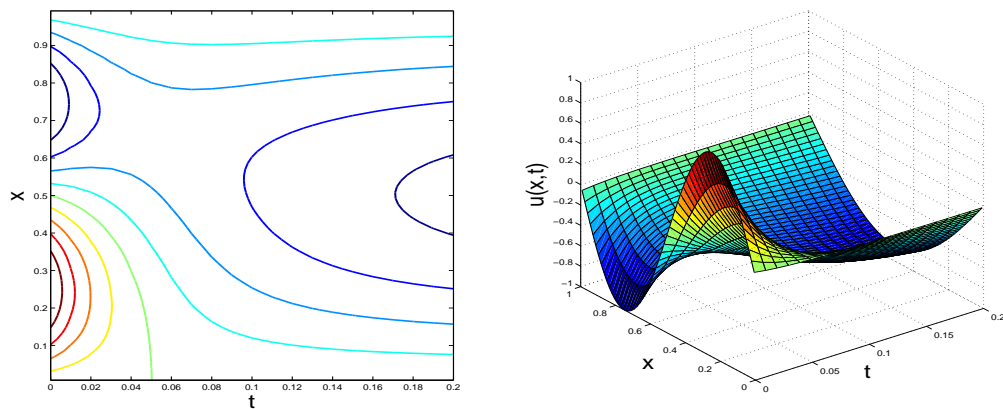**Figure 2:** Physical behaviour of the HWCM solution of $u(x, t)$ of Example 1
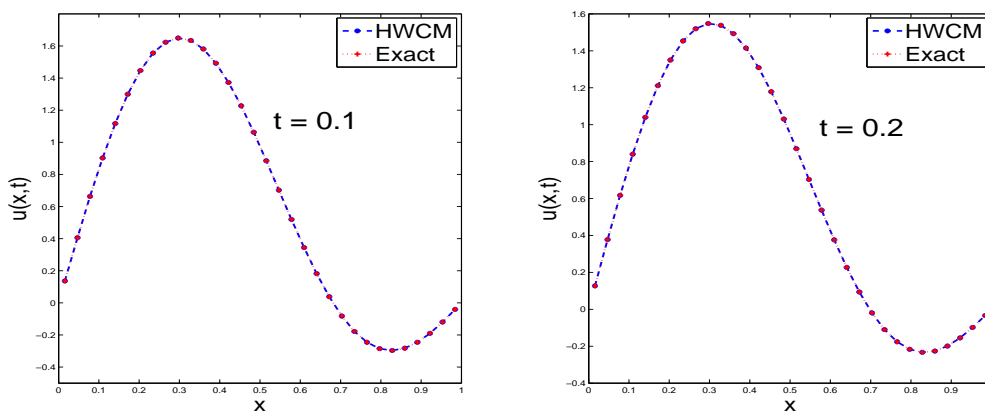
Figure 3: Comparison of the HWCM solution and exact solution of Example 2
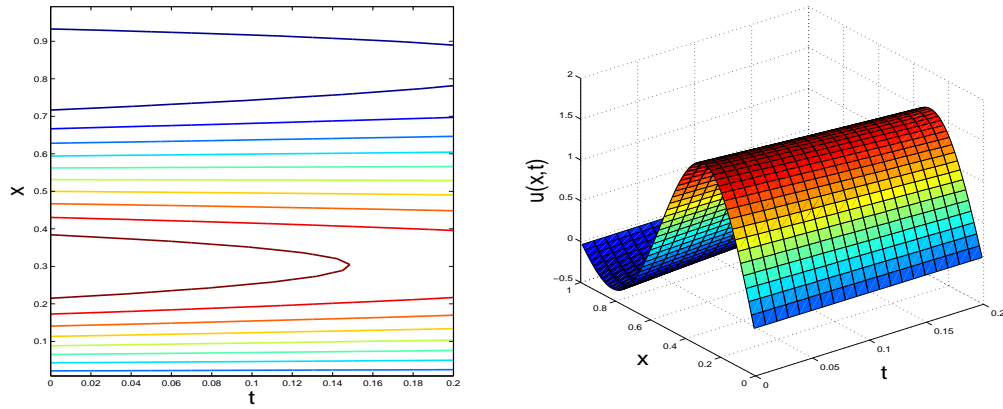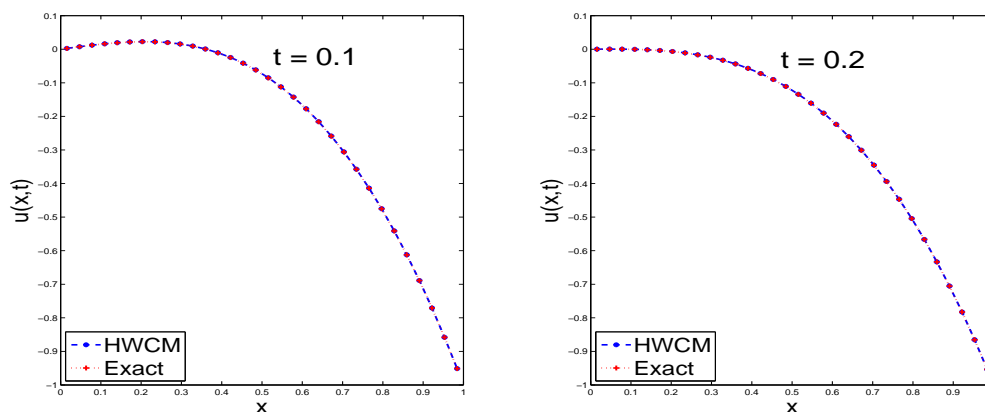
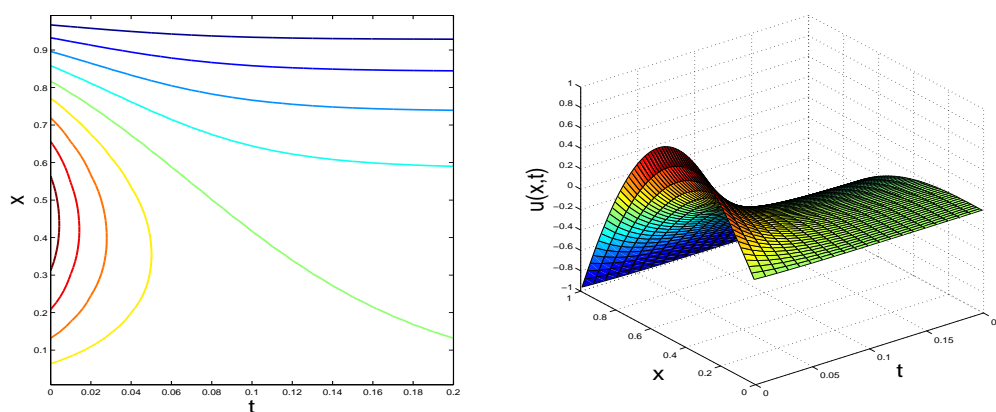**Figure 4:** Physical behaviour of the HWCM solution of $u(x,t)$ of Example 2

Figure 5: Comparison of the HWCM solution and exact solution of Example 3

Figure 6: Physical behaviour of the HWCM solution of $u(x,t)$ of Example 3

Figure 7: Comparison of the HWCM solution and exact solution of Example 4

Figure 8: Physical behaviour of the HWCM solution of $u(x,t)$ of Example 4

5 Conclusion

In this paper, an efficient numerical scheme based on uniform Haar wavelets is used to solve parabolic differential equations namely one-dimensional homogeneous and inhomogeneous heat equation. The numerical scheme is tested for four examples. The obtained numerical results are compared with the exact solutions and are found to be in good agreement. We observe that the error estimates are negligibly small compared to the number of grid points. Thus the Haar wavelet method guarantees the necessary accuracy with a small number of grid points.

References

[1] U. Lepik, H. Hein, *Haar wavelets with applications*, Springer, 2014.

[2] R.S. Sumana, L.N. Achala, *A short report on different wavelets and their structures*, Int. J. Res. Engg. Sci. 4(2) (2016) 31-35.

[3] C.F. Chen, C.H. Hsiao, *Haar wavelet method for solving lumped and distributed-parameter systems*, IEE Proc.-Control Theory Appl. 144(1) (1997) 87-94.

[4] U. Lepik, *Numerical solution of evolution equations by the Haar wavelet method*, Appl. Math. Comput. 185 (2007) 695-704.

[5] Z. Shi, T. Liu, B. Gao, *Haar Wavelet Method for Solving Wave Equation*, Int. Conf. Comp. Appl. Sys. Model. (ICCASM 2010).

[6] R. Jiwari, *A Haar wavelet quasilinearization approach for numerical simulation of Burgers Equation*, Comp. Phys. Comm. 183 (2012) 2413-2423.

[7] G. Hariharan, K. Kannan, *Haar Wavelet Method for Solving Cahn-Allen Equation*, Appl. Math. Sci. 3 (2009) 2523-2533.

[8] G. Hariharan, K. Kannan, K.R. Sharma, *Haar wavelet method for solving Fisher's equation*, Appl. Math. Comput. 211 (2009) 284-292.

[9] G. Hariharan, K. Kannan, *Haar wavelet method for solving FitzHugh-Nagumo equation*, Int. J. Comput. Math. Sci. 4(6) (2010) 281-285.

[10] G. Hariharan, *Haar Wavelet Method for Solving the Klein-Gordon and the Sine-Gordon Equations*, Int. J. Nonlin. Sci. 11 (2011) 180-189.

[11] G. Hariharan, K. Kannan, *Haar wavelet method for solving some nonlinear Parabolic equations*, J. Math. Chem. (2010)

[12] S. Dhawan, S. Arora, S. Kumar, *Numerical approximation of heat equation using Haar wavelets*, Int. J. Pure Appl. Math. 86(1) (2013) 55-63.

[13] U. Lepik, *Solving PDEs with the aid of two-dimensional Haar wavelets*, Comput. Math. Appl. 61 (2011) 1873-1879.

[14] M. Wang, F. Zhao, *Haar wavelet method for solving two-dimensional Burgers equation*, Adv. Intell. Soft Comput. 145 (2012) 381-387.

[15] I. Celik, *Haar wavelet approximation for magnetohydrodynamic flow equations*, Appl. Math. Model. 37 (2013) 3894-3902.

[16] I. Celik, *Haar wavelet method for solving generalized Burgers-Huxley equation*, Arab. J. Math. Sci. 18 (2012) 25-37.

[17] N. Bujurke, C. Salimath, R. Kudenatti, S. Shiralashetti, *A fast wavelet-multigrid method to solve elliptic partial differential equations*, Appl. Math. Comput. 185 (2007) 667-680.

[18] M. Kumar, S. Pandit, *A composite numerical scheme for the numerical simulation of coupled Burgers equation*, Comp. Phys. Comm. 185 (2014) 809-817.

MES BULLETIN OF APPLIED SCIENCES

AUTHOR GUIDELINES

MES Bulletin of Applied Sciences (MESBAS): It is a peer-reviewed biannual journal that publishes both theoretical and experimental quality papers in any applied field. Aim is to promote research culture in teachers and students of UG, PG and higher. Scope of the journal includes: Biology, Chemistry, Physics, Mathematics, Statistics, Computer Science, Social Sciences, Economics, Business, Environmental Science, Food Science, Geology, Medicine, Engineering.

GUIDE FOR AUTHORS

The following categories will be considered for publication:

Original Research Papers, Original Research Reports, State-of-the-art Reviews, Short Communications / Technical notes.

PREPARING MANUSCRIPT:

Ensure that the following items are present:
- One author has been designated as the corresponding author with contact details:
  i. E-mail address   ii. Full postal address
- Paper should be in English.
- Enclose a covering letter.
- The papers for Mathematics, Physics, Computer Science and Engineering should strictly be in LaTeX. LaTeX template will be provided. Others can be in Docx format.

STRUCTURE OF THE PAPER:

Title, Authors details, Abstract, Key words, Introduction, Text, Conclusion, Acknowledgment, References, Figures and Tables.

PAPER SUBMISSION:

Please send your paper as attached file to mail id: mesbas.rcam@gmail.com

Subscription: Rs. 1200.00 per year (2 issues)

MES BULLETIN OF APPLIED SCIENCES

CONTENTS